

Chapter 1

Introduction

1.1 Introduction to uricase

The enzyme uricase (E. C. 1.7.3.3; urate oxidase, urate oxygen oxidoreductase) is involved in purine degradation; it catalyzes the oxidative breakdown of uric acid to allantoin (Fig. 1-1). This enzyme is present in various living organisms including mammals (1, 2), plants (3), fungi (4, 5), yeasts (6, 7, 8), and bacteria (9). In some organisms the degradation of purines is not as complete as in others, with some uricolytic enzymes being absent. For example, birds, reptiles and hominoids including humans, lack uricase, and excrete uric acid as the final product of purine degradation. Microorganisms such as bacteria and yeast further catalyze the oxidation of uric acid to allantoin, and subsequently to allantoinic acid, urea and ammonia.

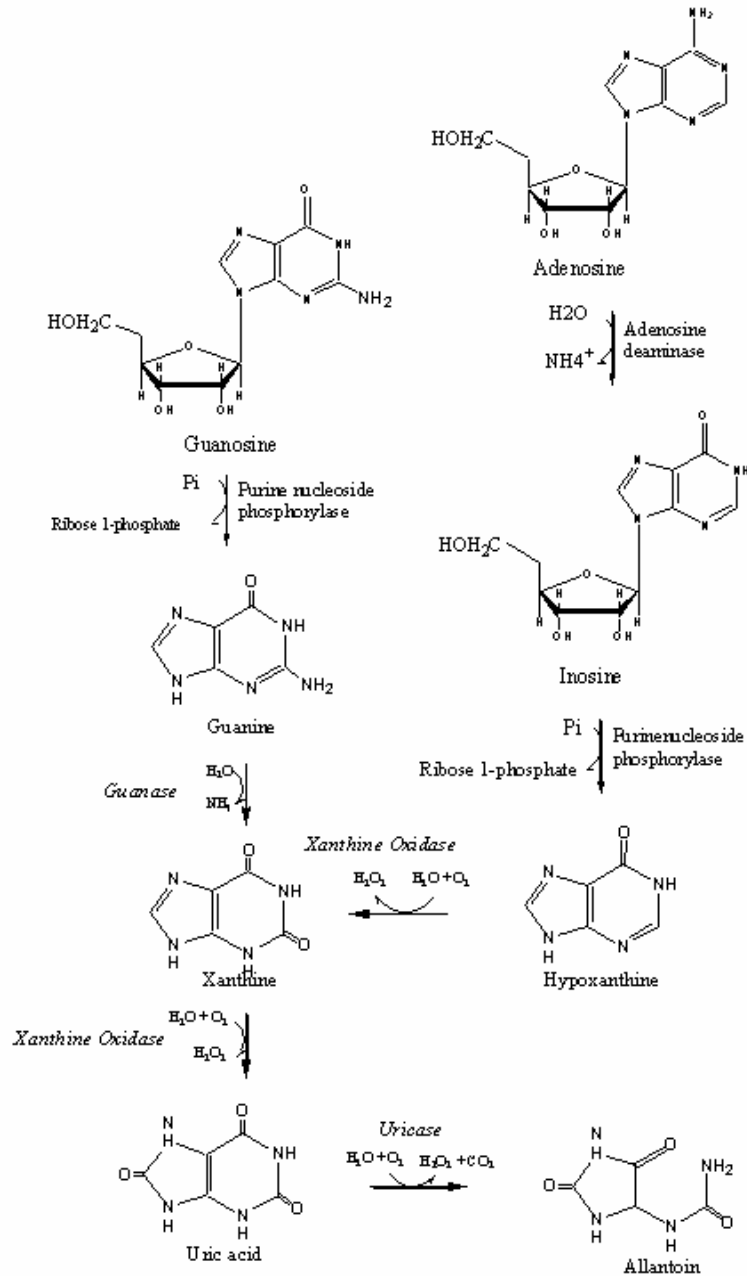
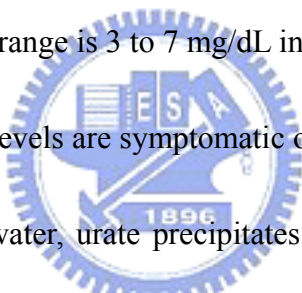


Figure 1-1. Metabolic degradation of purines. AMP and GMP are metabolized to the same product, a compound called xanthine. Xanthine is thought to be metabolized in the peroxisome, although the degree to which it is metabolized depends on the animal. Primates, birds, reptiles, and insects only degrade xanthine to uric acid, while other vertebrates metabolize it to allantoin. It is further metabolized in some animals, with marine invertebrates metabolizing it all the way to ammonia.

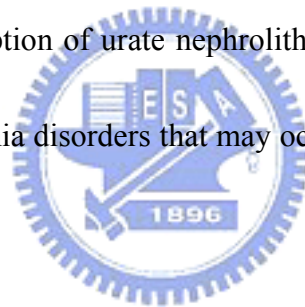
In humans, uric acid is present in the blood largely as the monosodium salt. Both the free acid and the urate salt are relatively insoluble in water, and in some individuals, uric acid can precipitate, causing symptoms of gout. Uric acid is a product of the biochemical breakdown of the purine bases that compose DNA and RNA. As cells die and release DNA, purines are converted into uric acid which is then excreted in the urine, and to a lesser extent, the intestinal tract. The concentration of uric acid in the blood is related to the balance between uric acid production and excretion. The normal blood concentration in children is 2 to 5 mg/dL. At puberty, the level of uric acid increases in males by 1 mg/dL, but not in females. In adults the normal range is 3 to 7 mg/dL in males and 2 to 6 mg/dL in females.



Abnormally high uric acid levels are symptomatic of various diseases. At concentrations exceeding 6.5 to 7 mg/dL in water, urate precipitates in the form of sodium urate crystals. At uric acid blood levels of above 10 mg/dL, the chance of an acute attack of gout (see below) exceeds 90 percent. Only 10% of individuals with hyperuricemia are over-producers of uric acid owing to diseases of the blood and bone marrow, inherited enzyme abnormalities, and metabolic alterations owing to obesity. In patients who overproduce uric acid owing to a deficiency of hypoxanthine-guanine phosphoribosyltransferase, gout attacks may begin before puberty. Increased destruction of body cells causes increased uric acid production with examples being malignancies, especially lymphoreticular cancers, hemolytic anemia, polycythemia, leukemias and nonmalignant conditions of increased cellular proliferation.

Uric acid production also increases with the accelerated breakdown of adenosine triphosphate (ATP) in glucose-6-phosphatase deficiency, tissue ischemia and myophosphorylase deficiency.

Gout is a painful disorder, characterized by uricemia, recurrent acute arthritis, deposition of sodium urate in and around joints and, in many cases, formation of uric acid calculi (10). Gout treatments generally include allopurinol, a potent competitive inhibitor of xanthine oxidase, which catalyzes the conversion of hypoxanthine to xanthine and xanthine to uric acid. However, for gout associated with renal complications, direct injection of uricase permits a significantly more rapid resorption of urate nephrolithiases. Such injection is performed to prevent or resolve hyperuricemia disorders that may occur during chemotherapeutic treatment (11).



Uricase derived from *Aspergillus flavus*, under the name uricozyme, has been used therapeutically over the past two decades in patients with primary or secondary hyperuricemia, including those treated with cytoreductive drugs for a malignant hemopathy (12). The cDNA coding for this enzyme has been cloned and expressed in several microorganisms (13, 14). *Saccharomyces cerevisiae* is now used for production scale owing to its higher yield. The recombinant enzyme accumulates intracellularly in an active and soluble form. The resulting purified enzyme, rasburicase, is now available (15) and has recently been approved for clinical use in Europe under the trade name Fasturtec.

The determination of the enzymes kinetic parameters was a critical step in the characterizing of uricase, and precise assessments of those parameters are required for regulatory reasons on each drug substance batch (purified enzyme) and drug product batch. These studies (characterization, stability, quality control) generated numerous uricase kinetic parameter determinations. Several different approaches are used for measuring uricase activity, but most involve monitoring substrate decrease (uric acid). Uric acid consumption is classically monitored using spectrophotometry at 293 nm (16). More recently, a colorimetric method has been used to measure uricase kinetic parameters on a 96-well microtiter plate that allows the use of a wide concentration range of substrate (17). Figure 1-2 shows the reactions occurring in the horseradish peroxidase (HRP) based system. The colorimetric by-product measured is a red quinoneimine dye.

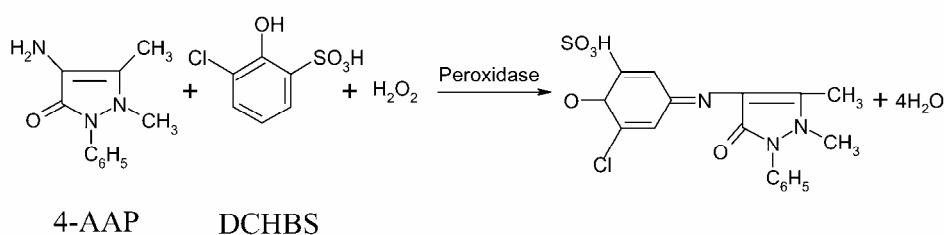


Figure 1-2. DCHBS oxidation catalyzed by HRP in the presence of hydrogen peroxide, and phenoxyl radical reaction with 4-AAP, producing a red quinoneimine dye. DCHBS, 3,5-dichloro-2-hydroxybenzene sulfonate. 4-AAP, 4-aminoantipyrine.

Spectrophotometry at 293 nm is frequently used to measure the level of uric acid. Haeckel's method (18) detects the hydrogen peroxide produced by the uricase-catalyzed oxidation of uric acid through the uricase-catalyzed oxidation of ethanol to acetaldehyde, combined with the oxidation of the latter to acetate in the presence of NAD^+ (or NADP^+) and aldehyde dehydrogenase. The change in absorbance of NADH (or NADPH) at 340 nm is also measured. An initial reading must be made for use as a sample blank. This arrangement makes the method quite laborious to conduct manually. Furthermore, highly purified aldehyde dehydrogenase is not always readily available.

Numerous attempts have been made to fabricate uric acid sensors, using uricase as a biocatalyst (19-23). Uricase catalyzes the *in vivo* oxidation of uric acid in the presence of oxygen, which acts as an oxidizing agent, and produce allantoin and CO_2 . Hydrogen peroxide is the reduction product of O_2 (Fig. 1-3). Several forms of uricase from microorganisms are used as diagnostic reagents for detecting uric acid. These enzymes either have high thermostability or are active over a wide pH range (5, 6, 8, 23). Among these enzymes, only *Bacillus* sp. TB-90 was noted to produce both high activity and thermostability over a wide pH range, from 6 to 9.

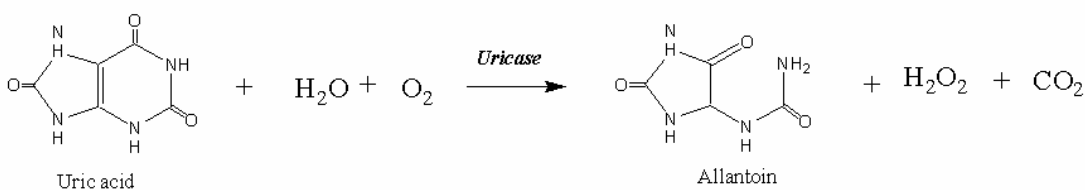


Figure 1-3 Uricase catalyzes the reduction of dissolved oxygen to peroxide in the presence of uric acid.

Allantoin, and its enzymatically reductive product, allantonic acid, represent 70-80% of the organic nitrogen in the xylem of nitrogen-fixing soybean plants and other species of tropical grain legumes (24). Uric acid has been demonstrated to adsorb rapidly onto carbon paste electrode surfaces (25-27). This phenomenon has stimulated the development of a controlled adsorption process to selectively determine uric acid in flowing streams.

Earlier electrochemical procedures, based on the oxidation of uric acid at carbon-based electrodes in acidic solutions, suffered from interference by ascorbic acid, which is oxidized at a potential close to that of uric acid (28). Various types of electrochemical enzyme sensors have been reported to be useful in determining uric acid levels. Nanjo and Guilbault developed the amperometric method of quantitatively measuring uric acid in biological fluids. This method is based on the consumption of dissolved oxygen (21). Janchen et al. conducted similar studies in the presence of oxygen (29). Coulometry, using a porous carbon field electrode, has also been applied to determine in human urine. The compound of

interest has been electrolysed with almost 100% current efficiency at the carbon surface.

However, hydrogen peroxide is not electroactive at this surface (30).

As previously noted, uricase specifically catalyzes uric acid oxidation. The disappearance of oxygen, or the production of H_2O_2 or CO_2 may be exploited for sensing uric acid. Dissolved O_2 can also be consumed by compounds such as ascorbic acid and thiol-containing substances (31). Ascorbate and thiols may react with peroxide produced by the uricase-catalysed reaction of uric acid. Notably, electrochemical enzyme sensors have been designed based on the amperometric determination of H_2O_2 enzymatically liberated from the uricase reaction. These systems exploit the anodic electroactivity of peroxide. Unfortunately, its oxidation has been reported to depend on relatively high applied potentials ($>0.4\text{V}$) and thus is susceptible to interference from easily oxidized molecules. Kulys and colleagues eliminated this interference by using horseradish peroxidase (HRP) to catalyze the reaction between H_2O_2 and hexacyanoferrate (II) and the reduction of the resulting hexacyanoferrate (III) at 0V vs. Ag/AgCl (32).

Owing to its inherent high sensitivity and low detection limit, chemiluminescence has been applied frequently to analysis of numerous biomedical or clinically important analytes. The analyte can be measured based on either the chemiluminescence induced by the reaction of analyte with chemiluminescence reagents or the inhibition of chemiluminescence resulting from the reaction of analyte with chemiluminescence reagents or oxidants before the

chemiluminescence reaction. For uric acid analysis, procedures based on the direct measurement of chemiluminescence induced by the oxidation of luminol with H_2O_2 , HRP and peroxyoxalate have been developed. Since chemiluminescence intensity resulting from the luminol and H_2O_2 system can be increased markedly in the presence of HRP (33,34). Application of the microdialysis sampling coupled to a chemiluminescence reaction has proved to be sufficiently sensitive for monitoring of uric acid *in vivo* in real time with high selectivity and accuracy (35).



1.2 Biosensor for biomolecular technology

A biosensor comprises a biological element (for example - antibody, enzyme, protein, nucleic acid, whole cells, tissues, or whole organisms) and a signal transducer. When the analyte interacts with the biological element, which produces an energy change is converted into a measurable signal detected by the transducer. Miniaturization, cost reductions and the improved processing power of modern microelectronics have further improved the analytical capability of such devices, and extended the possibilities for applications. The most common types of biological recognition elements are based on enzymatic interactions, nucleic acid interactions, antibody-antigen interactions, cellular interactions, or interactions using synthetic bioreceptors. The commonly used transducers are optical, electrochemical and mass-sensitive measurement.



Most current biosensors can be classified based on four different principles: bioaffinity, catalytic, transmembrane and cell sensor. Most transmembrane and cell sensors are based on affinity or catalytic principles. Current research development is focused on improvement of the stability, selectivity and sensitivity of biosensing devices. On the other hand, there is a growing trend towards the miniaturization of the spectrometers, chromatographs and detectors that are traditionally used in analytical chemistry, achieved through micro- and nano-fabrications techniques. Consequently, it has become increasingly difficult to make clear distinctions between miniaturized instruments and classical biosensors. This statement holds particularly true for recent trends in the development of optical and CMOS (complementary

metal oxide semiconductor) biosensors. Additionally, the practical application of any sensor or analytical instrument requires the use of complete analysis systems and thus the development and optimization of the same components for sample handling, pumps, filters, membranes, and sample conditioning. For real biosensors, the detection occurs by direct conversion of biochemical information to electronic information via a suitable transducer. The biochemical composition of complex mixtures can be characterized in selected cases with arrays of biosensors. The data pretreatment results from different individual sensors determining suitable feature vectors, and biochemical analysis is performed via subsequent pattern recognition.



1.2.1 Stable interfaces in biosensor

The selectivity of biosensors is generally obtained by utilizing natural or artificial biomolecular functional units such as antibodies, enzymes, transmembrane proteins, and so on (36). Owing to the huge amount of electrical and optical transducers available in thin film technology, most developments of new biosensors focus on preparation of controlled thin film structures in which these biomolecular functional units can be arranged and addressed in reproducible and controlled geometric surroundings (37). This requires the preparation of arrays of biomolecules on planar surfaces, and making it necessary to scale down the processes of covalent immobilization of complete molecules, the *in situ* synthesis of molecules on surfaces (for example by self-assembly) and the physical entrapment of

molecules in defined areas to micro- and nanometer dimensions (38). Various methods of preparation include entrapment in polymeric matrices, physisorption, direct covalent attachment, ionic attachment, embedding in lipid membranes, coupling to ordered Langmuir-Blodgett, or self-assembling monolayers with covalent or affinity-like linkers. Another recent example, involving the immobilization of enzymes in polymers, was presented by Geckeler and Muller (39). Electrochemical polymerization is a promising method for the controlled immobilization of various enzymes. The simultaneous entrapment or covalent coupling to monomer units occurs either before or after the polymerization (40). Direct covalent coupling of enzymes to the substrate is another common technique as described by Moser *et al.* (41). Patterning of molecules on surfaces using photolithography or laser techniques has recently attracted growing interest (42). Applications of the high binding specificity of the biotin-avidin system have become increasingly popular. As the first step, avidin or streptavidin can be coupled to the surface of interest either directly or via biotin covalently bound to the surface (43). In this concept, any species that can be biotinylated may be coupled to the surface. Examples include enzymes (44), antibody fragments (45), labeled antibodies (46), and even multilayers (47).

Four substrates are important for most practical thin film devices, namely platinum, carbon, modified silicon surface or glasses, and gold (43). Perfect order in the monolayer system is generally not the only important property to be optimized in biosensors. Another

criterion is that the biomolecular functional units, which often must be immobilized to maintain their biological activity. The large size and necessary accessibility to biomolecules that are detected in solution of these units generally requires some spatial separation of their active sites in ordered monolayers.

Suitable molecules with biomolecular functional units for use in thin film formation may contain short and long chain thiol coupling groups for attachment to the substrate, and also specific end groups for their mutual coupling to form a stable two-dimensional system. The spatial separation of active sites may use a mixture of active and non-active molecules. In this case, two-dimensional phase separation should be avoided. Another possibility is the embedding of active biomolecules into suitable matrices. Examples include sol-gel materials (48) and polyethyleneglycol (49) or dextran (50) overlayers with attached biomolecular functional units.

1.2.2 Transducers

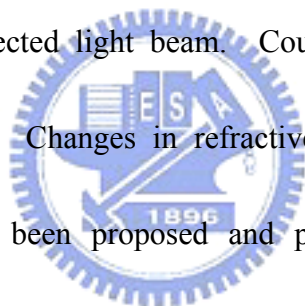
Optical transducers:

Optical transducers permit the quantitative determination of one or more of the fundamental characteristics of optical radiation, including amplitude, phase, frequency and polarization. For biosensor application a change in activity, the concentration of a biochemical, or the biological structure must cause a change of one of these fundamental

quantities. The following discussion briefly characterizes the different transducer principles used in biomolecular studies.

A. Surface plasmon resonance (SPR)

Surface plasmons are collective fluctuations of the electron plasma on the surface of an electrically conducting material. Surface plasmons can be excited via evanescent light waves using the basic attenuated total reflection (ATR) configuration. SPR occurs when the photon momentum along the surface matches the plasmon frequency and is detected as a strong attenuation of the reflected light beam. Coupling conditions are sensitive to the surface refractive index (57). Changes in refractive index below 10^{-6} can be resolved. Various optical set-ups have been proposed and partially commercialized. Moreover, detection limits below $1 \text{ pg protein/mm}^2$ have been reported (58, 59).



B. Reflectometric interference spectroscopy (RIFS)

The detection of binding reactions by reflectometric interference spectroscopy (RIFS) is based on the interference occurring at thin planar transparent films. A light beam passing a weakly reflecting thin film is partially reflected at each of the interfaces. Because the two reflected beams follow different optical paths, a phase difference is introduced. Interference of the two beams causes modulation of reflected light intensity owing to constructive and

destructive interference (60). The transducer is simply a nonstructured thin film system on a transparent substrate. The detection limits are in the range of 2 pg/mm^2 (61).

C. Integrated optical devices (IOD)

Integrated optics with monomode channel waveguides are routinely used in long range, high speed telecommunications. Monomode channel waveguides permit the very straightforward implementation of interferometer structures. A waveguide is split into a measurement and a reference path and recombined after a distance. Any phase difference introduced on beams splitting can be detected based on interference effects (62). Binding of organic matter on the surface of the measurement arm causes a modulation of intensity at the interferometer output. Detection limits are approximately 10 pg/mm^2 (63). Currently such devices are prohibitively expensive to produce, but the implementation of IO devices in silicon or in polymers, driven by the needs of future information technologies, may change this situation (64). As an example Bookham Technology (UK) devises integrated systems based on its patented silicon technology.

D. Grating coupler

The first integrated optical device used in bioaffinity analysis was a grating coupler structure embossed in a monomode film waveguide devised by Lukkosz and co-workers (65).

A periodic grating on the surface of a waveguide can be used for in- or out-coupling of radiation from the waveguide. Meanwhile, the angle of deflection (coupling angle) depends on the wavelength and grating period. Binding of organic or biological matter on top of the grating changes the coupling angle. The detection limit is approximately 10 pg protein/mm².

Electrochemical transducers:

Electrochemical techniques can be used to quantify redox-active substances. Cyclic voltammetry is probably the most widely used of the electrochemical techniques. Cyclic voltammetry is used to characterize electrode materials, surface coverages, electron transfer properties, and electron transfer mechanisms including adsorption phenomena and chemical reactions at the surface (54). The special electrode reactions that occur when the redox species are confined to the surface can also be applied to characterization of surface redox processes, for example square-wave voltammetry (55) or normal pulse voltammetry.

Electrochemical methods have attracted particular attention in modern analytical chemistry with the availability of miniaturized electrodes, microdot electrode arrays and interdigitated microelectrode arrays. These devices can achieve detection limits in the lower nanomolar range without preconcentration. Moreover, these miniaturized devices permit the investigations of small sample volumes (<0. μ L). An array of microdot electrodes (56) demonstrates a typical example of such a transducer comprising two working electrodes,

counter- and reference-electrode. In the steady-state, one electrode generates electroactive species (the generator electrode) which diffuse to the neighboring electrode (the collector electrode) where the electrochemical regeneration occurs. This effect causes an electrochemical feedback. The resulting current is typically amplified by one order of magnitude or more, thus markedly enhancing the detection limit (56).

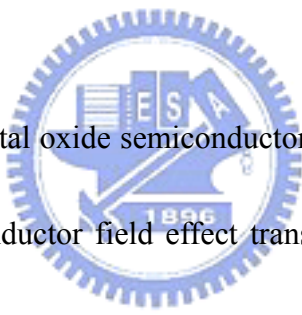
Mass-sensitive transducers:

Mass-sensitive signal transducers are based on the propagation of acoustic waves in a piezoelectric crystal. The device generally operates as a frequency-determining element in an oscillator circuit. Bulk acoustic wave devices such as the quartz crystal microbalance (QCM) typically operate at resonance frequencies of a few to 10 MHz. The measurement effect employed is the frequency decrease of the QCM with increasing mass loading. The sensitivity of QCM-devices thus depends strongly on the resonance frequency. Higher operating frequencies are thus required to achieve higher sensitivities. This can be realized by using very thin quartz substrates or by assessing overtones. Typical detection limits achieved with 10 MHz QCM are approximately 10 pg/mm^2 (51, 52).

Another type of mass-sensitive transducer is known as a surface acoustic wave device. In this device a surface acoustic wave (SAW) is generated on an elastic transducer surface between interdigital electrodes. Unlike the QCM, the SAW-technique only detects the

surface part of the acoustic wave. Devices that operate at higher frequency ranges and lower detection limits than the QCM have been reported (50). However, noise problems are generally more severe, and the SAW technique must be modified to deal with possible damping before application in aqueous solution, for example, by combining the use of horizontal polarized shear waves with mass gratings on the sensor device. The resulting wave type is termed the surface transverse wave and causes only minor energy losses in water.

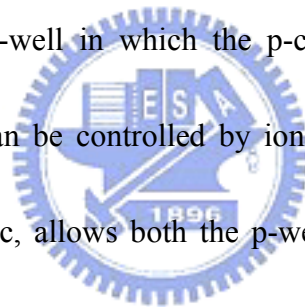
1.3 CMOS technologys



CMOS (complementary metal oxide semiconductor) uses a combination of p-channel and n-channel metal-oxide-semiconductor field effect transistors (MOSFET) to implement logic gates and other digital circuits for computers and signal processing equipment (66). The p-well process is a widespread technique for CMOS circuits. The process begins with a fairly low doped n-type silicon substrate in which the p-channel MOSFET is fabricated. A diffused p-region, called a p-well, is formed in which the n- channel MOSFET is fabricated. In most cases, the p-type substrate doping level must exceed the n-type substrate doping level to obtain the desired threshold voltages. The larger p-doping can easily compensate for the initial n-doping to form the p-well. Figure 1-4a displays a simplified cross section of the p-well CMOS structure. The notation FOX indicates field oxide, which is a relatively thick

oxide separating the devices. The field oxide prevents inversion of either the n- or p substrates and helps isolate the two devices. In practice, additional processing steps are required, for example, providing connections so that the p-well and b-substrate can be electrically connected to the appropriate voltages. The n-substrate must always have a higher potential than the p-well, therefore, this p/n junction is always reverse biased.

With ion implantation now being widely used for threshold voltage control, both the n-well CMOS and twin-well CMOS processes can be used. The n-well CMOS process, shown in Fig. 1-4b, begins with an optimized p-type substrate that is used to form the n-channel MOSFETs. The n-well in which the p-channel devices are fabricated is then added. The n-well doping can be controlled by ion implantation. The twin-well CMOS process, illustrated in Fig. 1-4c, allows both the p-well and n-well regions to be optimally doped to control the threshold voltage and transconductance of each transistor. The twin-well process enables a higher packing density owing to on self-aligned channel stops.



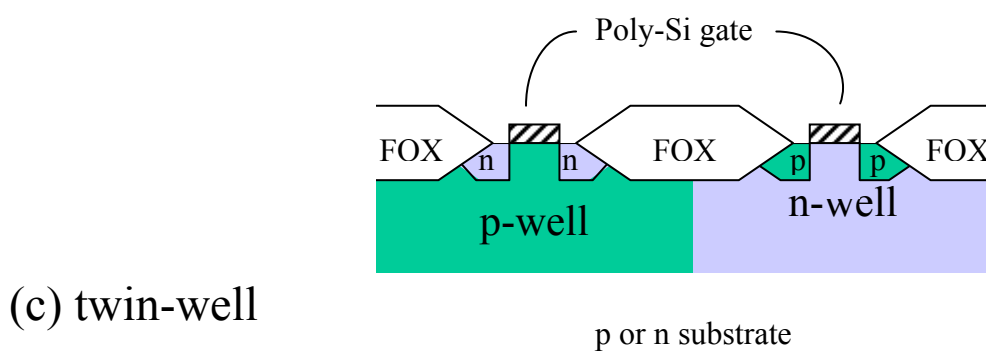
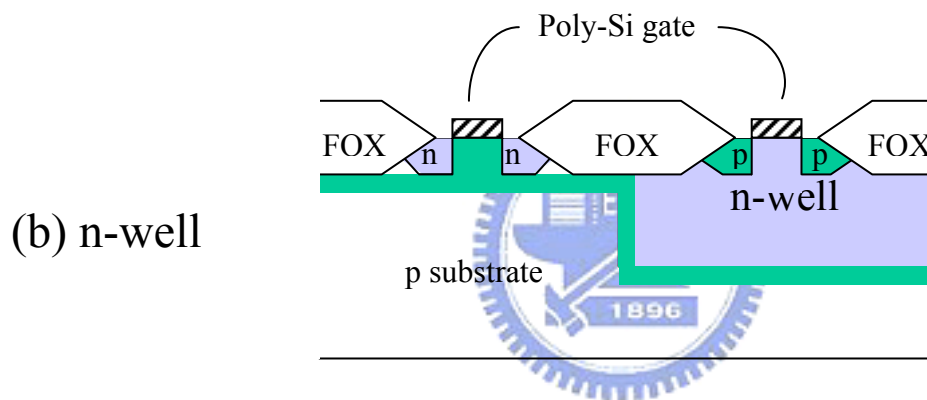
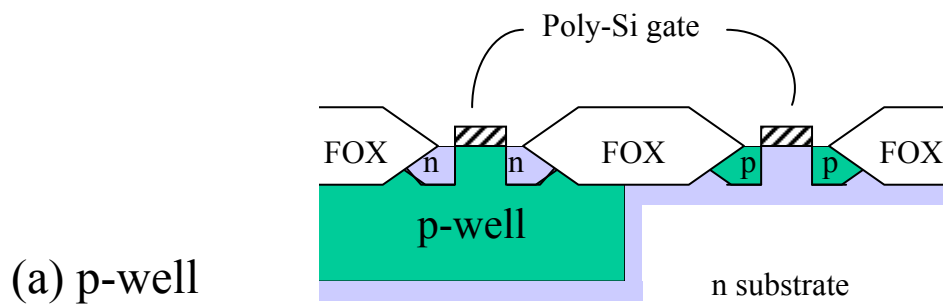
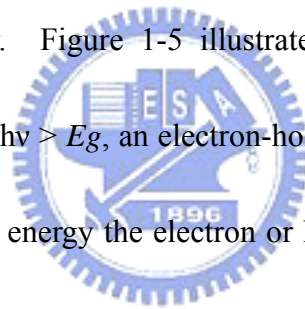


Figure 1-4 CMOS structures. (a) p-well, (b) n-well, and (c) twin well

When a semiconductor is illuminated, the photons may either be absorbed or may propagate through the semiconductor, depending on the photon energy and the bandgap energy E_g . If the photon energy is below E_g , the photons are not readily absorbed. In this case, the light is transmitted through the material and the semiconductor appears transparent. If $E = h\nu > E_g$, the photon can interact with a valence electron and elevate the electron into the conduction band. The valence band contains numerous electrons and the conduction band contains numerous empty states, so the probability of such interaction is high when $h\nu > E_g$. This interaction creates an electron in the conduction band and a hole in the valence band — an electron-hole pair. Figure 1-5 illustrates the basic absorption processes for different values of $h\nu$. When $h\nu > E_g$, an electron-hole pair is created and the excess energy may provide additional kinetic energy to the electron or hole, which is dissipated as heat in the semiconductor.



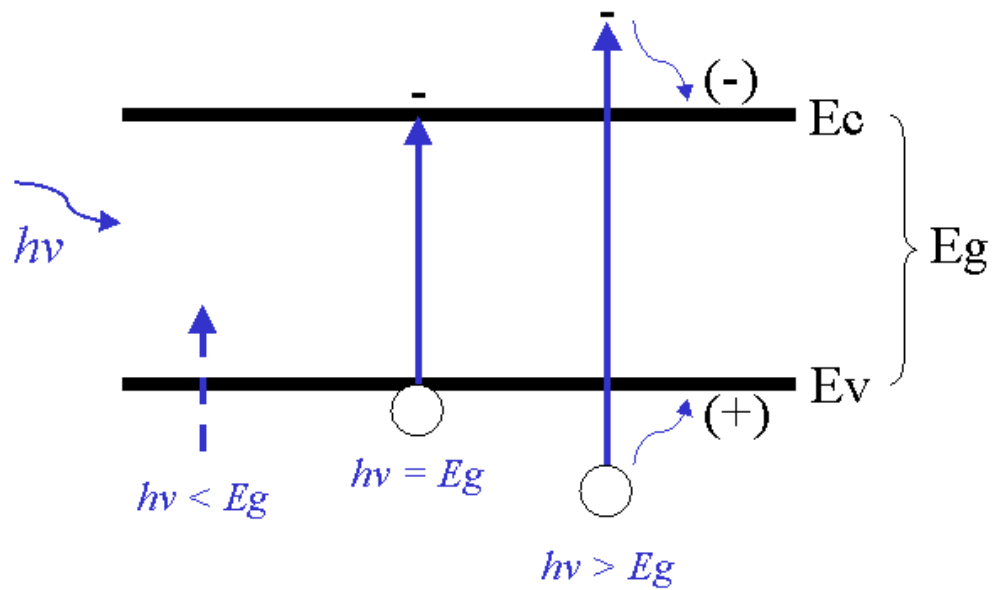


Figure 1-5. Optically generated electron-hole pair formation in a semiconductor.

Several different applications have been developed using the IC biochip system designed for the microchip photosensing elements and associated data treatment based on CMOS technology. These highly integrated biochip systems have been in development during the last couple of years. One DNA biochip device is being used to detect a gene segment of the AIDS virus (67). Recently, an antibody-based biochip was developed that had a 2-dimensional photosensor array detector directly coupled to a microfluidics sample / reagent delivery system for rapid, on-chip detection of *E. coli* (68). This compact system features a 4×4 array of independently operating photodiodes which are integrated along with amplifiers, discriminators and logic circuitry on a single platform via the CMOS process. The potential for implementing the CMOS technology to combine photosensors and associated

microelectronics into a compact, inexpensive integrated circuit (IC) chip is the main advantage of this sensor over other 2-dimensional detectors, such as charge-coupled devices (CCDs) and charge injection devices (CIDs). The fluidics system includes a single 0.4 mL reaction chamber housing a sampling platform that selectively captures detection probes from a delivered complex sample by using of immobilized bioreceptors. More recently, an integrated CMOS-based microchip system was designed using capillary array electrophoresis for detecting bacterial pathogen amplified by polymerase chain reaction (69). Use of the miniaturized CMOS microchip system as a detector in electrophoresis shows excellent potential for compatibility with conventional microfabricated devices. Therefore, these microchips should contribute to the further development of miniaturized systems for more rapid and high-throughput bioassays.



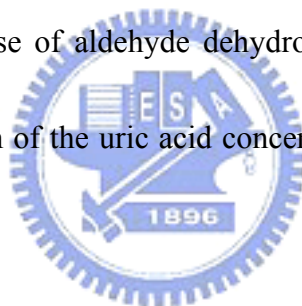
1.4 References

1. Keilin, J. (1959) The biological significance of uric acid and guanine excretion. *Biol. Rev.* 34, 265-296.
2. Wallrath, L. L. and Friedman, T. B. (1991) Species differences in the temporal pattern of drosophila urate oxidase gene expression are attributed to trans-acting regulatory changes. *Proc. Natl. Acad. Sci. U.S.A.* 88, 5489-5493.
- 3.. Montalbini, P., Redondo, J., Caballero, J. L., Cárdenas, J. and Pineda, M. (1997) Uricase from leaves: its purification and characterization from three different higher plants. *Planta.* 202(5), 277-283.
4. Nahm, B. and Marzluf, G. A. (1987) Induction and de Novo synthesis of uricase, a nitrogen-regulated enzyme in *Neurospora crassa*. *J. bacteriol.* 169, 1943-1048.
5. Montalbini, P., Aguilar, M. and Pineda, M. (1999) Isolation and characterization of uricase from bean leaves and its comparison with uredospore enzyme. *Plant Science* 147, 139-147.
6. Yuichi, H., Tetsuhiko, S. and Hajime, I. (2000) Cloning, sequence analysis and expression in *Escherichia coli* of the gene encoding a uricase from the yeast-like symbiont of the brown planthopper, *Nilaparvata lugens*. *Insect Biochemistry and Molecular Biology* 30, 173-182.
7. Koyama, Y., Ichikawa, T. and Nakano, E. (1996) Cloning, sequence analysis and expression in *Escherichia coli* of the gene encoding the *candida utilis* urate oxidase. *J. Biochem.* 120,

969-973.

8. Adamek, V., Suchova, M., Demnerova, K., Kralova, B., Fort, I. and Morava, P. (1990)
Fermentation of *candida utilis* for uricase production. *J. Indu. Microbiol.* 6, 85-90.
9. Yamamoto, K., Kojima, Y., Kikuchi, T., Shigyo, T., Sugihara, K. and Takashio, M. (1996)
Nucleotide sequence of the uricase gene from *Bacillus* sp. TB-90. *J. Biochem.* 119, 80-84.
10. Eswara, U. S., Dutt, H. and Mottola, A. (1974) Determination of uric acid at the microgram level by a kinetic procedure based on a pseudo-induction period. *Anal. Chem.* 46, 1777-1781.
11. Burtic, C. A. and Ashwood, E. R. (1994) Teitz textbook of clinical chemistry, 2nd ed.
Philadelphia: WB saunders company.
12. Kissel, P., Manuary, G., Royer, R. and Toussain, P. (1975) Treatment of malignant haemopathies and urate oxidase. *Lancet.* 25, 229.
13. Legoux, R., Delpuch, B., Dumont, X., Guillemot, J. C., Ramond, P., Shire, D., Caput, D., Ferrara, P. and Loison, G. (1992) Cloning and expression in *Escherichia coli* of the gene encoding *Aspergillus flavus* urate oxidase. *J. Biol. Chem.* 267 (12), 8565-8570.
14. Leplatois, P., Douarin, L. and Loison, G. (1992) High-level of a peroxisomal enzyme: *Aspergillus flavus* uricase accumulates intracellularly and is active in *Saccharomyces cerevisiae*. *Gene* 122, 139-145.
15. Pui, C. H., Mahmoud, H. H., Wiley, J. M., Woods, G. M., Leverger, G., Camitta, B.,

- Hastings, C., Blaney, S., Relling, M. V. and Reaman, G. H. (2000) Recombinant urate oxidase for the prophylaxis or treatment of hyperuricemia in patients with leukemia or lymphoma. *J. Clin. Oncol.* 19 (3), 697-704.
16. Kalckar, H. M. (1947) Differential spectrophotometry of purine compounds by means of specific enzymes. *J. Biol. Chem.* 167, 429.
17. Fraisse, L., Bonnet, M. C., Farcy, J. P., Agut, C., Dersigny, D. and Bayol, A. (2002) A colorimetric 96-well microtiter plate assay for the determination of the urate oxidase activity and its kinetic parameters. *Anal. Biochem.* 303, 42-49.
18. Haeckel, R. (1976) The use of aldehyde dehydrogenase to determine H₂O₂-producing reaction: The determination of the uric acid concentration. *J. Clin. Chem. Clin. Biochem.* 14, 101-106.
19. Yutaka, A., Hiroshi, I., Hiroomi, N., Tsugutoshi, A. and Mitsutak, Y. (1992) Effects of serum bilirubin on determination of uric acid by the uricase-peroxidase coupled reaction. *Clin. Chem.* 38, 1350-1352.
20. Bhargava, A. K., Lal, H. and Pundir, C. S. (1999) Discrete analysis of serum uric acid with immobilized uricase and peroxidase, *J. Biochem. Biophys. Methods* 39, 125-136.
21. Nanjo, M. and Guilbault, G. G. (1974) Enzyme electrode sensing oxygen for uric acid in serum and urine. *Anal. Chem.* 46, 1769-1772.
22. Uchiyama, S., Shimizu, H. and Hasebe, Y. (1991) Chemical amplification of uric acid



- sensor responses by dithiothreitol. *Anal. Chem.* 66, 1873-1876.
23. Miland, E., Ordieres, A. J. M., Blanco, P. T. and Smyth, C. Ó. (1996) Poly (o-aminophenol)-modified bienzyme carbon paste electrode for the detection of uric acid, *Talanta* 43, 785-796.
24. Reynolds, P. H. S., Boland, M. J., Blevins, D. G., Randall, D. P. and Schubert, K. R. (1982) Ureide biogenesis in leguminous plants. *Trends Biochem. Sci.* 7:366-368.
25. Gonzalez, E. (1991) Amperometric sensor for hypoxanthine and xanthine based on the detection of uric acid. *Anal. Chim. Acta.* 242, 267-273.
26. Markas, T., Gilmartin, J. and Hart, P. (1994) Novel reagentless, amperometric biosensor for uric acid based on a chemically modified screen-printed carbon electrode coated with cellulose acetate and uricase. *Analyst.* 119, 833-840.
27. Cai, X., Kalcher, K., Neuhold, C. and Ogorevc, B. (1994) An improved voltammetric method for the determination of trace amounts of uric acid with electrochemically pretreated carbon paste electrodes. *Talanta.* 41, 407-412.
28. Shukla, M. K. and Mishra, P. C. (1996) electronic structures and spectra of two antioxidants uric acid and ascorbic acid. *J. Mol. Struct.* 377, 247-259.
29. Janchen, M., Walzel, G., Neef, B., Wolf, B., Scheller, F. and Kuhn, M. (1983). Uric acid determination in dilute serum with an enzyme electrochemical and enzyme-free sensor. *Biomed. Biochim. Acta* 9,1055-1059.

30. Uchiyama, S., Obokata, T. and Suzuki, S. (1990) Flow-coulometric detector for uric acid in human urine. *Anal. Chim. Acta.* 230, 195-198.
31. Gilmartin, M. A. T., Haetand, J. P. and Birch, B. J. (1994) Development of amperometric biosensor for uric acid based on chemically modified graphite poxyresin and screen-printed electrode containing cobalt phthalocyanine. *Analyst.* 119, 243-252.
32. Kulys, J. J., Laurinavicius, V. S. A., Pesliakiene, M. V. and Gureviciene, U. V. (1983) The determination of glucose, hypoxanthine and uric acid with use of bi-enzyme amperometric electrodes. *Anal. Chim. Acta* 148, 13-18.
33. Hong, H. C. and Huang, H. J. (2003) Flow injection analysis of uric acid with a uricase- and horseradish peroxidase-coupled sepharose column based luminol chemiluminescence system. *Anal. Chim. Acta* 499, 41-46.
34. Kasai, S., Hirano, Y., Motochi, N., Shiku, H., Nishizawa, M. and Matsue, T. (2002) Simultaneous detection of uric acid and glucose on a dual-enzyme chip using scanning electrochemical microscopy/ scanning chemiluminescence microscopy. *Anal. Chim. Acta* 458, 263-270.
35. Yao, D., Vlessidis, A. G. and Evmiridis, N. P. (2003) Microdialysis sampling and monitoring of uric acid in vivo by a chemiluminescence reaction and an enzyme on immobilized chitosan support membrane. *Anal. Chim. Acta* 478, 23-30.
36. Gopel, W. and Heiduschka, P. (1994) Introduction to bioelectronics: "Interfacing biology

- with electronics". *Biosens. Bioelectron.* 9, iii-xiii.
37. Gopel, W. (1995) Controlled signal transduction across interfaces of "Intelligent" molecular system. *Biosens. Bioelectron.* 10, 35-60.
38. Connolly, P. (1994) Bioelectronic interfacing: micro- and nanofabrication techniques for generating predetermined molecular arrays. *Trends Biotechnol.* 12, 123-127.
39. Geckeler, K. E. and Muller, B. (1993) Polymer materials in biosensors. *Naturwissenschaften* 80, 18-24.
40. Bartlett, P. N. and Cooper, J. M. (1993) A review of the immobilization of enzymes in electropolymerized films. *J. Electroanal. Chem.* 362,1-12.
41. Moser, I., Urban, G. and Pittner, F. (1992) Advanced immobilization and protein techniques on thin film biosensors. *Sens. Actuators B* 7, 356-362.
42. Calvert, J. M. (1993) Lithographic patterning of self-assembled films. *J. Vac. Sci. Technol.* B 11, 2155-2163.
43. Mittler-Neher, S. and Knoll, W. (1995) Spectroscopic and surface-analytical characterization of self-assembled layers on Au. *Biosens. Bioelectron.* 10, 903-916.
44. Pantano, P. and Kuhr, W. G. (1993) Covalent modification utilizing avidin-biotin technology. *Anal. Chem.* 65, 623-630.
45. Muller, W. and Spinke, J. (1993) Attempts to mimic docking processes of the immune system: Recognition-induced formation of protein multilayers. *Science* 262, 1706-1708.

46. de Alwis, U. and Wilson, G. S. (1989) Strategies for the reversible immobilization of enzymes by use of biotin-bound anti-enzyme antibodies. *Talanta* 36, 249-253.
47. Spinke, J. and Guder, H. J. (1993) Molecular recognition at self-assembled monolayers: The construction of multicomponent multilayers. *Langmuir*. 9, 1821-1825.
48. Dave, B. C. and Zink, J. I. (1994) Sol-gel encapsulation methods for biosensors. *Anal. Chem.* 66, 1120-1127.
49. Harris, J. M. (1992) Poly (ethylene glycol) chemistry. Biotechnical and Biomedical Applications. Plenum Press, New York and London.
50. Lundstrom, I. (1994) Real-time biospecific interaction analysis. *Biosens. Bioelectron.* 9, 725-736.
51. Rickert, J., Brecht, A. and Göpel, W. (1997) Quartz microbalances for quantitative biosensing and characterizing protein multilayers. *Biosens. Bioelectron.* 12, 567-575.
52. Rickert, J., Brecht, A. and Göpel, W. (1997) QCM operation in liquids: constant sensitivity found during formation of extended protein multilayers by affinity. *Analyt. Chem.* 69, 1441-1448.
53. Tommoy, M., Baer, R. L., Spirasolomon, D. and Doherty, T. P. (1995) Atrazine measurements using surface transverse wave. *Anal. Chem.* 67, 1510-1516.
54. Rusling, J. F. and Suib, S. L. (1994) Characterizing materials with cyclic voltammetry. *Adv. Mater.* 6, 922-930.

55. Odea, J. J. and Osteryoung, J. G. (1993) Characterization of quasi-reversible surface processes by square-wave voltammetry. *Anal. Chem.* 65, 3090-3097.
56. Niwa, O., Xu, Y., Halsall, H. B. and Heineman, W. R. (1993) Small-volume voltammetric detection of 4-aminophenol with interdigitated array electrodes and application to electrochemical enzyme immunoassay. *Anal. Chem.* 65, 1559-1563.
57. Liedberg, B. and Nylander, C. (1983) Surface plasmon resonance for gas detection and biosensing. *Sens. Actuators* 4, 299-304.
58. Jorgenson, R. C. and Yee, S. S. (1993) Optical biosensors. *Sens. Actuators* B12, 213-220.
59. Lavers, C. R. and Wilkinson, J. S. (1994) Design principles of biosensors. *Sens. Actuators* B 22, 75-81.
60. Striebel, C. h. and Brecht, A. (1994) Characterization of biomembranes by spectral ellipsometry, surface plasmon resonance and interferometry with regard to biosensor application. *Biosens. Bioelectron.* 9, 139-146.
61. Piehler, J. and Brecht, A. (1996) Affinity detection of low molecular weight analytes. *Anal. Chem.* 68, 139-143.
62. Lukosz, W. (1995) Integrated optical chemical and direct biochemical sensors. *Sens. Actuators* B 29, 37-50.
63. Gauglitz, G. G. and Ingenhoff, J. (1994) Design of new integrated optical substrates for immuno-analytical applications. *Fresenius J. Anal. Chem.* 349, 355-359.

64. Lai, Q., Bachmann, M., Hunziker, W., Besse, P.A. and Melchior, H. (1996) Arbitrary ratio power splitters using angled silica on silicon multimode interference couplers. *Elect. Letters* 32, 1576-1577.
65. Nellen, P. h. and Lukosz, W. (1993) Integrated optical input grating couplers as direct affinity sensors. *Biosens. Bioelectron* 8, 129-147.
66. Neamen, D. A. Semiconductor physics and devices, 2nd ed. New York: McGraw-Hill, 1997.
67. Vo-Dinh, T., Alarie, J. P., Isola, N., Landis, D., Wintenberg, A. L. and Ericson M. N. (1999) DNA biochip using a phototransistor integrated circuit. *Anal. Chem.* 71, 358-363.
68. Stokes, D. L., Griffin, G. D. and Vo-Dinh, T. (2001) Detection of *E. coli* using a microfluidics-based antibody biochip detection system. *Fresenius J. Anal. Chem.* 369, 295-301.
69. Song, J. M., Mobley, J. and Vo-Dinh, T. (2003) Detection of bacterial pathogen DNA using an integrated complementary metal oxide semiconductor microchip system with capillary array electrophoresis. *J. chromatogr. B* 783, 501-508.

Chapter 2


Experimental

2.1 Experimental of Materials

2.1.1 Strains and vectors

The strain, *Bacillus subtilis* CCRC 14199, was obtained from the Culture Collection and Research Center (Food Industry Research and Development Institute, Hsinchu, Taiwan). XL1-Blue competent cell, pBluescript IISK(+) cloning vector, and pMAL-c2 expression vector were used in cloning.

2.1.2 Reagents



Restriction enzyme, ligase, and amylose resin were purchased from New England Biolab. SYBR green nucleic acid gel stain, *rTth* polymerase, and PCR reagents were purchased from Roche. DNA primers were purchased from Biobasic Inc. Agarose was purchased from USB. Ammonium persulfate (APS) and sodium dodecyl sulfate (SDS) were purchased from Gibco BRL. Sodium phosphate, β -mercaptoethanol, coomassie brilliant R250, isobutanol, and sodium chloride were purchased from Merck. Phenylmethylsulfonyl fluoride (PMSF), lysozyme, methanol, acetic acid, proteinase K, uricase, uric acid, horseradish peroxidase, 4-aminoantipyrine, and 3,5-dichloro-2-hydroxybenzene sulfonate were purchased from Sigma. Tris-HCl,

tris(hydroxymethyl) methylamine, and glycine were purchased from BDH. Acrylamide, and methylene-bis-acrylamide were purchased from Amersham Pharmacia Biotech. LB medium, tryptone, and yeast extract were purchased from Difco.

2.1.3 Buffers and solution

LB broth: 10 g tryptone, 5 g yeast extract, 10 g NaCl. Adjust to pH 7.0 with NaOH and make up to a final volume of 1 L with distilled water. Autoclave.

LB agar: As for LB broth except for the addition of 15 g bactoagar.

1000x Ampicillin : dissolve ampicillin in distilled water to make a 100 mg / ml (w/v) solution, and sterilize by filtration through a 0.2 μ m filter.

5-bromo, 4-chloro 3-indolyl β -D-galactoside (X-gal): dissolve X-gal in dimethylformamide (DMF) to make a 20 mg/mL solution. Wrap the tube that contains the solution in aluminum foil.

Isopropyl β -D-thiogalactopyranoside (IPTG) : dissolve 2 g IPTG in 8 mL distilled water and adjust the volume of the solution to 10 mL. Sterilize by filtration through a 0.2 μ m filter. Dispense the solution into 1 mL aliquots.

SYBR green nucleic acid gel stain: add 10,000 \times concentration reagent purchased from Roche into DMSO and dilute to 1/300 concentration. Keep the solution in dark.

Acrylamide-Urea gel solution : dissolve 38 g acrylamide, 2 g bis-acrylamide (methylenebisacrylamide) and 360 g urea in sufficient distilled water to bring the total volume to 800 ml. Filter through a 0.2 μm paper and then refrigerate.

Stacking buffer (1M Tris, pH 6.8) : dissolve 24.22 g of Tris base into 100 mL distilled water and adjust the pH to 6.8 using 6 N HCl.

30% acrylamide : add 300 g acrylamide into 300 mL distilled water and make up the final volume to 1 L. Filter the solution through 0.45 μm paper. Keep the solution in the dark and store at 4 °C. Perform this step carefully using a mask.



1 % bis-acrylamide (N, N-Methylene-bis acrylamide) : add 5 g ultrapure bis-acrylamide into water and make up the total volume to 500 mL with distilled water. Filter the solution through 0.45 μm paper. Keep the solution in the dark and store at 4 °C.

50 \times TAE buffer : add 242 g Tris base and 57.1 g glacial acetic acid to distilled water. Add 100 mL 0.5 M EDTA and make up final volume to 500 mL.

10 \times TBE buffer : add 108 g Tris base, 55 g boric acid and 0.5 M EDTA 40 mL into distilled water. Make up the final volume to 1 L.

5 \times sample buffer : mix 1 mL 1 M Tris-HCl (pH6.8), 0.8 mL glycerol, 1.6 mL 10% SDS,

0.4 mL 2-mercaptoethanol, and 0.05% bromophenol blue. Then make up the final volume 8 mL.

20 % SDS solution : dissolve 4 g ultrapure SDS in distilled water and make up the final volume to 20 mL. Store at room temperature.

Gel stain solution (0.1% Coomassie blue R-250 stain solution) : add 0.5 g Coomassie blue R-250 to 200 mL methanol. then, add 50 mL acetic acid and make up the final volume to 500 mL using distilled water.

Gel destain solution I : mix 400 mL methanol with 100 mL acetic acid , and make up volume to 1 L with distilled water.

Gel destain solution II : mix 50 mL methanol with 70 mL acetic acid , and make up volume to 1 L with distilled water.

Rich medium + glucose & ampicillin (per liter) : 10 g tryptone, 5 g yeast extract, 5 g NaCl, 2 g glucose autoclave; add sterile ampicillin to 100 μ g/ mL.

0.1 M IPTG stock : 1.41 g IPTG (isopropyl- β -D-thiogalactoside); add H₂O to 50 mL filter sterilize.

0.5M sodium phosphate buffer, pH 7.2 (stock):

(A) 69.0 g NaH₂PO₄· H₂O to 1 L with H₂O.

(B) 134.0 g Na₂HPO₄· 7H₂O to 1 L with H₂O.

Mix 117 mL (A) with 383 mL (B). The pH of this stock should be ~ 7.2.

Diluted to 10 mM in column buffer, the pH should be 7.0.

Lysis buffer (per liter) : 20 mL 0.5 M Na_2HPO_4 , 1.75 g NaCl, 10 mL 25% Tween 20,
0.7 mL β -mercaptoethanol, 20 mL 0.5 M EDTA (pH 8), and adjust to pH 7.0
with HCl or NaOH.

Column buffer (per liter) : 20 mL 0.5 M sodium phosphate (pH 7.2) , 29.2 g NaCl, 1
mL 1 M sodium azide, 0.7 mL β -mercaptoethanol, 2 mL 0.5 M EDTA (pH 8),
and adjust to pH 7.0 with HCl or NaOH.

2.1.4 Equipment

PCR machine :

Geneamp PCR 9700



Centrifuges :

1. Beckman, Allegra 21 Series
2. Eppendorf 5415D
3. Sorval RC 5C

Electrophoretic system:

1. Mighty Small II SE250/SE260 (protein)
2. Hoffer HE 33 (nuclic acid)

DNA sequence:

ABI PRISM model 377.

CMOS sensor chip detection system:

1. A radiation source : GaAlAs red (wavelength peak at 660 nm, full spectrum from 610 nm to 710 nm) light emitting diode (LTL-283CK, TAIWAN LITON ELECTRONIC CO.)
2. A polymeric biochip
3. CMOS sensor chip : designed and provided by Prof. Chung-Yu Wu and Yu-Chuan Shih of the Department of Electric Engineering, National Chiao Tung University, Taiwan. The sensor chip was a 100 x 100 photodiode array with single pixel size of 10 μm x 10 μm , designed with an N⁺/P well structure and manufactured using a standard 0.5 μm CMOS process.
4. Agilent 34401A multimeter
5. A personal computer

2.2 Experimental of Methods

2.2.1 Culture of bacterial strain

The bacterial strains used in this study are *Bacillus subtilis* CCRC 14199 obtain from the Culture collection and Research Center (CCRC), Food Industry Research and Development Institute (Hsinchu, Taiwan). *Bacillus subtilis* CCRC 14199 isolated from fruit soils (Hualien, Taiwan) by the Bergey's manual of systematic bacteriology are identified. Cultures were maintained on LB medium plate. For isolation of genomic DNA by *Bacillus subtilis*, overnight fresh cultures on LB medium plate were inoculated into LB medium broth.



2.2.2 Isolation of genomic DNA

1. According to the QIAamp Boold kit and QIAamp tissue kit handbook methods.
2. Take 1.5 mL culture cells and centrifuge at 7500 rpm for 10 min to precipitate the cells, then add 180 μ L ATL buffer into the cells, vortex until to the cells are mixed well.
3. Add 20 μ L Proteinase K and mix well, put at 55 $^{\circ}$ C for 1 h.
4. Add 20 μ L RNase A (20 mg/mL) and put at room temperature. for 2 min, and then add 200 μ L AL buffer and mix well, put at 70 $^{\circ}$ C for 10 min.
5. Add 210 μ L ethanol mix thoroughly, then put in 2 mL collection tube of QIAamp spin

- column, centrifuge at 8000 rpm for 1 min.
6. Open QIAamp spin column carefully and add 500 μ L AW buffer, centrifuge at 8000 rpm for 1 min.
 7. Add 500 μ L AW buffer again, centrifuge for 3 min.
 8. Add the distilled water which was preheat 70 $^{\circ}$ C, reaction at room temperature for 5 min and centrifuge for 1 min at full speed.

2.2.3 Polymerase chain reaction

Two oligonucleotide primers that spanned the uricase gene were designed as a 5'-premer (5'-TCT AGA ATT CCA TAT GTT CAC AAT GGA TGA CCT G-3') and a 3'-premer (5'-GCT GCA GAA GCT TCG CCG CTG GTT TGC CGC AGG -3'). The PCR amplification reaction was performed in final volume of 50 μ L containing 0.5 μ L Template DNA, 10 pmol of each primer, 200 μ M of each dNTP, 25 mM Mg(OAc)₂, 3.3x XL buffer and two unit of *rTth* polymerase (Applied Biosystems). The reaction involved an initial denaturation step at 94 $^{\circ}$ C for 1 min, and then adding the enzyme, followed by 30 cycles at 94 $^{\circ}$ C for 15 sec, 58 $^{\circ}$ C for 2 min, and 72 $^{\circ}$ C for 8 min and a final elongation step at 72 $^{\circ}$ C for 10 min.

2.2.4 Construction of recombinant DNA

PCR products were digested with *EcoRI/HindIII* and ligated to *EcoRI/HindIII* digested pMAL-c2 vector using a DNA ligation Kit, to transform *E.coli* DH5 α . The products were transferred into LB medium for incubation at 37 °C for 1 h with shaking. The culture was spread on LB plate with ampicillin for plasmid selection. X-gal and isopropylthio- β -D-galactoside (IPTG) were mixed and spread on LB plates for blue-white screening of recombiants.

2.2.5 Gene-spin™ Miniprep Purification Kit

1. Transfer an overnight 1-2 mL culture to a microcentrifuge tube. Spin down the cells for 30 sec ~ 1 min at maximum speed (12 ~ 14,000 rpm).
2. Add 200 μ L Solution I and pipette up and down (or vortex) until the cells are completely resuspended.
3. Add 200 μ L Solution II and mix by gently inverting the capped tube 5-6 times.
4. Add 200 μ L Solution III and mix by gently inverting the capped tube 5-6 times.
5. Centrifuge for 5 min at maximum speed (12 ~ 14,000 rpm). A compact white pellet will be formed along the side or at the bottom of the tube.
6. Insert the spin column into a collection tube, carefully remove the cleared lysate at step 5 directly to spin column, spin for 30 sec.

7. Remove the spin column from the collection tube, discard the filtrate and add 700 μL washing solution and spin for 1 min.
8. Discard the filtrate then centrifuge for 3 min at top speed to remove any residual trace of ethanol.
9. Remove the spin column and place the column in a new microcentrifuge tube. Add 50-100 μL H_2O or TE into the column. For plasmid larger than 7 kb, use preheated 60-70 μL H_2O or TE to elute.
10. Elute the DNA by centrifugation for 1min and store the eluted DNA at $-20\text{ }^\circ\text{C}$.

Repeat step 9-10 may give 10-15% more DNA, but DNA concentration will be diluted.

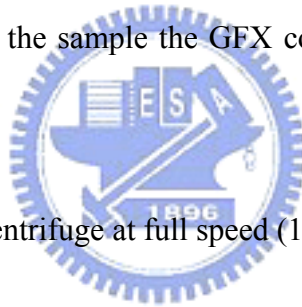


2.2.6 Purification of DNA from Gel Bands

1. Weigh an empty 1.5 mL microcentrifuge tube to the nearest 10 mg and record the weight.
2. Using a clean razor blade or scalpel, excise the slice of agarose containing the DNA band to be purified. Cut as close to the DNA band as possible. Cut the slice into several smaller pieces and transfer them to the pre-weighed 1.5 mL microcentrifuge tube.
3. Weigh the tube containing the agarose slice to the nearest 10 mg, and subtract the

weight of the empty tube to determine the weight of the slice.

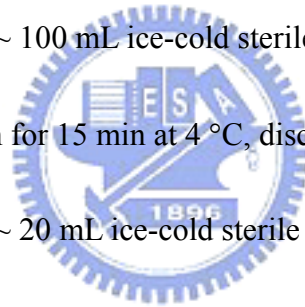
4. To the gel slice add 10 μL of capture buffer for each 10 mg of gel slice.
5. Close the tube and mix by vortexing vigorously. Incubate at 60 °C until the agarose is completely dissolved (5-15 min).
6. During the incubation, place one GFX column in collection tube for each purification to be performed.
7. After the agarose is completely dissolved, centrifuge briefly to collect the sample at the bottom of the tube.
8. Transfer the sample to the sample the GFX column. Incubate at room temperature for 1 min.
9. Centrifuge in a microcentrifuge at full speed (10,000 to 16,000 rpm) for 30 sec.
10. Discard the flow-through by emptying the collection tube. Place the GFX column back inside the collection tube.
11. Add 500 μL of wash buffer to the column. Centrifuge at full speed for 30 sec.
12. Discard the collection tube and transfer the GFX column to a fresh 1.5 mL microcentrifuge tube.
13. Apply 50 μL of elution buffer directly to the top of the glass fiber matrix in the GFX column.
14. Incubate the sample at room temperature for 1 min.



15. Centrifuge at full speed for 1 minute to recover the purified DNA.

2.2.7 Preparation of competent cells for electroporation

1. Inoculate single colony from LB-agar plate to 5 mL LB, incubate overnight at 37 °C
2. Transfer 5 mL overnight mixture to 500 mL SOB, incubate for 2-3 h at 37 °C ($A_{550} = 0.8$)
3. Transfer 500 mL mixture to 500 mL sterile centrifuge tubes
4. Centrifuge at 5000 rpm for 15 minutes at 4 °C, discard supernatant.
5. Resuspend pellet with ~ 100 mL ice-cold sterile water, and combine to one tube.
6. Centrifuge at 5000 rpm for 15 min at 4 °C, discard supernatant.
7. Resuspend pellet with ~ 20 mL ice-cold sterile water, and combine to one tube.
8. Centrifuge at 5000 rpm for 15 min at 4 °C, discard supernatant.
9. Rinse pellet with ~1 mL 10 % ice-cold glycerol.
10. Apply ~50 μ L cell solution to eppendorff, and store in - 80 °C



2.2.8 Transformation of *Escherichia coli* in electroporation

1. Mix 40 μ L competent cells and 1 μ L ligation mixture
2. Wash cuvette with ethanol, and applied the mixture to cuvette.
3. Locate cuvette into electroporation, pulse at 1.5 kV, 200 Ω , 25 μ F

4. Apply 1 ml LB to cuvette, pipetting and cycle to eppendorf
5. Incubate at 4 °C for 15 min.
6. Apply to LB/amp plate, incubate overnight at 37 °C

2.2.9 DNA sequencing

Using an ABI PRISM BigDye Terminator Cycle Sequencing Ready Reaction Kit, PCR reagents were mixed to a total volume of 20 μL including 2 μL RR Mix, 5 μL of the plasmid DNA recovered from the overnight culture colony, 1 μL of the primer, and 12 μL H_2O . PCR was performed 96 °C for 5 min and then 25 cycles 96 °C of 10 sec, 50 °C for 5 sec and 60 °C for 4 min were repeated, before holding at 72 °C for 10 min. After the PCR reactions were completed, the mixtures were transferred to a microfuge tube, and 64 μL 95% or absolute ethanol, and 16 μL H_2O were added. The solution was vortexed briefly and incubated in an ice bath for at least 15 min or stored overnight in a -20 °C box. It was centrifuged at 15000 rpm for 15 min at 4 °C, and then the supernatant was carefully decanted. Resuspended with 250 μL 70% ethanol and centrifuge under the same conditions. The supernatant was removed. The step of washing with 250 μL 70% ethanol was repeated and tube was vacuum dried for 5 min. 4 μL sequencing loading dye was added and the mixture vortexed for at least 90 sec and stored at -20 °C. Before being loaded into the sequencing gel, the sample was heated

at 95 °C for 2 min and then immediately placed on ice. A sequencing gel was mixed, by adding 10 mL 5x TBE stock solution to 40 mL acrylamide-urea gel solution and degas for 5 min, then 250 µL (TEMED) and 25 µL freshly made 10% ammonium persulfate (APS) (w/v) in H₂O were added just before the gel was cast, with care taken not to introduce air bubbles. The polymerization reaction of the gel took 4-5 h, and then the instructions for operating the ABI PRISM 377 DNA Sequencer were followed.

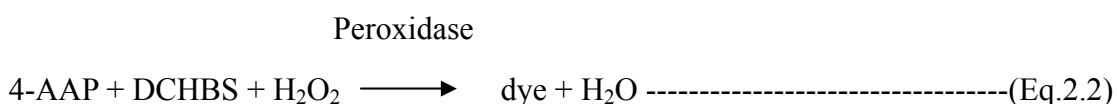
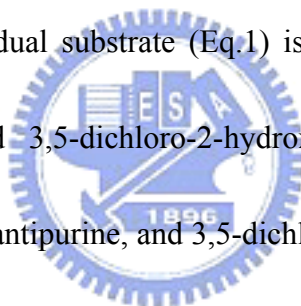
2.2.10 Staggered-extension process (StEP)

The primers that flanked 5'-primer and 3'-primer were used for recombination. The StEP condition contained 200 mM dNTPs, 15 µL of 3.3 x XL bufferII, 1.25 mM Mg(OAc)₂, 2 µg of 5'-primer and 3'-primer, 0.5 µL of plasmid DNA mixture and one unit of *rTth* DNA polymerase. The program was as followed: 95 °C for 5 minutes, 80 cycles of 30 sec for 94 °C and 56 °C. The amplified products were digested with *EcoRI* and *HindIII*, and then purified and ligated to pMAL-c2. The ligation mixture was then transformed into *E. coli* DH5α with electroporation. These colonies were selected by the way of colorimetric assay.

2.2.11 Modified colorimetric assay for screening of mutant gene

After each transformation for StEP uricase is completed, the coupled stage was

screened for activity from about 10 to 100 colonies on each plate. 50 μL of LB medium was put into each well of a 96-well microtiter plate. Single colonies were inoculated into this medium and incubated for 4 h at 37 $^{\circ}\text{C}$. The absorbance of blank was balanced using the same medium, and then 50 μL of substrate solution (0.1 mM uric acid, 0.1 U peroxidase, 4-aminoantipurine, and 3,5-dichloro-2-hydroxybenzene sulfonate dissolved in 50 mM borate buffer pH 8.5) was added to the well for further 5 min at 37 $^{\circ}\text{C}$. The result were obtained according to the known indicator reactions used in the assay of oxidases in the visible range. The H_2O_2 generated during the oxidation of the individual substrate (Eq.1) is visualized by a peroxidase-catalyzed 4-aminoantipurine, and 3,5-dichloro-2-hydroxybenzene sulfonate reaction which transforms the 4-aminoantipurine, and 3,5-dichloro-2-hydroxybenzene sulfonate into a dye (Eq2.2).



2.2.12 Purification of uricase

1. Inoculate 1 L rich broth + glucose and ampicillin with 10 mL of an overnight culture

- of cells containing the fusion plasmid.
2. Grow to 2×10^8 cells/mL ($A_{600} \sim 0.5$). Add IPTG to a final concentration of 0.3 mM, e.g. 85 mg or 3 mL of a 0.1 M stock in H₂O. Incubate the cells at 37 °C for 2 h.
 3. Harvest the cells by centrifugation at 4000 x g for 20 min and resuspend in 50 mL lysis buffer.
 4. Freeze sample in a dry ice-ethanol bath (or overnight at 20 ° C). Thaw in cold water.
 5. Sonicate: monitor cell breakage until it reaches a maximum (usually about 2 min).
 6. Add NaCl to 0.5 M. Centrifuge at 9000 x g for 30 min.
 7. Swell the amylose resin (1.5 g) for 30 min in 50 mL column buffer in a 250 mL filter flask. De-gas with an aspirator. Pour in a 2.5 x 10 cm column. Wash the column with 3 column volumes of the same buffer + 0.25% Tween 20.
 8. Dilute the crude extract 1:5 with column buffer + 0.25% Tween 20. Load the diluted crude extract.
 9. Wash with 3 column volumes column buffer + 0.25% Tween 20.
 10. Wash with 5 column volumes column buffer without Tween 20.
 11. Elute the fusion protein with column buffer + 10 mM maltose. Collect 5-10 1 mL fractions.

2.2.13 Quantitative assay of protein

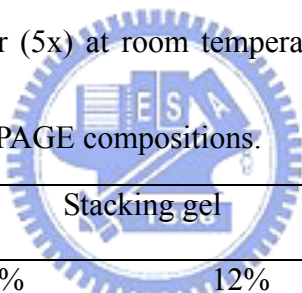
The protein content was determined using the dye binding methods of bicinchoninic

acid (BCA). This method combines the well-known reduction of Cu^{2+} to Cu^{1+} by protein in an alkaline medium with the highly sensitive and selective colorimetric detection of the cuprous cation using a unique reagent that contains bicinchoninic acid. A standard curve was constructed using BSA.

2.2.14 Electrophoresis

SDS-PAGE was performed essentially according to the method of Davis and Laemmli (1970) using a gel system (mightly Small II SE250). In SDS-PAGE, the sample was diluted in sample buffer (5x) at room temperature and a constant voltage of 150 V.

Table 2-1 lists the SDS-PAGE compositions.



Reagents	Stacking gel			Separation gel	
	4%	12%	12%	10%	
Acrylamide/Bis (mL)	1.2	2.4	3.5	14	13.32
Gel buffer B (mL)	-	-	2.5	10	10
Gel buffer C (mL)	1.25	2.5	-	-	-
SDS solution (μL)	100	200	100	400	400
Distilled water (mL)	7.4	14.8	2.94	11.76	12.44
TEMED solution (λ)	40			40	
10 % Ammonium persulphate solution (λ)	80			80	

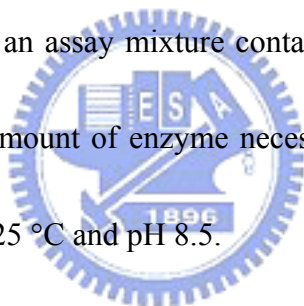
Table 2-1 Compositions of SDS-PAGE.

2.2.15 Coomassie blue staining

After electrophoresis, the gel was soaked in Coomassie Blue R 250 staining solution for 20 min. Then the gel was destained with destaining solution I and II until the stained band were distinct against a clear background.

2.2.16 Uricase activity

Uricase activity was routinely determined from the decline in absorbance at 293 nm caused by the aerobic enzymatic oxidation of uric acid. During enzyme purification, activity was measured in an assay mixture containing 0.1 M Tris buffer pH 8.5. One unit was defined as the amount of enzyme necessary to transform 1 μmol of uric acid into allantoin in 1 min at 25 °C and pH 8.5.



Chapter 3

Cloning and Expression the Gene Encoding Bacillus subtilis Uricase in Escherichia coli

3.1 Abstract

The uricase gene has been cloned from *Bacillus subtilis* CCRC 14199 isolated from soils of a papaya fruit farm (Hualien, Taiwan). DNA sequence analysis revealed an open reading frame of 1491 nucleotides encoding a protein of about 55 kDa. A MBP-uricase fusion protein of the expected size (98 kDa) was expressed. Uricase protein was found to exhibit high uricase activity (9.1 U/mg). The uricase was similar (61% identical) to the uricase from *Bacillus* sp. TB-90 and contained the conserved three cysteines, one of which is required for enzyme activity.

Keywords: *Bacillus subtilis* ; cloning; sequence; uricase; enzyme activity

3.2 Introduction

Uricase (urate oxidase, EC 1. 7. 3. 3.) is an enzyme involved in the purine degradation pathway where it catalyzes the oxidation breakdown of uric acid to allantoin. Uricase is present in various living organisms such as mammals (1, 2), plants (3), fungi (4, 5), yeasts (6,7,8), and bacteria (9). Uric acid, the primary end-product of purine metabolism, is present in biological fluids such as blood and urine (10). Increased uric acid levels are associated with a number of conditions including gout, chronic renal disease, some organic acidemias and Lesch-Nyhan syndrome (11).

Several attempts have been made to fabricate uric acid sensors using uricase as a biocatalyst (12-16). This enzyme is denoted here as uricase molecules, which catalyzes *in vivo* oxidation of uric acid in the presence of oxygen as an oxidizing agent, producing allantoin and CO₂ as oxidation products of uric acid hydrogen peroxide as reduction product of O₂ (Eq. 1).



Allantoin and its enzymatically reduced product, allantoic acid, account for 70-80% of the organic nitrogen in the xylem of nitrogen fixing soybean plants and other species of tropical grain legumes (17). Uric acid has been shown to rapidly adsorb onto carbon paste electrode surfaces (18-20): this phenomenon has led to the development of a controlled adsorption process for its selective determination in flowing streams.

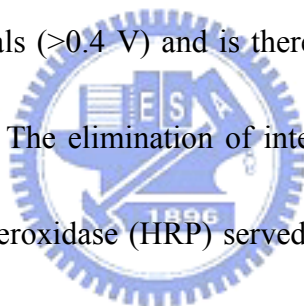
Ascorbic acid and uric acid are both present in biological fluids such as blood and urine.

Earlier electrochemical procedures based on the oxidation of uric acid at carbon-based electrodes in acidic solutions suffered from interference from ascorbic acid which can be oxidized at a potential close to that of uric acid (21).

The spectrophotometric method at 293 nm is often used as a comparison method when testing new detection methods. In Haeckel's method (22), the hydrogen peroxide produced by the uricase-catalyzed oxidation of uric acid is detected through the uricase-catalyzed oxidation of ethanol to acetaldehyde, coupled to the oxidation of the latter to acetate in the presence of NAD^+ (or NADP^+) and aldehyde dehydrogenase by measuring the change of absorbance of NADH (or NADPH) at 340 nm. An initial reading to be used as sample blank is needed, and this makes the method quite laborious as a manual procedure. In addition, highly purified aldehyde dehydrogenase is not always readily available.

Various types of electrochemical enzyme sensors have been reported for uric acid determination. The amperometric method for its quantitative determination in biological fluids based on the consumption of dissolved oxygen was reported by Nanjo and Guilbault (14). Janchen *et al.* carried out similar studies in the presence of oxygen (23). Coulometry, using a porous carbon felt electrode, has also been applied to its determination in human urine. The compound of interest was electrolysed with nearly 100% current efficiency at the carbon surface. Hydrogen peroxide however, is not electroactive at this surface (24).

As previously stated, uricase specifically catalyzes the oxidation of uric acid. The disappearance of oxygen or H_2O_2 , or the production of CO_2 may be exploited for uric acid sensing. In the first situation, dissolved O_2 may also be consumed by compounds such as ascorbic acid and thiol-containing substances (25). Moreover, ascorbate and thiols may also react with peroxide produced by the uricase-catalysed reaction of uric acid. Electrochemical enzyme sensors have been developed based on the amperometric determination of enzymatically liberated H_2O_2 from the uricase reaction. These systems exploit the anodic electroactivity of peroxide. Unfortunately, its oxidation has been reported to require relatively high applied potentials (>0.4 V) and is therefore susceptible to interferences from readily oxidizable molecules. The elimination of interferences was achieved by Kulys and colleagues when horseradish peroxidase (HRP) served as a catalyst for the reaction between H_2O_2 and hexacyanoferrate(II) followed by reduction of the resulting hexacyanoferrate(III) at 0V vs. Ag/AgCl (26). In this study, we describe cloning and DNA sequences of the uricase gene, and its successful expression in *Escherichia coli*.



3.3 Experimental

3.3.1 Cultures and media

The bacterial strain used in this study is *Bacillus subtilis* CCRC 14199 obtained from the Culture Collection and Research Center (CCRC), Food Industry Research and Development Institute (Hsinchu, Taiwan). *B. subtilis* CCRC 14199 was originally isolated from soils of papaya farmland (Hualien, Taiwan) and identified using criteria from Bergey's Manual of Systematic Bacteriology. Cultures were maintained on LB medium plate. For isolation of genomic DNA, overnight colonies on LB medium plate were inoculated into LB medium broth containing (g/L): tryptone 10.0, yeast extract 5.0, NaCl, 10.0. The culture was incubated at 37 °C for 18 h.



3.3.2 Isolation of genomic DNA for uricase

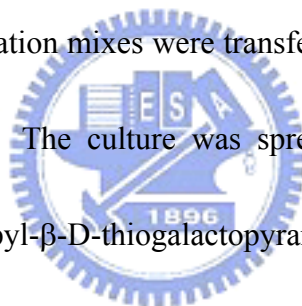
Genomic DNA extraction from *B. subtilis* was performed using a QIAamp Tissue Kit (Qiagen). Cells were grown in LB medium at 37 °C for 18 h with shaking, and processed according to the manufacturer's instruction. The purified DNA was resuspended in sterile water and stored at -20 °C.

3.3.3 Cloning of the uricase gene

Two oligonucleotide primers that flank the uricase gene were designed based on known *B.*

subtilis uricase sequences. The PCR amplification reaction was performed in final volume of 50 μ L containing 0.5 μ L Template DNA, 10 pmol of each primer, 200 μ M of each dNTP, 25 mM Mg(OAc)₂, 3.3 x XL buffer and two unit of *rTth* polymerase (Applied Biosystems). The reaction involved an initial denaturation step at 94 °C for 1 min, and then adding the enzyme, followed by 30 cycles at 94 °C for 15 sec, 58 °C for 2 min, and 72 °C for 8 min and a final elongation step at 72 °C for 10 min.

PCR products were digested with *EcoRI/HindIII* and ligated to *EcoRI/HindIII* digested pMAL-c2 vector or pBluescript IISK(+) using a DNA ligation Kit, and then transformed into *E. coli* DH5 α . The transformation mixes were transferred into LB medium for incubation at 37 °C for 1 h with shaking. The culture was spread on LB plates with ampicillin for selection and X-gal and isopropyl- β -D-thiogalactopyranoside (IPTG) for blue-white screening of recombinants.



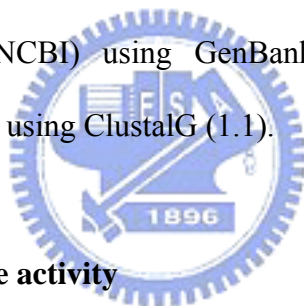
3.3.4 Expression and purification of the fusion uricase

The pMAL-c2 system (New England BioLabs) was used to express the uricase gene. Cells that contain plasmids that coded for fusion proteins under *lac* promoter control were grown to a concentration of 5×10^8 cell/mL at 37 °C with shaking in a rich medium with ampicillin. IPTG was then added to a final concentration of 0.3 mM, and the culture was grown for an additional 4 h. All subsequent steps were performed at 4 °C or on ice. The cells were harvested by low-speed centrifugation, resuspended in 1/10 vol. of 10 mM Tris buffer pH 7.2, and lysed by sonication. Cellular debris was then pelleted by high-speed centrifugation, and the supernatant was saved as crude cellular extract.

The fusion was purified as described by the manufacturer (20, 21) with some modification. The preparation of cross-linked amylose (New England BioLabs) and its use as an affinity chromatography matrix was as described by Kellerman and Ferenci (22). Fusion proteins were purified from crude extracts by binding to cross-linked amylose in a column, and were eluted with 10 mM Tris buffer that contained 10 mM maltose (20, 21).

3.3.5 DNA sequencing and computer analysis

The clones were sequenced using an ABI PRISM 310 auto-sequencer. Samples were prepared using a DNA Cycle Sequencing Kit and using a Big-Dye Terminator (Perkin Elmer). Appropriate oligonucleotides were used as primers. Computer analyses of DNA sequence data and the deduction of amino acid sequences were performed at the National Center for Biotechnology Information (NCBI) using GenBank databases and BLAST Programs. Protein sequences were aligned using ClustalG (1.1).



3.3.6 Measurements of uricase activity

Uricase activity was routinely measured aerobically from the decrease in absorbance at 293 nm due to the enzymatic oxidation of uric acid (5,6,8). During purification, the activity of the enzyme was measured in an assay mixture that contained 0.1 M Tris buffer (pH 8.5). One unit was defined as the amount of enzyme required to transform 1 μ mol of uric acid into allantoin in 1 min at 25 °C at pH 8.5.

3.4 Results

3.4.1 Cloning of the Uricase gene

The uricase gene from *B. subtilis* CCRC 14199 was cloned by PCR using primers designed to the uricase gene region of other *B. subtilis* strains. It was cloned as a 1.5 kB PCR product into either pMAL-c2 or pBluescript IISK(+) (Figure 3-1).

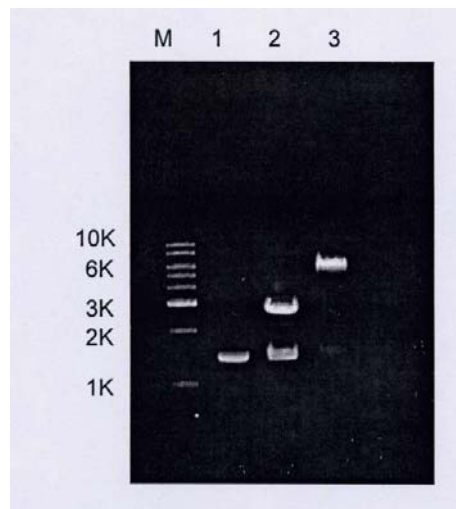


Figure 3-1. Agarose electrophoresis gel results of cloning. M, Molecular weight markers.

1, the uricase gene (1491 bp DNA fragments) was amplified by PCR. 2, DNA fragments were inserted into pBluescript IISK(+), and DNA fragments digested by *EcoRI/HindIII*. 3, DNA fragments were inserted into pMAL-c2, and DNA fragments digested by *EcoRI/HindIII*.

3.4.2 Expression and Purification of the uricase

To facilitate purification, a uricase-MBP fusion protein was created by cloning the entire uricase gene into the expression vector pMAL-c2. The fusion protein was expressed in *E. coli* DH5 α . Cells were lysed after IPTG induction and centrifuged. The uricase-MBP fusion protein was purified in single step, using amylose resin and eluted with 50 mM Tris buffer containing 10 mM maltose (24, 25). The uricase-MBP fusion protein had an apparent Mr of 98 kDa by SDS-polyacrylamide gel electrophoresis (Fig. 3-2)

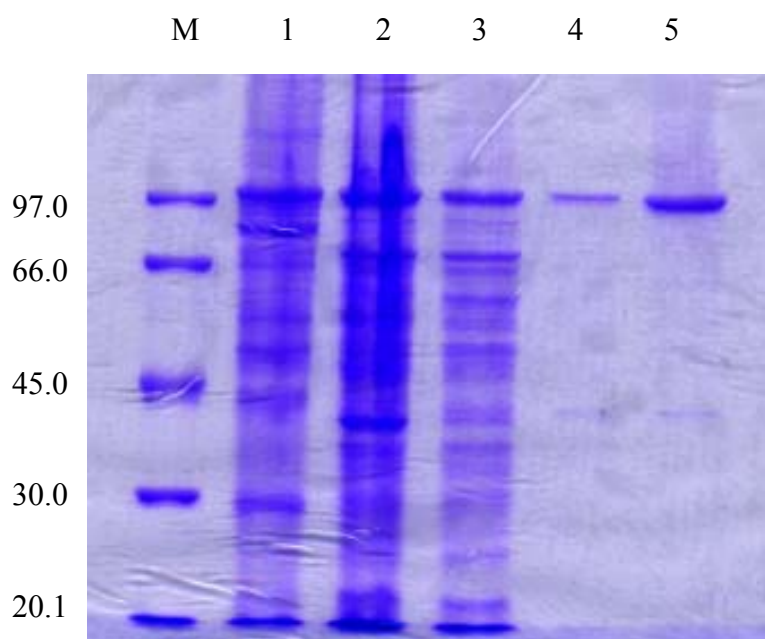


Figure 3-2. SDS-PAGE analysis of the uricase-MBP fusion protein produced in *E. coli*, and purified by amylose affinity spin column. M, marker; lane 1, pellet; lane 2, crude extract; lane 3, flowthrough; lane 4-5, eluate. The samples were loaded onto a 12% polyacrylamide gel. The fusion protein is approximately 98 kDa.

3.4.3 Nucleotide and amino acid sequence of uricase

The DNA sequence of the CCRC 14199 uricase gene was determined by sequencing the uricase sequence cloned into pMAL-c2. Sequence analysis revealed, as expected, a large ORF encoding a protein of 494 amino acids with a calculated MW of 55 kDa that corresponds to the uricase gene (Fig. 3-3).



```

male...TCGAGCTCGAACAAACAACAATAACAATAACAACAACCTCGGGATCGAGGGAAGGATTTCA
GAATTCATATGTTCCACAATGGATGACCTGAACCAAAGGACACACAAACACTCAGAGACACACTTGGCT 60
      M F T M D D L N Q R T H K H S Q T H L A 20
CTATTTTTGAACACTCTTCATGGATTGCGGAGACTCCGCAGCACTACGGCCGTTTTTCGTCCCTTTCTG 129
L F L N T L H G L R R D P Q H Y G R F R P F L 43
ATCTTCACCGCAAAATCACTGGCATTGTTAAAGCTGCGGATCGCGAGACACAGCTTGATTTTAAATCAA 198
I F T A K S L A L L K L R I A R H S L I L I K 66
AAGCATCCCCGGCTCGGAACAAAGAAAACAATCAGCGATGACTCGGTACGAGAGCAGCAGAACGCAGGG 267
K H P R L G T K K T I S D D S V R E Q Q N A G 89
CTCGGCAAATTCGAACAGCAGGAATACGAGGAGTTTTCTCATGCTCAATGAACACTATTATGATCGCTTC 336
L G K F E Q Q E Y E E F L M L N E H Y Y D R F 112
GGCTTTCCCTTTTATTTTCGCGGTTAAGGGAAGACGAAACAGGACATTACCAAGCCCTGTCGGCAAGG 405
G F P F I F A V K G K T K Q D I H Q A L L A R 135
CTTGAGAGCGAACGAGAAAACGGAGTTCAGCAGGCCCTTATAGAAAATTTACCGAATCGCCCGCTTTCGT 474
L E S E R E T E F Q Q A L I E I Y R I A R F R 158
CTGGCTGACATCATCACTGAAAAAGGAGAGACGCAAATTAAGAACCATGTCTTATGGCAAAGGAAAC 543
L A D I I T E K G E T Q I K R T M S Y G K G N 181
GTATTTGCATACCGAATTCATTTCAAACCGCTCACTGGAGTTAAGCAAATCCCGGAATCATCTTTTGCC 612
V F A Y R T Y F K P L T G V K Q I P E S S F A 204
GGAAGAGATAATACCGTTGTCGGCTTGATGTTACATGCGAAATTTGGCGGAGAAGCCTTCCTGCCATCA 681
G R D N T V V G V D V T C E I G G E A F L P S 227
TTTACAGACGAGACAACACTCTCGTCTGGCAACGGATTCAATTAATAACTTTATCCAGCGCCATCTC 750
F T D G D N T L V V A T D S I K N F I Q R H L 250
GCATCCTATGAAGGAACGACAACCGAGGGTTCCCTACACTATGTCGCTCACCGATTTTTCGATACCTAT 819
A S Y E G T T T E G F L H Y V A H R F F D T Y 273
TCTCATATGGACACGATCACTCTCACTGGCGAAGACATTCCGTTTGAAGCAATGCCTGCATACGAGGAG 888
S H M D C T I T L T G E D I P F E A M P A Y E E 296
AAAGAGCTCAGCACAAGCCGCTCGTCTTCAGAAGATCGCGTAATGAACGAAGCCGCTCTGTGTGAAA 957
K E L S T S R L V F R R S R N E R S R S V L K 319
GCAGAACGAAGCGGGAATACCATCACGATTACAGAGCAATACAGCGAAATCATGGATCTTCAGCTCGTC 1026
A E R S G N T I T I T E Q Y S E I M D L Q L V 342
AAGTTAGCGGCAACTCCTTCGTCGGCTTCATCCGGGACGAATATACGACTCTCCCGGAAGACGGCAAC 1095
K V S G N S F V G F I R D E Y T T L P E D G N 365
CGCCCGCTGTTTGTCTATTTTAAACATCAGCTGGCAATATGAAAATACAAATGACTCATACGCTTCTGAT 1164
R P L F V Y F N I S W Q Y E N T N D S Y A S D 388
CCAGCAGCTACGTTGCGGCTGAACAAGTCCGCGACTTTGCGGACACCCTTTTTCACGAGCTCGAAACC 1233
P A R Y V A A E Q V R D F A S T V F H E L E T 411
CCTTCAATCCAAAACCTCATCTATCATATCGGCTGCAGAATATTAGCGAGGTTCCCGCAGCTCACTGAT 1302
P S I Q N L I Y H I G C R I L A R F P Q L T D 434
GTCAGCTTCCAATCTCAAATCACACGTGGGATACGGTTGTCGAAGAAATCCCGGGCTCAAAGGAAAA 1371
V S F Q S Q N H T W D T V V E E I P G S K G K 457
GTCTACACCGAACCTGCGCCCGCCATACGGTTTCCAACATTTTACCGTGACAAGAGAAGACGCCGAGAA 1440
V Y T E P A P A I R F P T F Y R D K R R R R E 480
AGAAAAACAGAAAGCCGCTGAAAAATGTCGGAGCCTGAAAGCCTGATGGGAAAACCTGACAACCCATATT 1509
R K T E S R 486
TTAGATTTAACCTGCGGCAAACAGCGGCGAAGCTTCTGCAGCGGCACTGGCCGTCGTTTTACAACGTC 1545
GTGACTGGGAAAACCTGGCGTTACCCAACTTAATCGCCTTG

```

Figure 3-3. DNA sequence of the uricase gene. The deduced amino acid sequence is shown under the nucleotide sequence.

3.5 Discussion

We have cloned and sequenced the uricase gene from genomic DNA of *B. subtilis* strain CCRC 14199. It encodes a 55 kDa protein with 497 amino acids residues. The nucleotide sequence of the 1.5 kb *EcoRI-HindIII* DNA fragment, including the uricase, was determined (Fig. 3-1). Figure 3-2 shows SDS-PAGE analysis of the fusion uricase produced in *E. coli*, and the uricase protein purified with amylose affinity spin column.

The putative amino acid sequence of the *B. subtilis* uricase showed 61%, 49%, 20%, 16%, 16%, 14% and 11% identity with that of uricase from *Bacillus naldurans*, *Bacillus* spp., *Streptomyces coelicolori*, *Aspergillus flavus*, pig liver, mouse liver, and *Corynebacterium glutam*, respectively (Fig. 3-4). Two consensus regions in *Bacillus* sp. TB-90 uricase have been identified (9). These sequences, motif 1 and motif 2, were completely conserved in the sequence of the *Bacillus subtilis* uricase at positions 231-247 and 339-374, respectively.

Recombinant uricase was expressed as a fusion to maltose binding protein in pMAL-c2 in *E. coli* DH5 α . The recombinant uricase was present in the soluble fraction and was purified in a single amylose affinity step. The uricase activity was determined by the decrease in absorbance at 293 nm (Figure 3-5). The activity of the uricase produced in *E. coli* was 9.1 U/mg protein.

```

pig -----
mouse -----
A.flavus -----
B.subtilis -----MPMFTMDLNLQMDTQTLTDTLGSIFEHSSWIAER SAALRPFSSLSDLHRKMTGIVK-----
B.spp. MRKKKVFLSVLSAAA ILSTVALNPNPSAGDARTFDLDFKGIQTITDVSQSPKQRQTGAAAFVLESSENVKLLKGLLKKLETVPANNKLIHVQFNGPILLEET

pig -----
mouse -----
A.flavus -----
B.subtilis AADRETQLDLIKKHPRLGTTK TMSDDSVREQQNAGLGLKLEQQEYEEFLMLNEHYDRFGFPFILA VKGKTKQDIHQALLARLESERETEFQOALIEIY
B.spp. KQKLETTGAKILDYIPDYAYI VEYEGDVQSKVRSIEHVESVEPYLPKYKIDPQLFTKGASTLVKALALDTKQNNKEVQLRGLIEIAQYVANSNDVHYIT

pig ---QREMAHYRNDYKKNDEVEFVRTGYGKDMTKVLHIQR-----DGKYHSIKEVATSVQLTLSS-----KKDYLHGDNSDVIPTDTIKN
mouse ---SGKMAHYHDNYGKNDEVEFVRTGYGKDMTKVLHIQR-----DGKYHSIKEVATSVQLTLRS-----KKDYLHGDNSDVIPTDTIKN
A.flavus -----MSAVKAARYGKDNVRVYKVKHDE-----KTGVQTVYEMTVCVLLEGEI-----ETSYTKADNSVIVATDSIKN
B.subtilis RIARFRLADII TEKGETQMKRMTSYGKGNVFAVRTYLPK-----LTGVKQIPESSFAGRDNTVGVVDVTCIEGGEAFLPSEFDGDNLTLVVATDSMKN
B.spp. AKPEYKVMNDVARGIVKADVAQSSYGLYGGQIVAVADTGLDTGRNDSMHEAFRQKITALYALGRITNNANDTNGHGTHVAGSLGNGATNKGMAPQAN

pig TVNVLAKFKGIKSIETFAVTICEHFLSSFKHVIRAQVYVEEVPWKRFEKNGVKHVHAFIYTPGTGLAKFKGIKSIETFAVTICEHFLSSFKHVIRAQVYV
mouse TVHVLAKLRGIRNIETFAVNI CEHFLSSFNHVTRAHVYVEEVPWKRFEKNGIKHVHAFIHTPTGLAKLRGIRNIETFAVNI CEHFLSSFNHVTRAHVYV
A.flavus TIIYITAKQNPVTPPELFGSILGTIIFIEKYNIHIAAIVNI VCIIRWTRMDIDGKPIPIHSFIRDSEETAKQNPVTPPELFGSILGTIIFIEKYNIHIAAIVNI
B.subtilis FIQRHLASVEGTTTEGFLHYVAHRFLDYSHMDTITLTGEDIPFEAMPAYEKEKELSTSRLVFRRLASVEGTTTEGFLHYVAHRFLDYSHMDTITLTG
B.spp. LVFQSIMDSSCG-LGGLPSNLQTLFSQAFSAGARITHNSWGAANGAYTTDSRNVDYVRKNDMSIMDSSCG-LGGLPSNLQTLFSQAFSAGARITHNS

pig EEVWPKRFEKNGVKHVHAFIYTPGTGTHFCEVEQIRNGP-----PVIHSGIKDLKVLKTTQSGFEG--FIKDQFTTLPEVKDRCFATQVYCKWRYHQ
mouse EEVWPKRFEKNGIKHVHAFIHTPTGTHFCEVEQMRNGP-----PVIHSGIKDLKVLKTTQSGFEG--FLKDQFTTLPEVKDRCFATQVYCKWRYOR
A.flavus VCIIRWTRMDIDGKPIPIHSFIRDSEKRNQVDVVEGKG-----IDIKSSLSGLTVLKSTNSQFVG--FLRDEYTTLKETWDRILSTDVDTQWQKN
B.subtilis EDIPFEAMPAYEKEKELSTSRLVFRSRNERSRSLKAERSGNTITITEQYSEIMDLQLVKVSNGSFGV--FIRDEYTTLPEDGNRPLFVYVNI SWQYEN
B.spp. WGAANGAYTTDSRNVDYVRKNDMTILFAAGNERPNQGTISAPGTAKNAITVGATENLRPSFGSYADNINHVAQFSSRCPTKDRIKPDVMAPGTIIL

pig G-----RDVDFEATWDTVRSIVLQKFAGPYDKGEYSP
mouse -----RDVDFEATWGAVRDVLQKFAGPYDKGEYSP
A.flavus FSGLQEVRS-----HVPKFDATWATAREVTLKTFAE--DNSASV
B.subtilis TN-----DSYASDPARYAAEQVRDLASTVFHELETP
B.spp. SARSSLAPDSSFWANIDSKYAYMGGTSMATPIVAGNVAQLREIFVKNRGI TPKPSLLKAALJAGAADVGLGYPNGQGVQVRLTDKSLNVAVYVNESSAL

pig SVQKTLYDIQVLTGQVPEIEDMEISLPNIHYFNIDMSKMGLINKE---EVLPLDNPYGRITGTVKR-KLTSRLCYG-----
mouse SVQKTLYDIQVLSLQVPEIEDMEISLPNIHYFNIDMSKMGLINKE---EVLPLDNPYGRITGTVKR-KLPSRLRHG-----
A.flavus QATMETYKMAEQILARQQLIETVEYSLPNKIHYFIDLSEWIKGLQNTGKNAEVFAQSDPNGLIKCTVGRSSLSKSL-----
B.subtilis SIQNLIIYHIGCRI LARFQPLTDVFSQSQ-NHTWDTVVEEIPGSKGK---VYTEPRPPYGFQHFVITREDAEKEKQAAEKCRSLKA-----
B.spp. STSQKATYFTATAGKPLKISLVWSDAPASTTASVTLVNDLVLITAPNGTRIVGNDFSAPFDNNWDRNNVENVFINSQSGTYITIEVQAYNVVPGPQ

pig -----
mouse -----
A.flavus -----
B.subtilis -----
B.spp. GNFSLATVN

```

Figure 3-4. Comparison of deduced amino acid sequence of the uricase with other uricases.

B. subtilis -----
 B. spp. -----
 B. halodurans -----
 Streptomyces -----
 Corynebacterium MDKPHIEDEGTTTNAVTTSTTTTRVKHPVDQVPPAPKLAALGLQHVLAFYAGAVIPLLLIAQSLNLDATTIHLINADLLTCGIATLIQSVGIGRHI GVRLP I

B. subtilis MPMFTMDDL NQMDTQTLTDITLGSIFEHSSWIAERSAALRPFSSLSDLHRKMTGI VKAADRETQLDLIKKHPRLCTKKTMSDDSVREQQNAQLGKLEQQEYEE
 B. spp. -----
 B. halodurans -----
 Streptomyces -----
 Corynebacterium VQGVTTTAVAPI IAIGLVTDGQGGVASLPAIYGAVIVSGI FTFFAAPVFARFLKFFPPVVTGTVLLVMGASLLSVSANDFVNYADGVAARDLAYGFGTLA

B. subtilis FLMLNEHYDRFGFPFILAVKGTKQDIHQALLARLESERETEFQQALIEIYRIARFRLADIITEKGETQMKRTMSYKGNVFAVRTYLYKPLTGKQIPESS
 B. spp. -----
 B. halodurans -----
 strept -MVKDVKVQKTEKRTMYCKGDFVVRTNASPLEGIIKAIPESS
 Corynebacterium VIILAQRFFRFGMTLAVLIGLVGTAVALILGDANLDEVGNAAEAFDITPFFYGVPEFNAVAIFSMIIVMIITMVETTGDFVATGEIVGKRTRRSVDVTRAL

B. subtilis FAGRDNTVVG-----VDVTCEIGGEAFLPSFTDGNLTVVATDSMKNFIQRHLASYEG-----TTTEGFLHYVAHRFLDTY
 B. spp. FSGRDHILFG-----VNVKISVGGTKLLTSFTKGNLSLVVATDSMKNFIQRHLASYEG-----TTTEGFLHYVATSFLLKYY
 B. halodurans FSGRKNVILG-----MDLKVALKGD AFLSSFTDGNLSLVIATDSMKNFILRKAAPFNG-----STMEDFLQFISKEFLNTY
 Streptomyces FNTLEETAAL-----AELHEACAATAWAR-----HLLAARPF-----ATAEDLYAASDAAMAELS
 Corynebacterium RADGLSTLMCGVMNSFPYTCFAQNVGLVRI TGVKSRWVAAAAAGFMIILGVLPKAGI VASIPSPVLGGASLALFANVAWVG I QTI AKSDLADSRNSVIVTS

B. subtilis SHMDTITLTGEDIPFEAMPAYEELKELSTSRVFRRSRNRSRSVLKAERS-GNTITITEQYSEIMDLQLVKVSNSFVGFIRDEYT--TLPEDGNRPLFVYL
 B. spp. SHIEKISLIGEEIPFETTFAVKNGNRAASELVFKKSRNEYATAYLNMVRNEDNTLNI TEQQSGLAGLQLIKVSNSFVGFIRDEYT--TLPEDSNRPLFVYL
 B. halodurans SHISSVSLSGDQLLEHEVPI PSTSGFOTSDLLFQQEES-VKPFKVEVRRMDTEYKVMQLSGIQGLRLIKVKESSFYGYIQDEYT--TLPEAYDRPLFVYL
 Streptomyces AEDLAEAMACHPPIGRPKPGDATSSRE-----QAGMACAAEELKAEMLELN--LAYQDKFCHVFLIC
 Corynebacterium ALGLAMLVSRPDAVAQAFPEWARIFVSSGMSVGAITAILLNLFFHVGRQSGGQVATSKSGERINLDAVNKMDRTDFVETFAPLFNSKTWPLETAWESQPPFA

B. subtilis NISWQYENTNDSYASDPARYVAEQVRDLASTVFHELETSPSQNLIYHIG-----CRILARFPQLTDVSFQSQNHITWDTVVEEIPGSK
 B. spp. NIKWKYKNTEDSFGTNPENYVAEQIRDIATSVFHETETLSIQHLIYLIG-----RRILERFPQLQEVYFESQNHITWDKIVEEIPESK
 B. halodurans NMFWAYENPEDATGIKPDRYVSAEQVAAIAYTVFHEMNCPISIQNLLYQIG-----LRVLMRFPQLVEISFESNRTWETVVEEAKDER
 Streptomyces ATGRIG-----EQMRDAALERIGNSPEQEREIVRTELG-----KINRIRLRLVEQDARP-----
 Corynebacterium NVTELREAIQVAVLTAPLSDREELIHDYDPAQLILATEEBAATI SQDRGSI GLDDLDDVDQEKLI TVTEQYRERFNMPYVAYFDTMDSVDTVVAAGLRRLD

B. subtilis G-KVYTEPRPPYGFQHFVTVREDAEKEKQAAEKCRSLKA-----
 B. spp. G-KVYTEPRPPYGFQCFVTQEDLPHENILMFSDEPDHKGALK----
 B. halodurans GGKVYTEPRPPYGFQCFSMTREDLLAAERAEK-----
 Streptomyces -----
 Corynebacterium NSDEQHRQALSEIIEIANDRFDILLADANPARSAFDRKFTETDFLG

Figure 3-4. Comparison of deduced amino acid sequence of the uricase with other uricases.

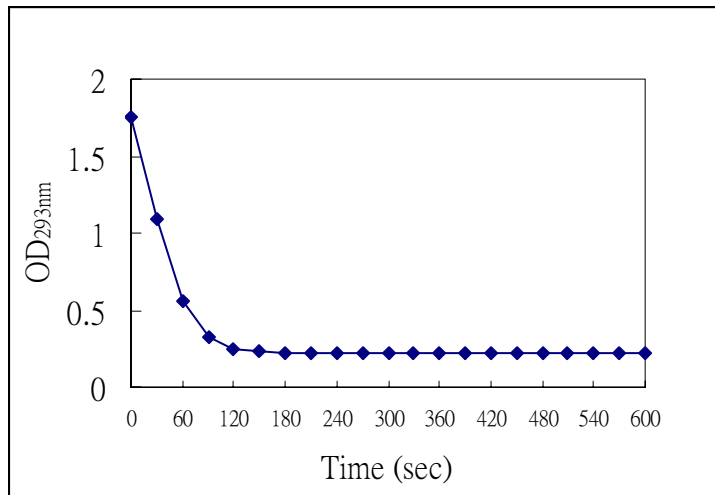


Figure 3-5. Uricase-MBP fusion activity. The curves show uricase activity as the change in optical density (OD) with time (0.05 M borate buffer containing 0.1 mM uric acid, pH 8.5).



3.6 References

1. Keilin, J. (1959) The biological significance of uric acid and guanine excretion. *Biol. Rev.* 34, 265-296.
2. Wallrath, L. L. and Friedman, T. B. (1991) Species differences in the temporal pattern of drosophila urate oxidase gene expression are attributed to trans-acting regulatory changes. *Proc. Natl. Acad. Sci. U.S.A.* 88, 5489-5493.
3. Montalbini, P., Redondo, J., Caballero, J. L., Cárdenas, J. and Pineda, M. (1997) Uricase from leaves: its purification and characterization from three different higher plants. *Planta.* 202, 277-283.
4. Nahm, B. and Marzluf, G. A., (1987) Induction and de Novo synthesis of uricase, a nitrogen-regulated enzyme in *Neurospora crassa*. *J. bacteriol.* 169, 1943-1048.
5. Montalbini, P., Aguilar, M. and Pineda, M. (1999) Isolation and characterization of uricase from bean leaves and its comparison with uredospore enzyme. *Plant Science* 147, 139-147.
6. Yuichi, H., Tetsuhiko, S. and Hajime, I. (2000) Cloning, sequence analysis and expression in *Escherichia coli* of the gene encoding a uricase from the yeast-like symbiont of the brown planthopper, *Nilaparvata lugens*. *Insect Biochemistry and Molecular Biology* 30, 173-182.
7. Koyama, Y., Ichikawa, T. and Nakano, E. (1996) Cloning, sequence analysis and expression in *Escherichia coli* of the gene encoding the *candida utilis* urate oxidase. *J. Biochem.* 120,

969-973.

8. Adamek, V., Suchova, M., Demnerova, K., Kralova, B., Fort, I. and Morava, P. (1990)
Fermentation of *candida utilis* for uricase production. *J. Indu. Microbiol.* 6, 85-90.
9. Yamamoto, K., Kojima, Y., Kikuchi, T., Shigyo, T., Sugihara, K. and Takashio, M. (1996)
Nucleotide sequence of the uricase gene from *Bacillus* sp. TB-90. *J. Biochem.* 119, 80-84.
10. Eswara, U. S., Dutt, H. and Mottola, A. (1974) Determination of uric acid at the
microgram level by a kinetic procedure based on a pseudo-induction period. *Anal. Chem.*
46, 1777-1781.
11. Burtic, C.A. and Ashwood, E. R. (1994) Teitz textbook of clinical chemistry, 2nd ed.
Philaclelphia: WB saunders company.
12. Yutaka, A., Hiroshi, I., Hiroomi, N., Tsugutoshi, A. and Mitsutatk, Y. (1992) Effects of
serum bilirubin on determination of uric acid by the uricase-peroxidase coupled reaction.
Clin. Chem. 38, 1350-1352.
13. Bhargava, A. K., Lal, H. and Pundir, C. S. (1999) Discrete analysis of serum uric acid
with immobilized uricase and peroxidase, *J. Biochem. Biophys. Methods* 39, 125-136.
14. Nanjo, M. and Guilbault, G. G. (1974) Enzyme electrode sensing oxygen for uric acid in
serum and urine. *Anal. Chem.* 46, 1769-1772.
15. Uchiyama, S., Shimizu, H. and Hasebe, Y. (1991) Chemical amplification of uric acid
sensor responses by dithiothreitol. *Anal. Chem.* 66, 1873-1876.

16. Miland, E., Ordieres, A. J. M., Blanco, P. T. and Smyth, C. Ó. (1996) Poly (o-aminophenol)-modified bienzyme carbon paste electrode for the detection of uric acid, *Talanta* 43, 785-796.
17. Reynolds, P. H. S., Boland, M. J., Blevins, D. G., Randall, D. P. and Schubert, K. R. (1982) Ureide biogenesis in leguminous plants. *Trends Biochem. Sci.* 7, 366-368.
18. Gonzalez, E. (1991) Amperometric sensor for hypoxanthine and xanthine based on the detection of uric acid. *Anal. Chim. Acta.* 242, 267-272.
19. Markas, T., Gilmartin, J. and Hart, P. (1994) Novel reagentless, amperometric biosensor for uric acid based on a chemically modified screen-printed carbon electrode coated with cellulose acetate and uricase. *Analyst.* 119, 833-840.
20. Cai, X., Kalcher, K., Neuhold, C. and Ogorevc, B. (1994) An improved voltammetric method for the determination of trace amounts of uric acid with electrochemically pretreated carbon paste electrodes. *Talanta* 41, 407-412.
21. Shukla, M. K. and Mishra, P. C. (1996) electronic structures and spectra of two antioxidants uric acid and ascorbic acid. *J. Mol. Struct.* 377, 247-259.
22. Haeckel, R. (1976) The use of aldehyde dehydrogenase to determine H₂O₂-producing reaction: The determination of the uric acid concentration. *J. Clin. Chem. Clin. Biochem.* 14, 101-106.
23. Janchen, M., Walzel, G., Neef, B., Wolf, B., Scheller, F. and Kuhn, M., (1983). Uric acid

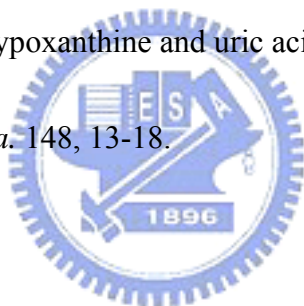
determination in dilute serum with an enzyme electrochemical and enzyme-free sensor.

Biomed. Biochim. Acta 9,1055-1059.

24. Uchiyama. S., Obokata. T. and Suzuki. S. (1990) Flow-coulometric detector for uric acid in human urine. *Anal. Chim. Acta.* 230, 195-198.

25. Gilmartin, M. A. T., Haetand, J. P. and Birch, B. J. (1994) Development of amperometric biosensor for uric acid based on chemically modified graphite poxyresin and screen-printed electrode containing cobalt phthalocyanine. *Analyst* 119, 243-252.

26. Kulys, J. J., Laurinavicius, V. S. A., Pesliakiene, M. V. and Gureviciene, U. V. (1983) The determination of glucose, hypoxanthine and uric acid with use of bi-enzyme amperometric electrodes. *Anal. Chim. Acta.* 148, 13-18.



Chapter 4

Detection of Serum Uric Acid Using the Optical Polymeric Enzyme Biochip System

4.1 Abstract

An optical polymeric biochip system based on the Complementary Metal Oxide Semiconductor (CMOS) photo array sensor and polymeric enzyme biochip for rapidly quantitating uric acid in a one-step procedure was developed. The CMOS sensor was designed with N⁺/P-well structure and manufactured using a standard 0.5 μm CMOS process. The polymeric enzyme biochip was immobilized with uricase-peroxidase and used to fill the reacting medium with the sample. This study encompasses the cloning of the *Bacillus subtilis* uricase gene and expression in *Escherichia coli*, as well as the purification of uricase and measurement of its activity. The cloned uricase gene included an open reading frame of 1491 nucleotides that encodes a protein of approximately 55 kDa. The expression of the putative MBP-fusion protein involved approximately 98 kDa of the protein. The CMOS sensor response was stronger at a higher temperature range of 20-40 °C, with optimal pH at 8.5. The calibration curve of purified uric acid was linear in the concentration range from 2.5 to 12.5 mg/dL. The results obtained for serum uric acid correlated quite closely with those obtained using the Beckman Synchron method.

Keywords: CMOS photo array sensor, polymeric enzyme biochip, uricase, peroxidase

4.2 Introduction

Uricase is an enzyme that participates in degrading purines by catalyzing the oxidative breakdown of uric acid to allantoin. This highly conserved enzyme is found in mammals (1,2), plants (3), fungi (4), yeasts (5, 6, 7), and bacteria (8). Uric acid, the primary end-product of purine metabolism, is present in biological fluids, such as blood and urine (9). Various disease states increase the amount of uric acid in biological fluids. Such conditions cause gout, chronic renal disease, some organic acidemias, and Lesch-Nyhan syndrome (10).

Several attempts have been made to fabricate uric acid sensors, using uricase (urate oxidase, EC 1. 7. 3. 3.) as a biocatalyst (11-15). Uricase catalyzes the *in vivo* oxidation of uric acid in the presence of oxygen to produce allantoin and CO₂ as oxidation products of uric acid, and hydrogen peroxide as a reduction product of O₂. Uricases from many microorganisms are used as diagnostic reagents for detection of uric acid. These enzymes exhibit high thermostability and are active over a wide pH range (5, 6, 8, 16). For example, the uricase of *Bacillus* sp. TB-90 demonstrated high activity and thermostability over a wide range of pH values.

Spectrophotometry at 293 nm is frequently used to detect the concentration of uric acid in solution. In Haeckel's method (17), the hydrogen peroxide produced by the uricase-catalyzed oxidation of uric acid is detected by the uricase-catalyzed oxidation of ethanol to acetaldehyde, coupled with the oxidation of the latter to acetate in the presence of NAD⁺ (or NADP⁺) and aldehyde dehydrogenase. The change in the absorbance of NADH (or NADPH) at 340 nm then is measured. An initial reading, to be used as a sample blank, must be taken. This method is a laborious and manual procedure. Furthermore, highly purified aldehyde dehydrogenase is not always readily available.

Various types of electrochemical enzyme sensors have been reported to be useful in uric acid determination. Nanjo and Guilbault developed an amperometric means of determining

the quantity of uric acid in biological fluids. This method is based on the consumption of dissolved oxygen (13). Janchen *et al.* performed similar studies in the presence of oxygen (18). Such systems exploit the anodic electroactivity of peroxide. Unfortunately, its oxidation has been reported to require relatively high applied potentials (>0.4 V), and thus, is susceptible to interference from readily oxidizable molecules. Kulys and colleagues eliminated interference using horseradish peroxidase (HRP) to catalyze the reaction between H_2O_2 and hexacyanoferrate (II) and the reduction of the resulting hexacyanoferrate (III) at 0 V versus Ag/AgCl (16).

This chapter describes the development of a polymeric enzyme biochip with a CMOS photosensor detection system to quantitate uric acid. In this chapter, a prototype CMOS array photosensor was designed and produced. To detect uric acid, a uricase-peroxidase-immobilized polymeric biochip was developed. The uricase gene of *Bacillus subtilis* was cloned, expressed in *Escherichia coli*, then the uricase was purified, and activity measured. Moreover, the polymeric biochip was immobilized simultaneously with uricase and peroxidase. Finally, we compare the measurements from 20 patients' serum uric acid samples using the CMOS biochip system to the Beckman Synchron analyzer.

4.3 Experimental

4.3.1 Optical detection system setup

Figure 4-1 schematically depicts the optical arrangement of the enzyme biochip detection system built to detect serum uric acid using a polymeric enzyme biochip. To eliminate infrared light, a white light LED lamp (HB5-439AWCA, Russia) was used as the light source and the light intensity was controlled with an adjustable driver. The LED projects a light beam vertically through a mini-lens to generate a 1mm diameter parallel light beam. The light beam passes through an interference filter wheel (a 520 nm interference filter, K43-069, Edmund, USA), then the self-developed polymeric biochip, and finally hits the surface of the prototypical CMOS photo array sensor. The polymeric biochip was immobilized with uricase-peroxidase and used to fill the reacting medium with the sample, the details of which are described below. The biochip is transparent so that the light could be transmitted to the sensor. The CMOS photo array sensor was designed with an N⁺/P-well structure and manufactured using a standard 0.5 μm CMOS process. To transfer the current signal of the CMOS photo sensor linearly to the voltage signal, a bias resistor (R_b) was connected between a 3 volts DC bias voltage source and the cathode (K) of the CMOS photosensor. A loading resistor (R_L) was connected between the anode (A) of the CMOS photo sensor and the ground of the bias voltage source. Then, the signal from the anode was used as the output voltage and connected to the positive probe of multi-meter (Agilent 34401A). The ground of the bias voltage source was connected to the negative probe of a multi-meter. The voltage signals were digitized and transferred as digital data to a personal computer with GPIB communication using a simple data collection program. The collected data were analyzed using Windows Excel that calculated the absorbance at 520 nm according to Beer-Lambert's law, *i.e.* $OD_{520nm} = -\log(I / I_0)$, where I is final reaction light signal, I₀ is blank light signal.

The results then were plotted graphically.

Figure 4-2 shows a pixel structure and circuit diagram of the CMOS photo array sensor. Each pixel of the array sensor was implemented with a P-N junction diode using a P-well and N⁺-active diffusion layer that could be fabricated using the 0.5 μm CMOS process. The array-sensor was a 240 pixels x 140 pixels in-parallel connection, as shown in Figure 4-3(a), with a single pixel size of 7.5 μm x 7.5 μm , as shown in Figure 4-3(b).



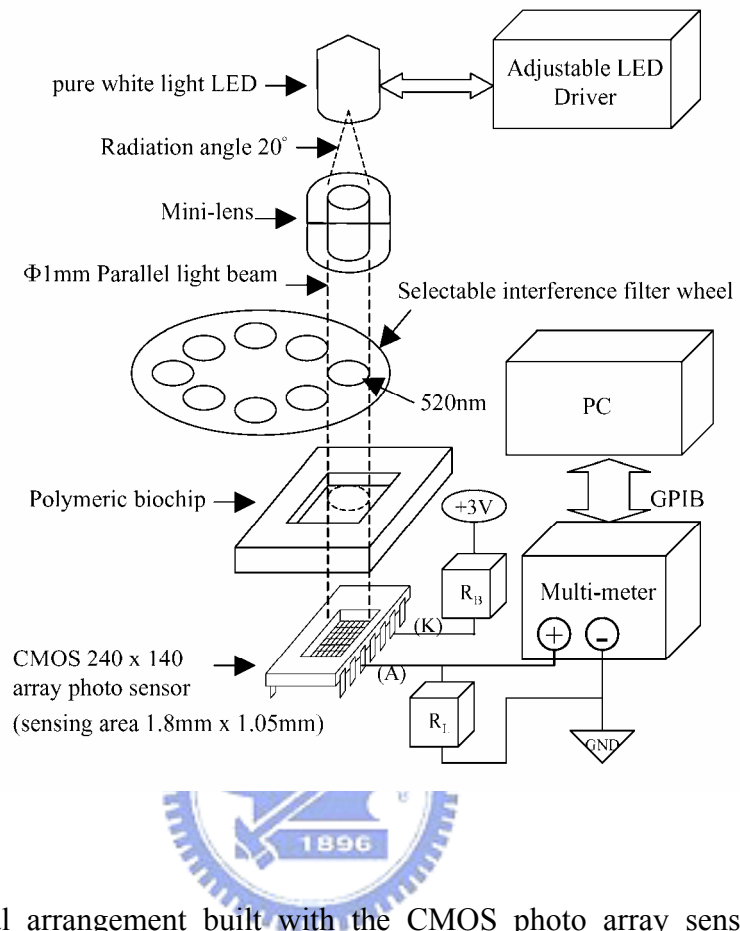


Figure 4-1. Optical arrangement built with the CMOS photo array sensor and used for polymeric enzyme biochip detection (see the text for details).

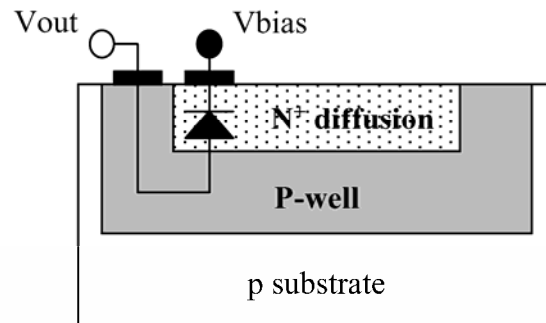
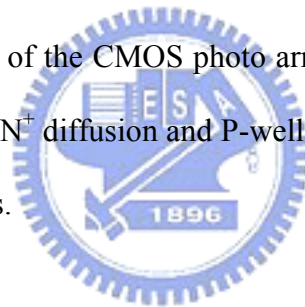


Figure 4-2. The pixel structure of the CMOS photo array sensor. The P-N junction diode is implemented with N⁺ diffusion and P-well and manufactured using a standard 0.5 μm CMOS process.



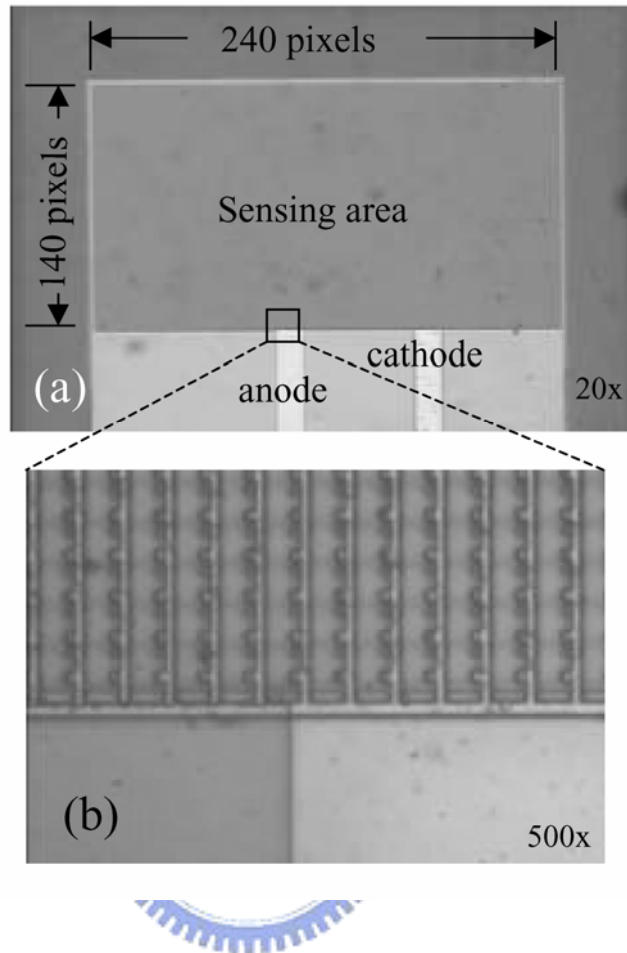


Figure 4-3. CMOS photodiode array sensor. (a) The layout of the 240 x 140 CMOS photo array sensor which occupies an area of 1.8 mm x 1.05 mm. (b) The close up microphotograph of the fabricated CMOS photo array sensor showing few pixels. Each pixel is $7.5 \mu\text{m} \times 7.5 \mu\text{m}$ in area.

4.3.2 DNA manipulations

Cloning and transformation were performed essentially as described by Sambrook and Russell (19). Genomic DNA from *Bacillus subtilis* CCRC 14199 was obtained from the Culture Collection and Research Center (Food Industry Research and Development Institute, Hsin-Chu, Taiwan). *Bacillus subtilis* uricase expression constructs were generated in a polymerase chain reaction (PCR). Briefly, the *Bacillus subtilis* uricase gene was amplified using the plasmid DNA of *Bacillus subtilis* (CCRC 14199) as a template, *rTth* DNA polymerase (Applied Biosystems) and the following primers: 5'-primer (5'-TCT AGA ATT CCA TAT GTT CAC AAT GGA TGA CCT G-3') and 3'-primer (5'-GCT GCA GAA GCT TCG CCG CTG GTT TGC CGC AGG -3'). The amplification reaction was performed in a total volume of 50 μ L: 0.5 μ L template DNA; 10 pmol of each primer; 0.2 mM dNTPs (dATP, dGTP, dTTP, dCTP); 1.5 mM Mg(OAc)₂; 1U of *rTth* polymerase; and 3.3x XL *rTth* polymerase buffer. PCR amplification was conducted in a thermal cycler (GeneAmp PCR System 9700) with an initial denaturation for 1 min at 94 °C, followed by 30 cycles (94 °C, 15 sec; 58 °C, 2 min; 72 °C, 8 min), and a final incubation for 10 min at 72 °C. The amplified products were digested with *Eco*RI and *Hind*III and cloned into the *Eco*RI-*Hind*III pMAL (or pBluescript II SK(+)), transformed into *E. coli* DH5 α competent cells and incubated at 37 °C for 1 h with shaking. The culture was spread on LB plates containing ampicillin for antibiotic selection. X-gal and isopropylthio- β -D-galactoside (IPTG) were mixed and spread on LB plates for blue-white screening of recombinants.

4.3.3 Expression and purification of the fusion uricase

For protein expression, the pMAL-c2 system (BioLabs) was used to express the uricase gene. Cells that contain plasmids encoding fusion proteins under control of the lac promoter were grown to a concentration of 5×10^8 cell/mL at 37 °C with shaking in a rich medium.

IPTG was added to a final concentration of 0.3 mM, and the culture was grown for an additional 4 h. All subsequent steps were performed at 4 °C or on ice. The cells were harvested by low-speed centrifugation, resuspended in 1/10 vol. of 10 mM Tris buffer pH 7.2, and lysed by sonication. Cellular debris then was pelleted by high-speed centrifugation, and the supernatant was saved as a crude cellular extract.

The purification procedure was adopted from the pMAL-c2 protein fusion and purification system (20, 21). The preparation of cross-linked amylose (BioLabs) and its use as an affinity chromatography matrix were as described by Kellerman and Ferenci (22). Fusion proteins were purified from crude extracts by binding to cross-linked amylose in a column, and were eluted with 10 mM Tris buffer that contained 10 mM maltose (20, 21).

4.3.4 Measurements of uricase activity

Uricase activity was routinely measured aerobically by the decrease in absorbance at 293 nm due to the enzymatic oxidation of uric acid (6, 8, 11). The assay mixture contained 0.1 mM uric acid in 50 mM borate buffer (pH 8.5), and 10 μ L of enzyme solution. One unit was defined as the amount of enzyme necessary to transform 1 μ mol of uric acid into allantoin in 1 min at 25 °C and pH 8.5.

4.3.5 Preparation of the uricase-peroxidase conjugate

The protocol for preparation of uricase-peroxidase was modified from Tresca *et al.*, (23). Briefly, 1 mg of peroxidase in 0.2 mL of 1M phosphate buffer at pH 6.8 was made to react with 0.25 ml of freshly prepared 0.1 M sodium periodate for 20 min, and the peroxidase reagent was removed by dialysis against 1 mM sodium acetate buffer at pH 4.6. Brown peroxidase-containing fractions were pooled and the uricase reagent was removed by dialysis against 0.1 M sodium carbonate buffer at pH 9.2. Finally, the reaction medium was mixed

with 0.2 mL of 4 mg/mL sodium borohydride and left for 2h. It then was dialyzed against 10 mM phosphate buffer at pH 7.4.

4.3.6 Immobilization of uricase-peroxidase conjugated on the biochip

An enzyme assay method using uricase-peroxidase probes was implemented, as shown in Figure 4-4. Briefly, the sensing region of polymeric biochip was wetted with a solution of p-azidotetrafluorobenzaldehyde in methanol (25 mg/mL), air-dried in the dark, exposed to UV-light for 10 min, washed with methanol twice, then with distilled water and 0.01 M carbonate buffer at pH 9.5. For covalent fixation, a pre-activated biochip region was incubated in a solution of uricase-peroxidase in 0.01 M carbonate buffer at pH 9.5 for 30 min then was washed.



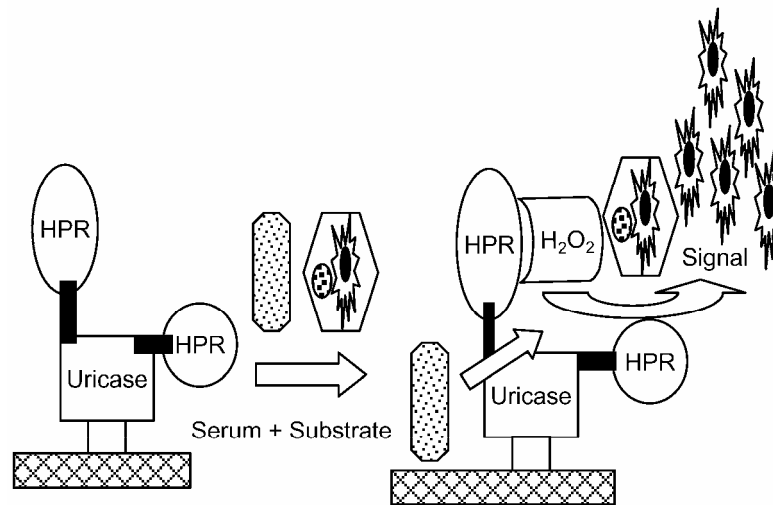


Figure 4-4. Schematic polymeric enzyme biochip assay method for detecting uric acid using immobilized uricase and peroxidase. Serum uric acid is oxidized by uricase to produce allantoin and hydrogen peroxide. The hydrogen peroxide reacts with 4-aminoantipyrine and 3,5-dichloro-2-hydroxybenzene sulfonate in a reaction catalyzed by peroxidase to produce a colored product.

4.3.7 Measurement of serum uric acid with optical enzyme biochip system and Beckman

Synchron analyzer

The absorbance of the biochip was detected with the optical enzyme biochip detection system. The system was especially adapted to quantitatively measure the absorbance of the biochip. A one part substrate solution (30 μ L) that contained 1 mM 4-aminoantipyrine, 4 mM 3,5-dichloro-2-hydroxybenzene sulfonate and 100 U/L ascorbate oxidase in 0.05 mM borate buffer at pH 8.5 and one part serum uric acid (30 μ L) was added to the biochip (immobilized with uricase-peroxidase). After reaction at room temperature for 1 min, the biochip was placed into the optical enzyme biochip detection system to measure the serum uric acid concentration. Hydrogen peroxide produced from the breakdown of uric acid (catalyzed by uricase) was measured by the oxidative coupling of 4-aminoantipyrine and 3,5-dichloro-2-hydroxybenzene sulfonate in the presence of peroxidase. To compare the detection ability of the developed biochip assay, a Beckman Synchron CX5 analyzer (USA) was used according to the manufacturer's instructions.

4.4 Results

4.4.1 Expression and purification of uricase

Genomic DNA from *Bacillus subtilis* (CCRC 14199) was isolated, using a QIAamp tissue kit (Qiagen, Hilden, Germany). The uricase gene was amplified by PCR resulting in a fragment of 1491 bp. The 1491 bp *EcoRI/HindIII* DNA fragment was ligated into pMAL-c2 and pBluescript II SK(+), and the cloned plasmid was double-digested with *EcoRI* and *HindIII* (Figure 4-5a). A uricase fusion protein was successfully purified from *E. coli* lysate only after it was enriched using an amylose column. The purified uricase fusion protein was eluted with maltose buffer and the fractions were pooled, concentrated and analyzed by sodium dodecyl sulfate-polyacrylamide gel electrophoresis (Figure 4-5b). For the uricase fusion protein, the major band on the gel had an apparent molecular mass of 98 kDa, corresponding to that predicted from the fusion gene sequence.

4.4.2 Measurements of uricase activity

The activity of the uricase expressed in *E. coli* and purified using SDS-PAGE was determined by a decrease in absorbance at 293 nm in the presence of uric acid. The effects of pH and thermal stability of the purified uricase also were examined. The pH stability was evaluated by incubation at different pH values (6 to 11) for 7 hrs. Optimal (100%) activity was found at pH values from 6 to 10. The thermal stability was examined by incubation for 30 min at different temperatures (4 to 80 °C) followed by cooling to room temperature. Complete inactivity was observed at 75 °C and 45% inactivity occurred at 70 °C. The residual activity maximum occurred between 4 and 55 °C.

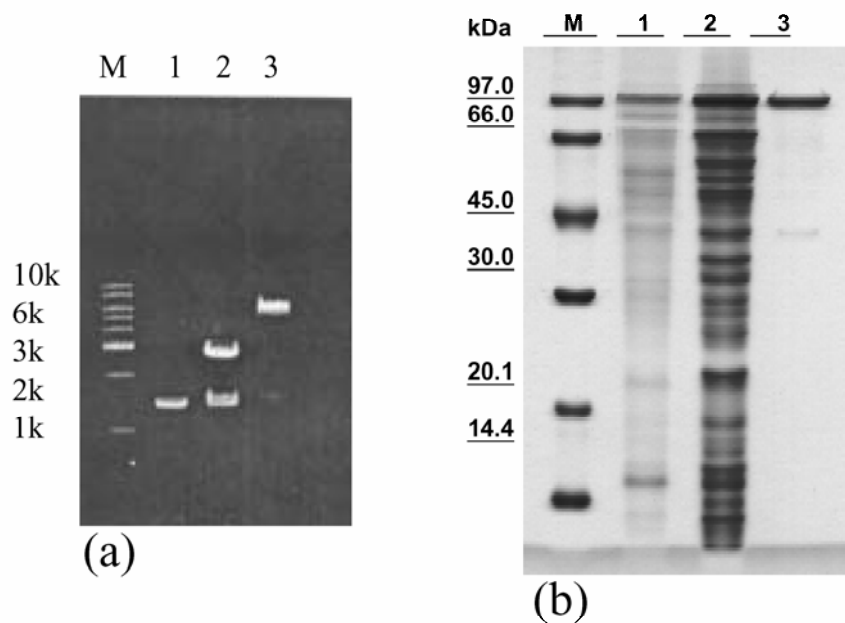


Figure 4-5. (a) Agarose electrophoresis gel analysis of cloning. M, molecular markers. Lane 1, the uricase gene (1491 bp DNA fragments) was amplified by PCR. Lane 2, DNA fragments were ligated into pBluescript II SK(+), and digested by *EcoRI* / *HindIII*. Lane 3, DNA fragment were ligated into pMAL, and were digested by *EcoRI* / *HindIII*. (b) SDS-PAGE analysis of the uricase fusion protein produced in *E. coli*, and purified on an amylose affinity spin column. Lane 1, pellet; Lane 2, crude extract; Lane 3, eluate. The samples were loaded onto 12% polyacrylamide gels. The uricase fusion protein produced in *E. coli* had an apparent molecular mass of 98 kDa.

4.4.3 Optimization of the uricase-peroxidase-immobilized biochip

The effects of temperature and pH on the uricase-peroxidase-immobilized biochip were evaluated. Figure 4-6a plots the relationship between pH and the absorbance of the uricase-peroxidase-immobilized biochip in a single part substrate buffer (30 μ L) that contained 1 mM 4-aminoantipyrine, 4 mM 3,5-dichloro-2-hydroxybenzene sulfonate, 100 U/L ascorbic acid and one part 5 mg/dL uric acid (30 μ L). The results showed that the absorbance of the uricase-peroxidase-immobilized biochip increased slowly with pH between 6 and 7.5, then increased sharply with pH from 7.5 to 8.5 and finally declined as the pH increased from 8.5 to 10. The absorbance response was maximal at pH 8.5, which is the optimal pH for the uricase-peroxidase-immobilized biochip.

Figure 4-6b plots the relationship between temperature and the maximum absorbance of the uricase-peroxidase-immobilized biochip. The reaction medium included one part substrate buffer (30 μ L) that contained 1 mM 4-aminoantipyrine, 4 mM 3,5-dichloro-2-hydroxybenzene sulfonate, 100 U/L ascorbic acid and one part 5 mg/dL uric acid (30 μ L) in 0.05 mM borate buffer at pH 8.5. The result showed that the absorbance increased with the temperature from 20 to 40 $^{\circ}$ C and the absorbance-temperature showed no signal. Hence, further experiments were performed at 25 $^{\circ}$ C, using 0.05 mM borate buffer at pH 8.5.

4.4.4 Evaluation of the uricase-peroxidase-immobilized biochip for measuring purified uric acid

In the application of the optical enzyme biochip detection system technology for assay of uric acid, success depends on combining of the efficiency of the immobilization enzyme reaction with that of photo-signal transduction. The calibration curve for uric acid was obtained using the uricase-peroxidase-immobilization biochip. Various quantities of uric

acid (1, 2.5, 5, 7.5, 10, 12.5, 15 mg/dL) were added to a polymeric biochip that contained 4-aminoantipyrine, 3,5-dichloro-2-hydroxybenzene sulfonate and various concentrations of uric acid. From these measurements, a calibration curve was obtained to evaluate of uric acid screening using the CMOS photosensor technology. Figure 4-7a plots the dose response curve between the purified uric acid concentration and the absorbance of the uricase-peroxidase-immobilized biochip. A calibrated value above or equal to a blank plus three standard deviations was considered positive. As shown by the calibration curve, the response was linear between 2.5 mg/dL and 12.5 mg/dL. The regression line for purified uric acid was $y = 0.0558x - 0.0692$ and the correlation coefficient had a value of $r^2 = 0.9931$.

4.4.5 Application of the optical polymeric biochip detection system for measuring serum uric acid

Serum samples from apparently healthy adults and patients with gout, leukemia, toxemia of pregnancy, and nephrolithiasis were collected from the Executive Yuan, Department of Health Hsin Chu Hospital. Serum samples were diluted 1:1 in substrate solution, then placed directly on the optical enzyme biochip detection system, and the concentration of uric acid present was estimated from a calibration plot. Results were within the linear range of the reaction, and the calibration graph was from 2.5 mg/dL to 12.5 mg/dL for serum uric acid. The results obtained by the optical enzyme biochip system were compared with those obtained using the Beckman Synchron analyzer. As shown in Figure 4-7b, the results indicated that the measured serum uric acid for 20 different serum sample using the optical enzyme biochip detection system correlated closely to results using the Beckman Synchron analyzer. The regression line for serum uric acid was $Y = 1.0142X + 0.1799$ and the correlation coefficient was $r^2 = 0.9951$. Results for serum uric acid obtained using a biochip did not significantly differ from those obtained using a Beckman Synchron analyzer.

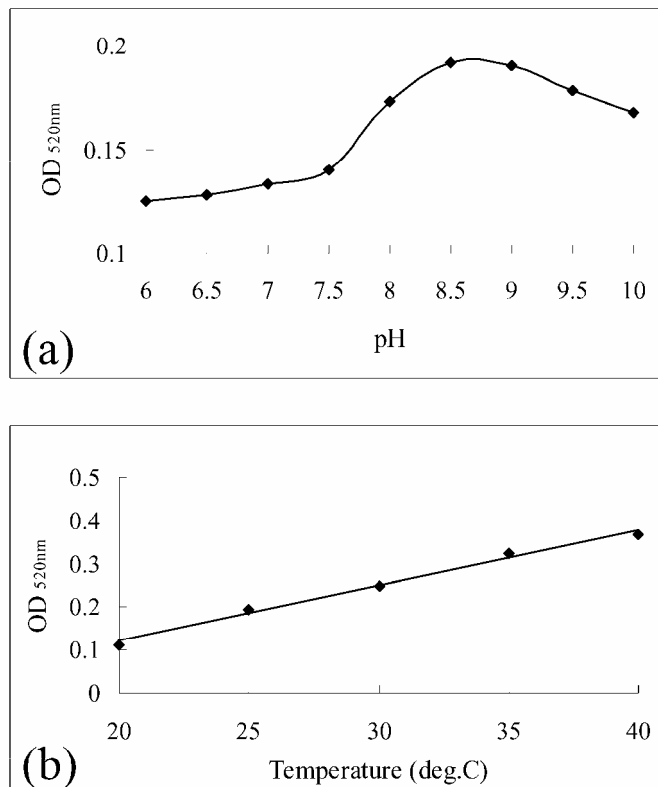


Figure 4-6. Effect of pH and temperature on the absorbance of the uricase-peroxidase immobilized biochip. (a) Effect of pH on the absorbance of the uricase-peroxidase immobilized biochip. (b) Effect of temperature on the absorbance of the uricase-peroxidase immobilized biochip.

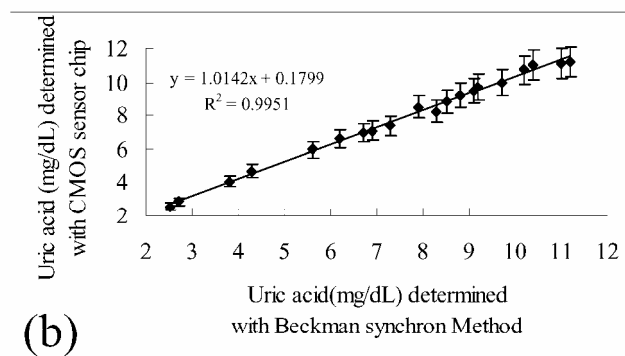
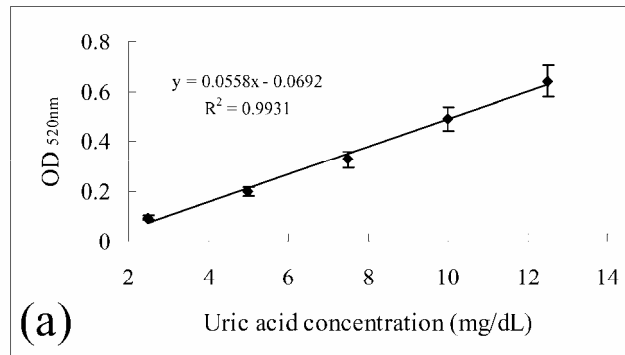


Figure 4-7. (a) Calibration curve of purified uric acid concentration and absorbance at 520 nm using the uricase-peroxidase immobilized biochip. (b) Comparison of serum uric acid results by Beckman Synchron method and polymeric enzyme biochip assay method.

4.5 Discussion

The study in this chapter used a CMOS photosensor, a biochip containing enzyme probes, in a rapid and sensitive method for accurately quantitating and directly monitoring enzyme-catalyzed reactions. The CMOS process is well established in the microelectronic industry, and has the potential to produce low-cost photosensors designed with an N⁺/P-well structure. By integrating an LED, a polymeric biochip, and a biased CMOS photosensor with a digitizing device, a low cost optical detection system could be built. Traditionally, glass has excellent properties for mechanics, thermodynamics and optics, and is popular as a biochemical material. The disadvantage of using glass is difficulties in processing and forming. However, polymer materials are superior in price, easy formation and easy mass production. Detection of uric acid using a biochip system is important to the clinical field of biotechnology, and depends on the simultaneous immobilization of uricase and peroxidase on the biochip. Two factors determine the overall response of the biochip in such a system: the influence of temperature and pH on enzyme activity, and the effect of temperature and pH on the generated absorbance. Temperature is an essential factor in enzymatic reactions. The effect of temperature on the biochip response was investigated over the range between 20 and 40 °C. The results indicate that the response of the CMOS sensor is stronger at higher temperatures in the tested temperature range of 20 – 40 °C. The optimal pH for immobilizing uricase and peroxidase on the biochip is 8.5. The calibration curve was accurate from 2.5 mg/dL to 12.5 mg/dL for purified uric acid. Measuring the concentration of serum uric acid in human serum samples demonstrates the usefulness of the assay in clinical chemistry. The results obtained agreed reasonably with those obtained by the Beckman Synchron method. Uric acid is oxidized by uricase to produce allantoin and hydrogen peroxide. The hydrogen peroxide reacts with 4-aminoantipyrine and 3,5-dichloro-2-hydroxybenzene sulfonate, in a reaction catalyzed by peroxidase to produce a

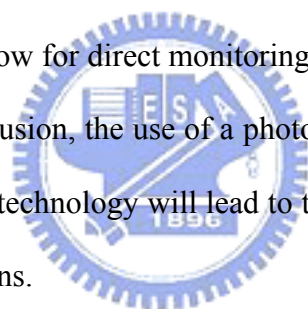
colored product. The Beckman Synchron system reagent was used to measure the uric acid concentration by a timed-end-point method (24). This system automatically apportions the appropriate sample and reagent volumes into a cuvette and monitors the change in absorbance at 520 nm where the change in absorbance is directly proportional to the concentration of uric acid in the sample.

The development of the optical enzyme biochip detection system, a device that includes a bioreceptor (for example, an enzyme) and a signal transducer (COMS photosensor) is presented here. When the analyte interacts with the bioreceptor, the resulting complex produces a change, which is translated into a measurable efferent (such as an electrical signal) by the transducer. The first application of the optical enzyme biochip detection system was in an enzyme-based biochip developed to detect uric acid. The application detects uric acid by the immobilization of the enzyme uricase-peroxidase as a bioreceptor. In the optical enzyme biochip detection system, the measured enzyme-catalyzed reactions and produced hydrogen peroxide directly with the quantity of uric acid. The catalysis by the enzymes and the small size of the CMOS photosensor, allow the continuous monitoring of the release of hydrogen peroxide from uric acid. Accordingly, data is presented demonstrating that the optical enzyme biochip detection system is useful for the detection of uric acid in human clinical samples.

The IC system designed for the microchip photosensor elements and associated data treatment is based on complementary metal oxide semiconductor (CMOS) technology. The development and evaluation of various elements of the DNA biosensor microchip technology have been described. The design of the gene probe immobilization techniques on the biosensor substrates as well as the development of integrated electro-optic systems on the IC biochip using a phototransistor multi-array system previously have been discussed. For example, the quantitation of HIV-1 using sequence-specific fluorescent-labeled DNA probes

and hybridization on the nitrocellulose sampling platform system was described (25). In another example, Stokes et al. evaluated the combined effectiveness of the IC biochip and antibody probe-based assay and determined that it yielded exceptional quantitative ability, sensitivity and selectivity (26). In this system, the sampling platform is a cellulose membrane that is exposed to *E. coli* and subsequently analyzed using a sandwich immunoassay involving a Cy5-labeled antibody probe.

A focus of our laboratory is the development of optical enzyme biochip assay technology and quantitation of various enzymes using CMOS technology. These studies include the design of the enzyme probe immobilization techniques on the polymeric biochip as well as the development of a photosensor using CMOS technology. We describe an application that detects uric acid by immobilized uricase-peroxidase probes. Measurements of enzyme-catalyzed reactions allow for direct monitoring of the degradation of the uric acid in a quantitative manner. In conclusion, the use of a photosensor based on complementary metal oxide semiconductor (CMOS) technology will lead to the development of low-cost diagnostic biochips for medical applications.



4.6 References

1. Keilin, J. (1959) The biological significance of uric acid and guanine excretion. *Biol. Rev.* 34, 265-296.
2. Wallrath, L. L. and Friedman, T. B. (1991) Species differences in the temporal pattern of drosophila urate oxidase gene expression are attributed to trans-acting regulatory changes. *Proc. Natl. Acad. Sci. USA* 88, 5489-5493.
3. Montalbini, P., Redondo, J., Caballero, J. L., Cardenas, J. and Pineda, M. (1997) Uricase from leaves: its purification and characterization from three different higher plants. *Planta* 202, 277-283.
4. Montalbini, P., Aguilar, M. and Pineda, M. (1999) Isolation and characterization of uricase from bean leaves and its comparison with uredospore enzyme. *Plant Science* 147, 139-147.
5. Yuichi, H., Tetsuhiko, S. and Hajime, I. (2000) Cloning, sequence analysis and expression in *Escherichia coli* of the gene encoding a uricase from the yeast-like symbiont of the brown planthopper, *Nilaparvata lugens*. *Insect Biochemistry and Molecular Biology* 30, 173-182.
6. Yasuji, K., Toshio, I. and Erichi, N. (1996) Cloning, sequence analysis and expression in *Escherichia coli* of the gene encoding the *candida utilis* urate oxidase. *J. Biochem.* 120, 969-973.
7. Adamek, V., Suchova, M., Demnerova, K., Kralova, B., Fort, I. and Morava, P. (1990) Fermentation of *candida utilis* for uricase production. *J. Ind. Microbiol.* 6, 85-90.
8. Yamamoto, K., Kojima, Y., Kikuchi, T., Shigyo, T., Sugihara, K. and Takashio, M. (1996) Nucleotide sequence of the uricase gene from *Bacillus* sp. TB-90. *J. Biochem.* 119, 80-84.
9. Eswara, U.S., Dutt, H. and Mottola, A. (1974) Determination of uric acid at the microgram level by a kinetic procedure based on a pseudo-induction period. *Anal. Chem.* 46, 1777.
10. Burtic, C. A. and Ashwood, E. R. (1994) Teitz textbook of clinical chemistry, 2nd ed.

Philadelphia: WB saunders company.

11. Yutaka, A., Hiroshi, I., Hiroomi, N., Tsugutoshi, A. and Mitsutatk, Y., (1992) Effects of serum bilirubin on determination of uric acid by the uricase-peroxidase coupled reaction. *Clin. Chem.* 38, 1350-1352.
12. Bhargava, A. K., Lal, H. and Pundir, C. S. (1999) Discrete analysis of serum uric acid with immobilized uricase and peroxidase. *J. Biochem. Biophys. Methods* 39, 125-136.
13. Nanjo, M. and Guilbault, G. G. (1974) Enzyme electrode sensing oxygen for uric acid in serum and urine. *Anal. Chem.* 46, 1769-1772.
14. Uchiyama, S., Shimizu, H. and Hasebe, Y. (1991) Chemical amplification of uric acid sensor responses by dithiothreitol. *Anal. Chem.* 66, 1873-1876.
15. Miland, E., Ordieres, A. J. M., Blanco, P. T. and Smyth, C. O. (1996) Poly (o-aminophenol)-modified bienzyme carbon paste electrode for the detection of uric acid. *Talanta* 43, 785-796.
16. Schiavon, O., Calicati, P., Ferruti, P. and Veronese, F. M. (2000) Therapeutic proteins: a comparison of chemical and biological properties of uricase conjugated to linear or branched poly(ethylene glycol) and poly(N-acryloylmorpholine). *Il Farmaco.* 55, 264-269.
17. Haeckel, R. (1976) The use of aldehyde dehydrogenase to determine H₂O₂-producing reactions. I. The determination of the uric acid concentration. *J. Clin. Chem. Clin. Biochem.* 14, 101-106.
18. Janchen, M., Walzel, G., Neef, B., Wolf, B., Scheller, F. and Kuhn, M. (1983) Uric acid determination in dilute serum with an enzyme electrochemical and enzyme-free sensor. *Biomed. Biochim. Acta* 9,1055-1059.
19. Sambrook, J. and Russell, D. W. (2001) Molecular cloning: A Laboratory Manual. Cold Spring Harbor Laboratory Press. Cold Spring Harbor, NY.

20. Guan, C., Li, P., Riggs, P. D. and Inouye, H. (1988) Vectors that facilitate the expression and purification of foreign peptides in *E. coli* by fusion to maltose-binding protein. *Gene* 67, 21-30.
21. Maina, C. V., Riggs, P. D., Grandea, A. G., Slatko, B. E., Moran, L. S. and Tagliamonte, J. A. (1988) An *E. coli* vector to express and purify foreign proteins by fusion to and separation from maltose-binding protein. *Gene* 74, 365-373.
22. Kellerman, O. K. and Ferenci, Y. (1982) Maltose-binding protein from *Escherichia coli*. *Methods Enzymol.* 90, 459-467.
23. Tresca, J. P., Ricoux, R., Pontet, M. and Engler, R. (1995) Comparative activity of peroxidase-antibody conjugates with periodate and glutaraldehyde coupling according to an enzyme immunoassay. *Ann. Biol. Clin.* 53, 227-231.
24. Fossati, P., Prencipe, L. and Berti, G. (1980) Use of 3,5-Dichloro-2-hydroxybenzenesulfonic acid / 4-aminophenazone chromogenic system in direct enzymic assay of uric acid in serum and urine. *Clin. Chem.* 26, 227-231.
25. Vo-Dinh, T., Alarie, J. P., Isola, N., Landis, D., Wintenberg, A. L. and Ericson, M. N. (1999) DNA Biochip using a Phototransistor Integrated Circuit. *Anal. Chem.* 71, 358-363.
26. Stokes, D. L., Griffin, G. D. and Vo-Dinh, T. (2001) Detection of *E. coli* using a microfluidics-based antibody biochip detection system. *Fresenius J. Anal. Chem.* 369, 295-301.

Chapter 5

Modified Colorimetric Assay for Uricase Activity and a Screen for Mutant *Bacillus subtilis* Uricase Genes Following StEP Mutagenesis

5.1 Abstract

This chapter describes a modified colorimetric assay for uricase activity in flexible 96-well microtiter plates using the uricase - uric acid - horseradish peroxidase - 4-aminoantipyrine - 3,5-dichloro-2-hydroxybenzene sulfonate colorimetric reaction. The utility of this assay was demonstrated in a screen for mutant uricase enzymes derived from the uricase gene of the thermophilic bacterium *Bacillus subtilis* by a modified staggered extension process (StEP) mutagenesis. An *Escherichia coli* library of StEP-derived uricase mutant clones was screened yielding two identical mutant uricase genes with activity. Two motifs conserved in eukaryotic and prokaryotic uricases are highly conserved in the mutant uricase. The mutant uricase protein was found to exhibit high uricase activity (13.1 U/mg). Finally, the modified colorimetric method is much more efficient than the conventional ones and greatly reduces assay time from 4 days to less than 20 hours.

Keywords: modified colorimetric assay; *Bacillus subtilis* uricase gene; maltose binding protein; horseradish peroxidase; staggered extension process (StEP).

5.2 Introduction

Uricase is an enzyme in the purine degradation pathway that catalyzes the oxidative breakdown of uric acid to allantoin. This enzyme is found in mammals (1,2), plants (3), fungi (4), yeasts (5-7), and bacteria (8). Uric acid, the primary end product of purine metabolism, is present in biological fluids, including blood and urine (9). Various medical conditions increase the amount of uric acid in biological fluids. Such conditions can lead to gout, chronic renal disease, some organic acidemias and Lesch-Nyhan syndrome (10).

Many attempts have been made to fabricate uric acid sensors, using uricase (urate oxidase, EC 1. 7. 3. 3.) as a biocatalyst (11-15). The uricase molecule catalyzes the *in vivo* oxidation of uric acid in the presence of oxygen, which oxidizes uric acid to allantoin and CO₂, leaving hydrogen peroxide as the reduction product of O₂. Several forms of uricase from microorganisms are currently used as diagnostic reagents to detect uric acid. Most of these enzymes either have high thermostability or are active over a wide pH range (5,6,8,16). Only one uricase, from *Bacillus* sp. TB-90, was observed to have both high activity and thermostability over a wide range of pH values, from 6 to 9.

This chapter describes the cloning of a modified uricase gene from thermophilic bacterium *Bacillus subtilis*. Molecular evolution by staggered extension process (StEP) mutagenesis was used to isolate potential uricase plasmid clones in *Escherichia coli*, which were screened in a microtiter well colorimetric assay for uricase activity. The 96-well microtiter LB medium plates containing potential uricase clones were incubated at 37 °C for a maximum of 18 h with shaking to induce protein expression. Then the plates were treated at 60 °C for 1 h to release soluble uricase protein. Substrate was added to 96-well microtiter LB medium plates to assay uricase activity. We identified a mutant uricase using this approach. We analyzed the enzymatic properties of this protein and its amino acid sequence for conserved uricase motifs.

5.3 Experimental

5.3.1 Materials

Restriction enzymes, ligase, and amylose resin were purchased from New England Biolabs (Beverly, MA, USA). SYBR green nucleic acid gel stain and PCR reagents were purchased from Roche (Mannheim, Germany). DNA primers were purchased from Biobasic Inc. (Toronto, Canada). Agarose was purchased from USB (Cleveland, OH, USA). Sodium dodecyl sulfate (SDS) was purchased from Gibco BRL (Gaithersburg, MD, USA). Sodium phosphate, β -mercaptoethanol, coomassie brilliant R250, isobutanol, and sodium chloride were purchased from Merck (Darmstadt, Germany). Phenylmethylsulfonyl fluoride (PMSF), lysozyme, proteinase K, uric acid, horseradish peroxidase, 4-aminoantipyrine, and 3,5-dichloro-2-hydroxybenzene sulfonate were purchased from Sigma (St. Louis, MO, USA). Tris(hydroxymethyl) methylamine were purchased from BDH (Poole, England). LB medium, tryptone, and yeast extract were purchased from Difco (Detroit, MI, USA). The 96-well microtiter plates were purchased from Nalge Nunc International (Roskilde, Denmark).

4.3.2 Mutagenesis of wild-type thermophilic bacterium *Bacillus subtilis* uricase gene

Thermophilic bacterium *B. subtilis* were isolated from soils of a papaya fruit farm and their special properties were described in the Culture Collection and Research Center internal information of strains (Food Industry Research and Development Institute, Hsinchu, Taiwan). The uricase gene from one of these wild-type thermophilic bacterium *B. subtilis* (TB-90) was cloned previously (24). That uricase gene was used as template in a polymerase chain reaction modified staggered extension process (StEP) mutagenesis protocol (17,18,20) using primers 5'-TCTAGAATTCCATATGTTTACAATGGATGACCTG-3' and 5'-GCTGCAGAAGCTTCGCCGCTGGTTTGCCGCAGG-3'. StEP conditions (50 μ L final

volume) were 0.5 μ L template DNA, 10 pmol of each primer, 0.2 mM of each dNTP, 1 x *Taq* buffer, 25 mM Mg (OAc)₂ and 2.5 U *Taq* polymerase. The program was 5 min at 95 °C, 80 cycles of 30 sec at 94 °C, and 5 sec at 56 °C. The 1.5 kb DNA fragment was purified from a 0.8% agarose gel, and ligated to *Eco*RI/*Hind*III pre-digested pMAL vector using a DNA ligation Kit to transform *E. coli* DH5 α selecting for ampicillin resistance. Isopropyl- β -D-thiogalactoside (IPTG) was spread on LB pates for screening.

5.3.3 Screening for uricase-producing microorganisms

The scheme used for screening for uricase-producing microorganisms, or in this case, *E. coli* carrying an active uricase mutant of the mutant thermophilic bacterium *B. subtilis* uricase gene, in 96-well microtiter LB medium plates, is depicted in Figure 5-1. Screening was performed in 96-well microtiter plates containing LB medium with 50 μ g/mL ampicillin and 0.3 mM IPTG, and using 0.1 mM uric acid, 0.1 U/mL horseradish peroxidase, 1 mM 4-aminoantipyrine, and 4 mM 3,5-dichloro-2-hydroxybenzene sulfonate in 0.1 M Tris buffer (pH 8.5) as the substrate. Mutant clones were grown on LB plates and transferred to 96-well microtiter LB medium plates containing 100 μ L LB/IPTG medium per well. These were incubated at 37 °C for a maximum of 18 h with shaking to induce the expression of mutant uricase. Then, they were treated at 60 °C for 1 h for cell lysis and release of the protein. Following the addition of substrate, the plate was incubated for 10 min at 37 °C, a bright purple color was observed and absorbance at 520 nm was read with a microplate reader.

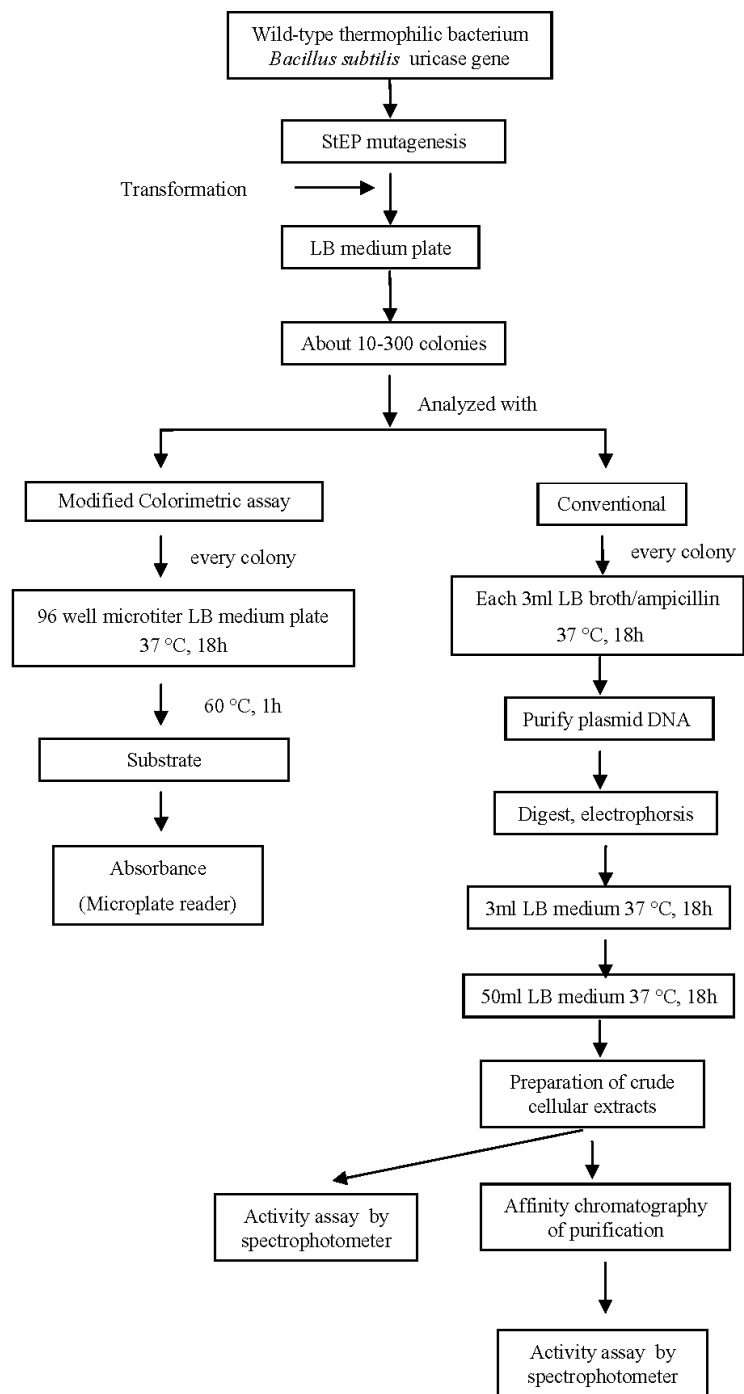


Figure 5-1. Flow chart for the detection of uricase activity by the conventional method and the modified colorimetric method.

5.3.4 DNA sequencing and computer analysis

Sequencing was performed using an ABI PRISM 3100 auto-sequencer. Samples were prepared using a DNA Cycle Sequencing Kit and a Big-Dye Terminator, according to the manufacturer's protocol (Applied Biosystem, Foster City, CA). Appropriate oligonucleotides were used as primers. Computer analyses of DNA sequence data and the deduction of amino acid sequences were performed at the National Center for Biotechnology Information (NCBI) website using GenBank databases and BLAST Programs. Protein sequences were aligned using Clustal W (1.1).

5.3.5 Expression and purification of the mutant fusion uricase protein

The pMAL-c2 system was used to express the uricase as a maltose binding protein fusion. Plasmid-bearing cells were grown to a concentration of 5×10^8 cell/ml at 37 °C with shaking in a rich medium at which point 0.3 mM IPTG was added and the culture was grown for an additional 4 h. All subsequent steps were performed at 4 °C or on ice. The cells were harvested by low-speed centrifugation, resuspended in 1/10 vol. of 20 mM Tris buffer pH 7.2, and sonically lysed. Cellular debris was then pelleted by high-speed centrifugation, and the supernatant was saved as crude cellular extract. Purification of the maltose binding protein fusions using the pMAL-c2 system was as per the manufacturer's instructions (19,20). Briefly, fusion proteins were purified from crude extracts by binding to cross-linked amylose in a column, as described by Kellerman and Ferenci (21), and eluted with 10 mM maltose in 20 mM Tris buffer (19,20). The purified fusion protein fractions were next loaded onto a DEAE-Sephacel column (0.7 x 2 cm) equilibrated with Tris buffer pH 8.0. The column was washed with 50 mL of Tris buffer and then eluted with 5 void volumes of Tris buffer containing 50 to 600 mM of NaCl with 50 mM interval. Fusion proteins were eluted between 300 and 350 mM NaCl.

5.3.6 Measurements of uricase activity

Uricase activity was routinely measured aerobically as the decrease in absorbance at 293 nm due to the enzymatic oxidation of uric acid (5,6,8). During purification, the activity of the enzyme was measured in an assay mixture that contained 0.1 M Tris buffer (pH 8.5). One unit was defined as the amount of enzyme required to transform 1 μmol of uric acid into allantoin in 1 min at 25 °C at pH 8.5. Protein concentration was estimated by the Bio-Rad Protein Assay (5), using bovine serum albumin as a standard. For determination of kinetic parameters, substrate concentrations of 5-100 μM , which showed linear relationships between the concentrations of allantoin as a function of time, were carried out. The data collected were next applied to the Lineweaver-Burk equation. Thermal stability of wild-type and mutant uricase was evaluated on the basis of the residual enzyme activity of the protein sample (10 U/mL^{-1} in 50 mM borate buffer pH 8.5) heated 1 h in closed vials at scheduled temperatures (20-80 °C) and cooled to room temperature. For the stability to pH, samples of wild-type and mutant uricase were dissolved at room temperature in a buffer containing 0.05 M sodium acetate (pH 4-6), 0.05 M potassium phosphate (pH 7), or 0.05 M sodium borate (pH 8-11). After 7 h of incubation, the enzyme activity was evaluated.

5.4 Results

5.4.1 Mutagenesis of wild-type thermophilic bacterium *Bacillus subtilis* uricase gene

As we reported previously (24), wild-type thermophilic bacterium *Bacillus subtilis* uricase gene showed a high thermostability and activity. We have isolated a mutant derivative of that enzyme using a modified StEP recombination approach. For the StEP procedure we used the uricase gene from wild-type thermophilic bacterium *Bacillus subtilis* as template and the resulting products were cloned into the expression plasmid pMAL-c2. The presence of the 1.5 kb uricase gene fragment in the library of clones was confirmed by restriction analysis (Fig. 5-2).

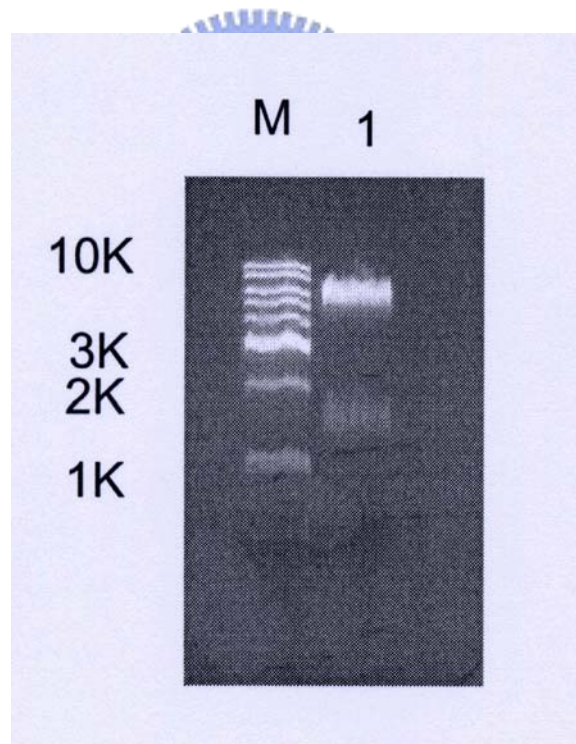


Figure 5-2. Agarose gel electrophoresis results of mutant uricase gene cloning. Lane 1, mutant DNA fragments were inserted into pMAL-c2, and DNA fragments were digested by *Eco* RI/*Hind* III. The uricase gene is present in the 1.5 kb DNA fragment.

5.4.2 Screening for uricase activity via a modified colorimetric assay

The modified colorimetric assay developed in this work was used to screen for uricase mutant genes derived from the thermophilic bacterium *Bacillus subtilis* uricase. A modified colorimetric assay was used with high-throughput screening using a microplate reader to quantify colorimetric level. About 150 *E. coli* DH 5 α transformants carrying potential uricase mutants from the aforementioned StEP procedure were transferred to 96-well microtiter LB medium plates to screen for uricase activity using a modified fast colorimetric 96-well plate assay. Plates were incubated shaking at 37 °C for a maximum of 18 h with IPTG to induce the expression of mutant uricase. Denatured cells were lysed under conditions compatible with rapid screening in 96-well microtiter plates and the lysed samples were transferred to 96-well microtiter LB medium plates in a 60 °C incubator for 1 h, causing the cells to facilitate release of the uricase. The soluble fraction was then bound to 96-well microtiter plates, and the recombinant protein was detected via substrate reactions that produced a chromophore (Fig. 5-3). Uricase produces hydrogen peroxide from uric acid, which is then acted upon by peroxidase and yields a chromophore via the peroxidase-dependent oxidative coupling of 4-aminoantipyrine and 3,5-dichloro-2-hydroxybenzene sulfonate (Fig. 5-3). Figure 5-4 presents the microplate reader results of screening 94 potential uricase mutants from the StEP recombined library for activity. Two mutants, designated B4 and B8, had uricase activity.

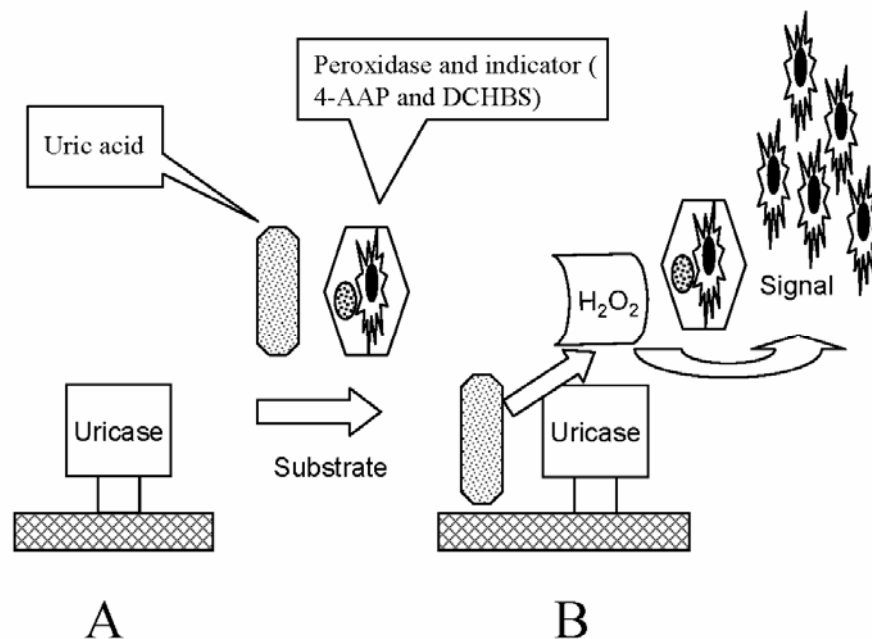


Figure 5-3. Depiction of the hydrogen peroxide based colorimetric assay. Substrate reaction mixture containing the hydrogen peroxide produced from uric acid with uricase, after measured by oxidative coupling of 4-aminoantipyrine and 3,5-dichloro-2-hydroxybenzene sulfonate in the presence of peroxidase to produce a colored product. (A) The 96-well microtiter LB medium plates are incubated at 37 °C for a maximum of 18 h with shaking to induce the expression of mutant uricase, and then treated for 60 °C for 1 h to cause lysis and release of the uricase protein. (B) Substrate is added to 96-well microtiter LB medium plates to assess uricase activity. The reaction measures uricase activity of mutant uricase gene by use of uric acid, peroxidase, and typical colorimetric indicator.

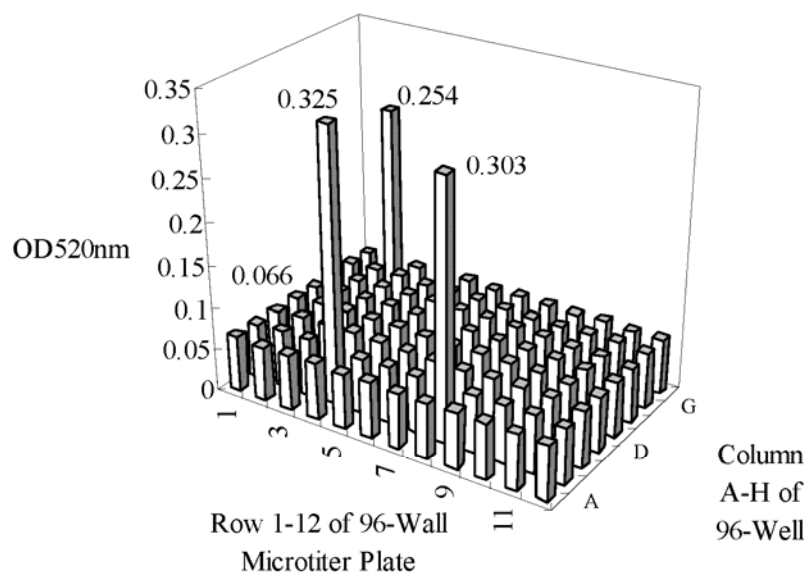


Figure 5-4. Screening potential uricase mutants in 96-well microtiter plates using a microplate reader. The reactions leading to colorimetric readout are described in the text. The H1 sample is the blank (0.066). H2 contains the wild-type uricase (positive control) (0.254). B4 (0.325) and B8 (0.303) are two variants that have activity.

5.4.3 Analyzing the motif sequence of mutant uricase

Two active variants (B4 and B8) were analyzed by sequence analysis and found to have identical nucleotide sequences. A BLAST search confirmed that the deduced amino acid sequence of the ORF maltose binding protein (MBP) sequence and the uricase sequence. The predicted amino acid sequence of the mutant uricase was 84% identical to that of wild-type uricase. Motif amino acid sequence analysis involved a BLAST search using the sequences of these motifs (motifs A-F). Two consensus motifs have been identified in both eukaryotic and prokaryotic uricases (6,8). Neither of these motifs [motifs A (Gly-Lys-X-X-Val) and B (Asn-Ser-X-Val/Ile-Val-Ala/Pro-Thr-Asp-Ser/Thr-X-Lys-Asn)] is altered in the variant uricase gene (Figure 5-5). Bairoch (22) and Legoux *et al.* (23) had identified consensus patterns of eukaryotic uricase (motifs C and D in Figure 5-5). The mutant sequence Leu-Val-Lys-Val-Ser-Gly-Asn and Thr-Pro-Ser-Ile Gln-Asn-Leu-Ile-Tyr (in Figure 5-5) differ from motifs C and D, respectively. Yamamoto *et al.*(8) presented consensus patterns of *Bacillus* sp. TB-90 uricase, which are motifs C (Leu-Ile-Lys-Val-Ser-Gly-Asn) and D (Thr-Leu-Ser-Ile-Gln-His-Leu-Ile-Tyr). Similarly, sequences of the mutant uricase were conserved but with slight modifications. Finally, motif E (Leu-Pro-Asn-Lys-His) was identified as a consensus pattern of prokaryotic uricases, but not in mutant uricase. The mutant uricase of *Bacillus subtilis* includes two cysteines, one of which is located at the active site of the enzyme. One hypothesis is that a chemically reactive sulfhydryl group on the surface of molecule is spontaneously oxidized during purification and forms a disulfide bond link between two molecules.

Motif A

Mutant	YGKGNVFA
<i>B. subtilis</i>	YGKGNVFA
<i>Bacillus</i> TB-90	YGKGDVFA
<i>A. flavus</i>	YGKDNV RV
<i>C. utilis</i>	YGKDNV KF
<i>N. lugens</i>	YGKDNV RV

Motif B

Mutant	DNTLVVATDSIKNF IQRHLASYEGTTTEGFLHYVAHRFF
<i>B. subtilis</i>	DNTLVVATDSMKNF IQRHLASYEGTTTEGFLHYVAHRFEL
<i>Bacillus</i> TB-90	DNSLVVATDSMKNF IQKHLASYTGTTTEGFLHYVAHRFEL
<i>A. flavus</i>	DNSVIVATDSIKNT IYITAKQNPVTPPELFGSILGTHFI
<i>C. utilis</i>	DNSSIVPTD TVKNT ILVLAKTTEIWP IERFGAKLATHFV
<i>N. lugens</i>	DNSLVVATDSIKNT IYILAKQHRVNPPELFASSISSEFI

Motif C

Mutant	LQLVKVSGNSFVGFIRDEYTTLPEDGNRPLFVYFNISWQ
<i>B. subtilis</i>	LQLVKVSGNSFVGFIRDEYTTLPEDGNRPLFVYLNISWQ
<i>Bacillus</i> TB-90	LQLIKVSGNSFVGFIRDEYTTLPEDSNRPLFVYLNISWK
<i>A. flavus</i>	LTVLKSTNSQFWGFLRDEYTTLKETWDRILSTDVDATWQ
<i>C. utilis</i>	LTVLKSTGSMFYGYNKCDFTTLQPTTDRIILSTDVDATWV
<i>N. lugens</i>	LSLLKSTGSAEGGFV RDEFTTLPESWDRILATDVDASWK

Motif D

Mutant	TPSIQNLIYHIGCRIL
<i>B. subtilis</i>	TPSIQNLIYHIGCRIL
<i>Bacillus</i> TB-90	TLSIQHLIYLIGRRIL
<i>A. flavus</i>	SASVQATMYKMAEQIL
<i>C. utilis</i>	SPSVQATMFNMATQIL
<i>N. lugens</i>	SPSVQNTMYKMCQQIL

Motif F

Mutant	TVVEEIPGSK
<i>B. subtilis</i>	TVVEEIPGSK
<i>Bacillus</i> TB-90	KIVEEIPPESE
<i>A. flavus</i>	LPNKKHYEEID
<i>C. utilis</i>	LPNKKHYFLID
<i>N. lugens</i>	LPNKKHNFELD

Figure 5-5. Motif sequence analysis of the mutant uricase.

5.4.4 Comparison of expression and purification of the wild-type and mutant fusion

uricase

Wild-type and mutant fusion uricase protein were successfully purified from *E. coli* lysates by amylose affinity chromatography. The uricase-MBP fusion protein was eluted with maltose buffer and concentrated. Analysis by sodium dodecyl sulfate-polyacrylamide gel electrophoresis (SDS-PAGE) demonstrates that the uricase-MBP fusion has an apparent molecular mass of 98 kDa (Fig. 5-6A), in close agreement with that estimated for uricase-MBP fusion protein. The uricase-MBP fusion protein was further purified by DEAE-Sephacel ion-exchange chromatography to homogeneity, as visualized by coomassie blue stained SDS-PAGE (Fig. 5-6B).



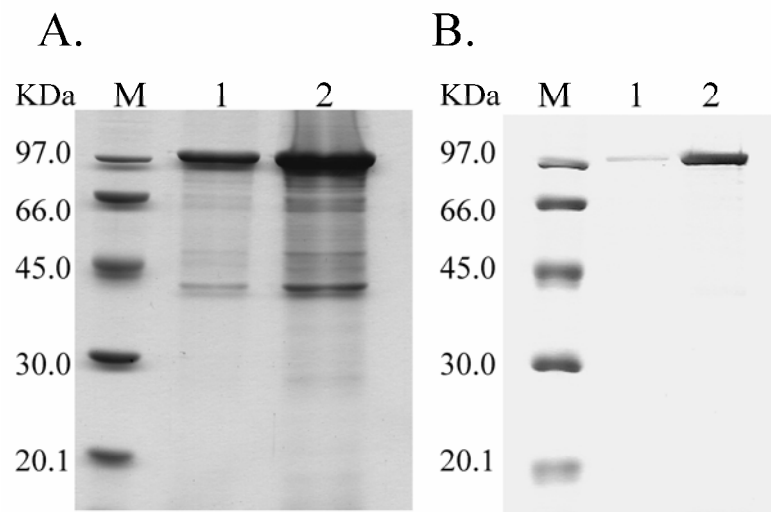


Figure 5-6. SDS-PAGE analysis of wild-type and mutant uricase-MBP fusion proteins. (A) Coomassie-stained uricase-MBP fusion proteins obtained from amylose affinity chromatography fractions. Lane M: marker proteins: phosphorylase b (97 kDa), bovine serum albumin (66 kDa), ovalbumin (45 kDa), carbonic anhydrase (30 kDa), trypsin inhibitor (20 kDa); lane 1, wild-type uricase-MBP fusion protein; lane 2, mutant uricase-MBP fusion protein. (B) Coomassie-stained uricase-MBP fusion proteins obtained from DEAE-Sepharose ion-exchange chromatography fractions. Lane 1, wild-type uricase-MBP fusion protein; lane 2, mutant uricase-MBP fusion protein. The samples were loaded onto 12% polyacrylamide gel. Both MBP-uricase proteins have an apparent molecular mass of 98 kDa.

5.4.5 Comparison of activity of the wild-type and mutant fusion uricase

Figure 5-7 shows the evaluation of uricase activity from both mutant and wild-type proteins, as detected by a decrease in absorbance at 293 nm in the presence of uricase. Clearly, the activity of enzyme purified from the mutant uricase exceeded that of the wild-type one. Specific uricase activities of the wild-type and mutant uricases were determined to be 11.5 and 13.1 U/mg, respectively. The apparent K_M values for wild-type and mutant uricase-MBP proteins were estimated to be 24 and 26 μM , respectively. Enzymatic properties of the mutant MBP-uricase were compared with the wild-type MBP-uricase. Thermal stability studies carried out by 1 h incubation at different temperatures showed that both wild-type and mutant uricase were completely inactivated at 75 °C and 80 °C, respectively. The temperature leading to 45-60% inactivation was 70 °C for both wild-type and mutant uricase. The residual activity of wild-type uricase was maximal when temperature from 4 to 60 °C (Fig. 5-8). However, mutant uricase, shows maximal residual activity of 4 to 65 °C. Thus the mutant might be slightly more thermostable. The pH stability studies performed using 7 h incubations at different pH (6-11) values showed that both wild-type and mutant uricase are at optimal activity at pH values from 6 to 10 (Fig. 5-9).

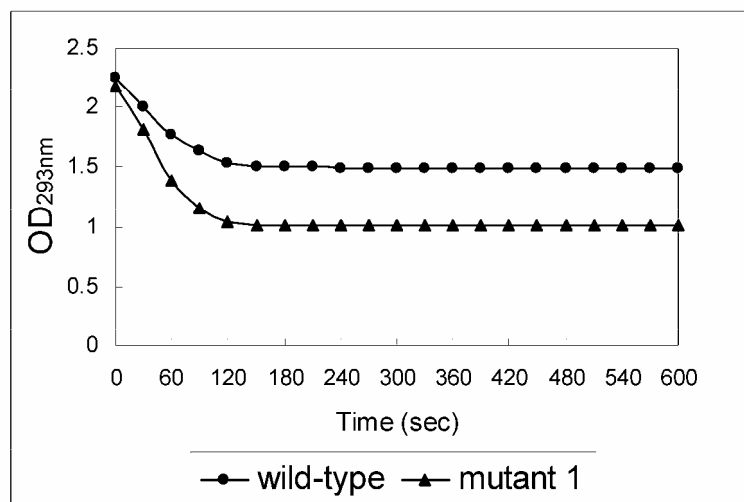


Figure 5-7. Comparison of the wild-type and mutant uricase activities. The curves show uricase activity as the change in the optical density (OD) with time. Decreasing OD₂₉₃ is an indication of uricase-dependent oxidation of uric acid (in 0.05 M borate buffer containing 0.1 mM uric acid, pH 8.5). One unit was defined as the amount of enzyme required to transform 1 μ mol of uric acid into allantoin in 1 min at 25 °C and pH 8.5.

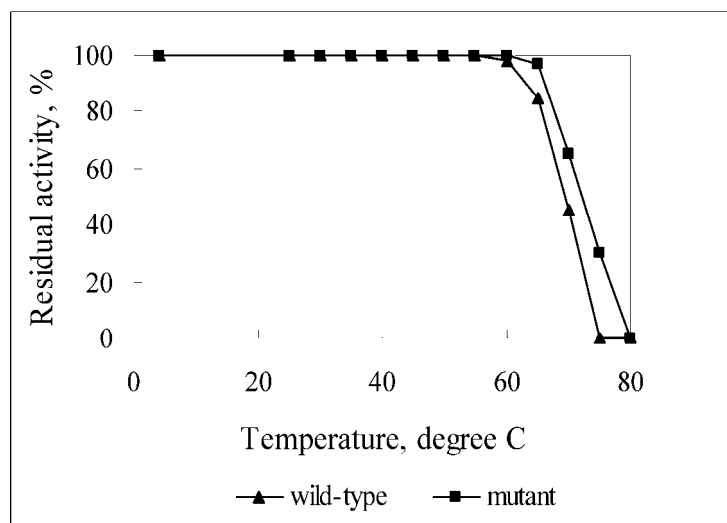
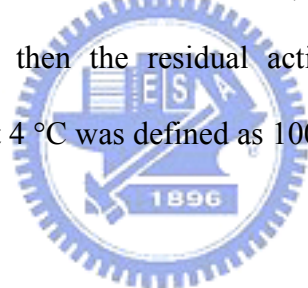


Figure 5-8. Thermal stability of wild-type and mutant uricase enzymes. The enzyme (10 U/mL of uricase in 50 mM borate buffer, pH 8.5) was treated for 1 h at various temperatures, and then the residual activity was determined. The residual activity after 1 h at 4 °C was defined as 100%.



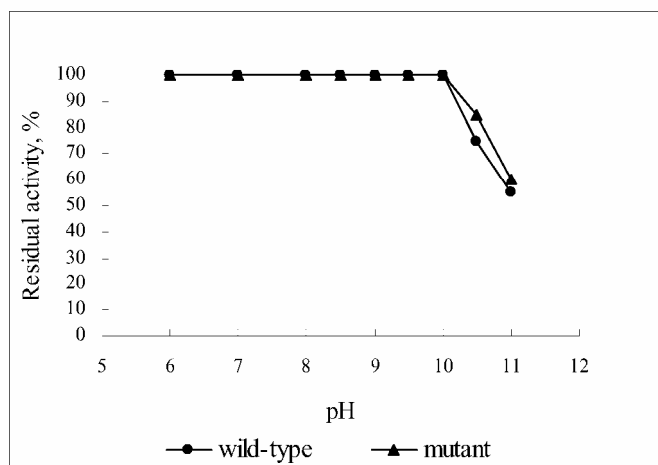
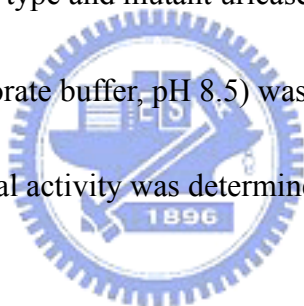


Figure 5-9. pH stability of wild-type and mutant uricase enzymes. The enzyme (10 U/mL of uricase in 50 mM borate buffer, pH 8.5) was treated at 25 °C for 7 h and various pHs, then the residual activity was determined. (● = Wild-type; ▲ = mutant)



5.5 Discussion

This chapter describes a modified colorimetric assay for uric acid in which uricase catalyzes the reduction of dissolved oxygen to hydrogen peroxide in the presence of uric acid. Horseradish peroxidase then catalyzes the production of a quinoneimine dye. One such colorimetric scheme utilizes the uricase - uric acid - horseradish peroxidase - 4-aminoantipyrine - 3,5-dichloro-2-hydroxybenzene sulfonate colorimetric reactions. This assay is compatible with high-throughput screening using a microplate reader. However, the success of the microtiter well plate assay is critically dependent upon a colorimetric indicator that will simultaneously support horseradish peroxidase and not inhibit the production of hydrogen peroxide (Fig. 5-4). The modified colorimetric assay takes only 20 h from isolation of uricase clones to measurements of uricase activity. This is much more efficient than conventional methods (Fig. 5-1), which take at least 4 days and include the following steps: 2 ml LB broth/ampicillin, purify plasmid DNA, digest, electrophoresis, 3 ml LB medium, 50 ml LB medium, preparation of crude cellular extracts, and affinity chromatography of purification and activity assay by spectrophotometry. We have demonstrated the usefulness of this assay and used it to screen for a mutant uricase enzyme.

The StEP recombination reaction can be carried out in a single tube. The staggered extension process (StEP) consists of priming the template sequence followed by repeated cycles of denaturation and extremely abbreviated annealing/ polymerase-catalyzed extension. In each cycle the growing fragments anneal to different templates based on sequence complementarity and extended further. This is repeated until full-length sequence is formed.

Due to template switching, most of the polynucleotides contain sequence information from different parental sequences. The key to successful recombination by StEP is to tightly contract the polymerase-catalyzed DNA extension. The nucleotide sequence of the 1.5 kb *Eco* RI-*Hind* III DNA fragment, including the mutant uricase, was identified (Fig. 5-2). Figure 5-4 shows the results of screening the StEP library for mutants using the microtiter plate colorimetric assay. Two clones with activity were identified and have an identical nucleotide sequence.

The predicted amino acid sequence of the mutant uricase was 84% identical to that of wild-type uricase. A BLAST search identified five motifs of wild-type uricase sequences. These motifs, except for motif B, are also conserved in mutant uricase (Fig. 5-5). Moreover, the mutant uricase includes two cysteines, one of which participates in activity of the enzyme. Wild-type and mutant uricase enzymes were purified from *E.coli* DH5 α as MBP fusions from the soluble fraction in a single amylose affinity step, then was further purified by DEAE-Sephacel ion-exchange chromatography to homogeneity. The specific uricase activities of the two enzymes were compared. Both wild-type and mutant uricase have optimal (100%) activity at a pH value from 6 to 10. Thermal stability studies demonstrate that both wild-type and mutant uricase are completely inactivated at 75 °C and 80 °C, respectively. Thus the mutant enzyme appears to be slightly more stable at high temperatures. In the temperature range between 4 and 80 °C, the residual activity of mutant uricase was maximal up to 65 °C.

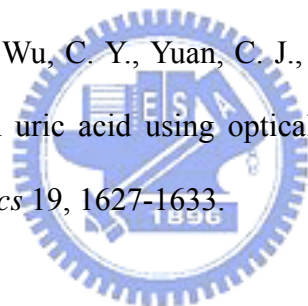
5.6 References

1. Keilin, J. (1959) The biological significance of uric acid and guanine excretion. *Biol. Rev.* 34, 265-296.
2. Wallrath, L. L. and Friedman, T. B. (1991) Species differences in the temporal pattern of drosophila urate oxidase gene expression are attributed to trans-acting regulatory changes. *Proc. Natl. Acad. Sci. U.S.A.* 88, 5489-5493.
3. Montalbini, P., Redondo, J., Caballero, J. L., Cárdenas, J. and Pineda, M. (1997) Uricase from leaves: its purification and characterization from three different higher plants. *Planta.* 202, 277-283.
4. Montalbini, P., Aguilar, M. and Pineda, M. (1999) Isolation and characterization of uricase from bean leaves and its comparison with uredospore enzyme. *Plant Science* 147, 139-147.
5. Yuichi, H., Tetsuhiko, S. and Hajime, I. (2000) Cloning, sequence analysis and expression in *Escherichia coli* of the gene encoding a uricase from the yeast-like symbiont of the brown planthopper, *Nilaparvata lugens*. *Insect Biochemistry and Molecular Biology* 30, 173-182.
6. Koyama, Y., Ichikawa, T. and Nakano, E. (1996) Cloning, sequence analysis and expression in *Escherichia coli* of the gene encoding the *candida utilis* urate oxidase. *J. Biochem.* 120, 969-973.
7. Adamek, V., Suchova, M., Demnerova, K., Kralova, B., Fort, I. and Morava, P. (1990) Fermentation of *candida utilis* for uricase production. *J. Indu. Microbiol.* 6, 85-90.
8. Yamamoto, K., Kojima, Y., Kikuchi, T., Shigyo, T., Sugihara, K. and Takashio, M. (1996) Nucleotide sequence of the uricase gene from *Bacillus* sp. TB-90. *J. Biochem.* 119, 80-84.
9. Eswara, U. S., Dutt, H. and Mottola, A. (1974) Determination of uric acid at the microgram level by a kinetic procedure based on a pseudo-induction period. *Anal. Chem.* 46, 1777.

10. Burtic, C. A. and Ashwood, E. R. (1994) Teitz textbook of clinical chemistry, 2nd ed. Philadelphia: WB saunders company.
11. Yutaka, A., Hiroshi, I., Hiroomi, N., Tsugutoshi, A. and Mitsutatk, Y. (1992) Effects of serum bilirubin on determination of uric acid by the uricase-peroxidase coupled reaction. *Clin. Chem.* 38, 1350-1352.
12. Bhargava, A. K., Lal, H. and Pundir, C. S. (1999) Discrete analysis of serum uric acid with immobilized uricase and peroxidase, *J. Biochem. Biophys. Methods* 39, 125-136.
13. Nanjo, M. and Guilbault, G. G. (1974) Enzyme electrode sensing oxygen for uric acid in serum and urine. *Anal. Chem.* 46, 1769-1772.
14. Uchiyama, S., Shimizu, H. and Hasebe, Y. (1991) Chemical amplification of uric acid sensor responses by dithiothreitol. *Anal. Chem.* 66, 1873-1876.
15. Miland, E., Ordieres, A. J. M., Blanco, P. T. and Smyth, C. Ó. (1996) Poly (o-aminophenol)-modified bienzyme carbon paste electrode for the detection of uric acid, *Talanta* 43, 785-796.
16. Schiavon, O., Calicati, P., Ferruti, P. and Veronese, F. M. (2000) Therapeutic proteins: a comparison of chemical and biological properties of uricase conjugated to linear or branched poly(ethylene glycol) and poly(N-acryloylmorpholine), *Il Farmaco* 55, 264-269.
17. Huimin, Z., Lori, G., Zhixin, S., Joseph, A. A. and Frances, H. A. (1998) Molecular evolution by staggered extension process (StEP) mutagenesis *in vitro* recombination. *Nat. Biotechnol.* 16, 258-261.
18. Zhao, H. and Arnold, F. H. (1997). Functional and nonfunctional mutations distinguished by random recombination of homologous genes. *Proc. Natl. Acad. Sci. U.S.A.* 94, 7997-8000.
19. Guan, C., Li, P., Riggs, P. D. and Lnouye, H. (1988) Vectors that facilitate the expression and purification of foreign peptides in *E. coli* by fusion to maltose-binding protein. *Gene*

67, 21-30.

20. Maina, C. V., Riggs, P. D., Granda, A. G., Slatko, B. E., Moran, L.S. and Tagliamonte, J. A. (1988) An E.coli vector to express and purify foreign proteins by fusion to and separation from maltose-binding protein. *Gene* 74, 365-373.
21. Kellerman, O. K. and Ferenci, Y. (1982) Maltose-binding protein from *Escherichia coli*. *Methods Enzymol* 90, 459-467.
22. Bairoch, A. (1991) Prosite : A dictionary of sites and patterns in proteins. *Nucleic Acids Res.* 19, 2241-2246.
23. Legoux, R., Delpech, B., Dumont, X., Guillemot, J. C., Ramond, P., Shire, D., Caput, D., Ferrara, P. and Loison, G. (1992) Cloning and expression in *Escherichia coli* of the gene encoding *Aspergillus flavus* urate oxidase, *J. Biol. Chem.* 267, 8565-8570.
24. Huang, S. H., Shih, Y. C., Wu, C. Y., Yuan, C. J., Yang, Y. -S., Li, Y. K. and Wu, T. K. (2004) Detection of serum uric acid using optical polymeric biochip detection system. *Biosensor and Bioelectronics* 19, 1627-1633.



Chapter 6

Expression and Purification of a PCR Synthesized Gene

Encoding *Bacillus* spp. Uricase

6.1 Abstract

This chapter presents a single-step assembly of DNA oligonucleotides via polymerase chain reaction (PCR) to generate a synthetic *Bacillus* spp. uricase gene. The *Bacillus* spp. uricase gene was designed using preferred codons common to all the three organisms. Sixteen oligonucleotides (each about 60-95 nucleotides in length), which had overlapping regions and spanned the length of the 999-base pair synthetic gene, were used in the synthesis. The synthetic gene was cloned in *Escherichia coli* and sequence analysis was used to verify that the method was successful. The synthetic gene was cloned into the pMAL-c2 vector for expression in *E. coli* as a fusion protein with the maltose-binding protein (MBP). The uricase-MBP fusion was purified in a one step procedure by affinity chromatography to crosslinked amylose resin. Uricase protein was purified from the fusion protein following cleavage with protease factor Xa and amylose affinity chromatography. The uricase protein yielded a single band on SDS-PAGE and was highly active.

Keywords: Oligonucleotides; Polymerase chain reaction; *Bacillus* spp. uricase; Synthesize; Expression and purification

6.2 Introduction

Uricase is an enzyme that participates in degrading purine by catalyzing the oxidative breakdown of uric acid to allantoin. This enzyme is found in various organisms including mammals (10, 23), plants (16), fungi (17), yeasts (1, 12, 25), and bacteria (24). Uric acid, the primary end product of purine metabolism, is present in biological fluids, such as blood and urine (5). Various conditions increase the amount of uric acid in biological fluids. Such conditions cause gout, chronic renal disease, some organic acidemias and Lesch-Nyhan syndrome (3).

Several attempts have been made to fabricate uric acid sensors, using uricase (urate oxidase, EC 1. 7. 3. 3.) as a biocatalyst (2, 15, 18, 22, 26). Uricase catalyzes the *in vivo* oxidation of uric acid in the presence of oxygen, which acts as an oxidizing agent to produce allantoin and CO₂ as oxidation products of uric acid, and hydrogen peroxide as reduction product of O₂. Many uricases from microorganisms are used as diagnostic reagents in detecting of uric acid. These enzymes either exhibit high thermostability or are active over a wide pH range (12, 20, 24, 25). Only *Bacillus* sp. TB-90 was found to produce both high activity and thermostability over a wide range of pH values.

Many publications have addressed the assembly of DNA sequences from oligonucleotides by ligation (6, 8, 21), by self-priming PCR (4, 8), and by the *FokI* method of gene synthesis (14). This paper presents a single-step PCR protocol that uses thermostable *rTth* polymerase to create a synthetic uricase gene based on *Bacillus* spp. genes and then successfully clone and express the uricase gene *E. coli*.

6.3 Experimental

6.3.1 Synthesizing oligonucleotides

Sixteen long oligonucleotides, spanning the entire single chain *Bacillus* spp. uricase gene, were synthesized by Biobasic, Inc. These single-stranded oligonucleotides (SSH-N1, SSH-C2, SSH-N3, SSH-C4, SSH-N5, SSH-C6, SSH-N7, SSH-C8, SSH-N9, SSH-C10, SSH-N11, SSH-C12, SSH-N13, SSH-C14, SSH-N15, and SSH-C16 in Table 5-1) each included 5-15 overlapping nucleotides, which upon annealing, serve as primers for the *rTth* polymerase (Applied Biosystems) in a PCR reaction.

6.3.2 Synthesizing a gene *Bacillus* spp. uricase by extending overlap and PCR

To generate full-length templates of SHH-N and SHH-C by overlap extension and PCR, 2 pmol of each oligonucleotide (SSH-N1, N3, N5, N7, N9, N11, N13, N15 and SHH-C2, C4, C6, C8, C10, C12, C14, C16) was mixed in a standard PCR (50 μ L final volume) that contained 0.2 mM of each deoxyribonucleoside triphosphate (dNTP), 1.0 unit of *rTth* polymerase, 1.5 mM Mg(OAc)₂ and 3x3 XL *rTth* polymerase buffer. All the PCRs were performed in a thermal cycler (GeneAmp PCR System 9700) using a program of predenaturation for 1 min at 94 °C, followed by 25 repeated cycles of 1 min denaturation at 94 °C, 2 min annealing at 55 °C, 2 min extension at 72 °C, and final extension at 72 °C for 5 min. Figure 6-1 presents experimental details.

Cloning and transformation were performed as described by Sambrook and Russell (19). The assembled *Bacillus* spp. uricase gene products were digested with *Eco*RI and *Hind*III and cloned into the *Eco*RI-*Hind*III digested pMAL-c2, and then transformed into *E. coli* DH5 α . The culture was spread on a LB plate with ampicillin for selection and X-gal and

isopropyl- β -D-thiogalactopyranoside (IPTG) for blue-white screening of recombinants.



SHH-N1 (1-90) 5' > tct aga att cca tal gac caa aca caa aga aag ggt lat gla cta cgg faa agg tga cgt tt cgc fta ceg tac cta ctt gan acc gct cac cgg tgt tag g <3'

SHH-C2 (170-85) 5' > ttg gta cca cca acg gag att tta acg tta aca ccg aag agg atg tgg tea cga ceg gag aac ggg gat tee ggg atg gte cta ac<3'

SHH-N3 (160-220) 5' > ggt ggt acc aaa ttc ctg acc tcc ttc acc aaa ggc gac aac agc ttg gtt gtt gct acc g <3'

SHH-C4 (275-215) 5' > atg gtg gta ccg gtg tag cta gcc aag tgt ttc tgg atg aag ttt ttc atg gag tgg gta g <3'

SHH-N5 (260-350) 5' > aca ccg gta cca cca teg aag gtt tet tgg aal acg ttg cta cct cct tet lga aaa aat act ccc aca teg aaa aga tet cct tga teg g <3'

SHH-C6 (420-340) 5' > gaa aac gag ctc gct agc agc cct gtt acc gtt ttt aac agc gaa ggt ggt ttc gaa cgg gat ttc ttc acc gat caa gga <3'

SHH-N7 (405-485) 5' > tag cga get cgt tt caa aaa atc ceg faa cga ata cgc tac cgc fta ctt gaa cat ggt teg faa cga aca cac cct <3'

SHH-C8 (535-470) 5' > ctt tga tea act gga gac cag cca gac cgc tot get gtt cgg tga tgt tca ggg tgt tgt ctt cgt <3'

SHH-N9 (520-590) 5' > ctc cag ttg atc aaa gtc agc ggt aac tcc ttc gtt ggt ttc atc cgt gac gaa tac acc acc ctc cgg ga <3'

SHH-C10 (670-580) 5' > ggt tgg tac cga atg agt ctt cgg tgt ttt tgt att tee att tga tgt tea agt aaa cga aca gcg gac ggt tgg agt ctt cgg gca ggg t <3'

SHH-N11 (655-735) 5' > tca ttc ggt acc aac ccg gaa aac tac gtt gct gct gaa cag atc cgt gac atc gct acc tcc gtt ttc cac gaa acc gaa <3'

SHH-C12 (810-725) 5' > aac ttc ctg cag ctg cgg gaa cct ttc caa gat cct act acc gat caa gta gat caa gtg ct gat gga cag ggt ttc ggt ttc gt <3'

SHH-N13 (795-850) 5' > goa got goa gga agt tta ctt cga atc cca gaa cca cac ctg gga caa aat cgt tg <3'

SHH-C14 (905-840) 5' > ccg tac ggc gga cgc ggt tgg gtg taa act tta cct tgg gat tcc ggg att tct tca acg att ttg <3'

SHH-N15 (885-950) 5' > cgg cgg tac ggt ttc cag tgc ttc acc gtt acc cag gaa gac ttg cgg cag gaa aa <3'

SHH-C16 (999-945) 5' > gct gca gaa gct ttc att tca gag cac ctt tat ggt cgg gtt cgt cgg aga aca tca gga tgt ttt cc <3'

Table 6-1. Schematic representation of sixteen long oligonucleotides.



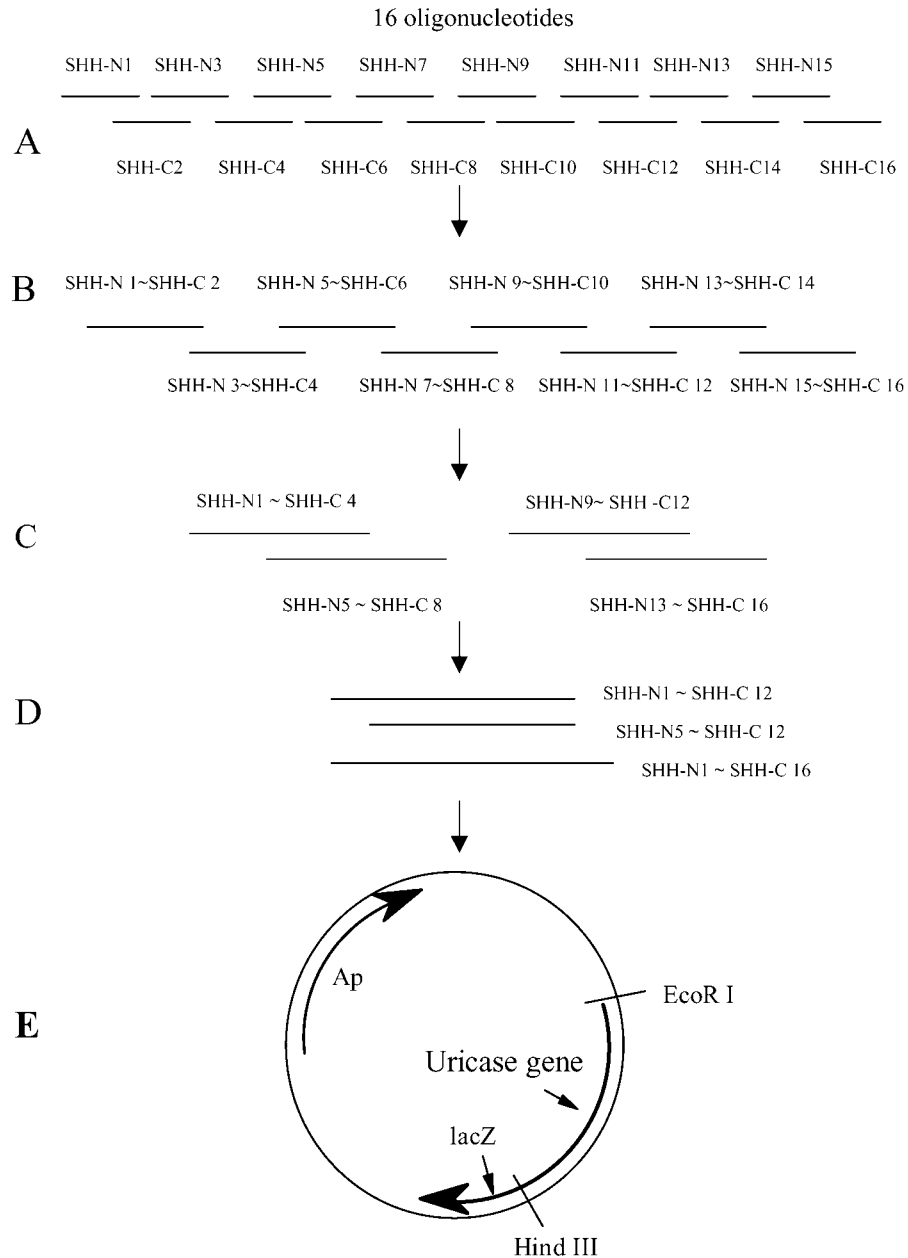


Figure 6-1. Protocol for assembling synthetic *Bacillus* spp. uricase-pMAL-c2. The synthetic *Bacillus* spp. uricase gene process included the following entities. (A) sixteen long oligonucleotides; (B) first PCR products; (C) second PCR products; (D) third PCR products. The reaction products were analyzed by 2% agarose-gel electrophoresis. The assembled product (E) and pMAL-c2 were both digested with *EcoRI* and *HindIII*, gel-purified, ligated, and used to transform *E. coli* XL1-blue.

6.3.3 Sequencing and computer analysis of DNA

The clones were sequenced using an ABI PRISM 310 auto-sequencer. Samples were prepared using a DNA Cycle Sequencing Kit and a Big-Dye Terminator (Perkin Elmer). Suitable oligonucleotides were used as primers. DNA sequence analysis was performed at the National Center for Biotechnology Information (NCBI) using GenBank databases and BLAST Programs. Protein sequences were aligned using ClustalG (1.1).

6.3.4 Expression and purification of the *Bacillus spp. uricase* protein

For protein expression, pMAL-c2 system (New England BioLabs) was used to express the assembled *Bacillus spp. uricase* gene. Cells that contained plasmids that coded for fusion proteins under *lac* promoter control were grown to a concentration of 5×10^8 cell/ml at 37 °C with shaking in a rich medium, IPTG was added to a final concentration of 0.3 mM, and the culture was grown for an additional 4 h. All subsequent steps were performed at 4 °C or on ice. The cells were harvested in low-speed centrifugation, resuspended in 1/10 vol. of 10 mM Tris buffer pH 7.2, and sonically lysed. Cellular debris was then pelleted by high-speed centrifugation, and the supernatant was saved as crude cellular extract. The purification procedure used the pMAL-c2 protein fusion and purification system (7, 13). Cross-linked amylose was prepared of from amylose (New England BioLabs) and used as an affinity chromatography matrix as described by Kellerman and Ferenci (11). Fusion proteins were purified from crude extracts by binding to cross-linked amylose in a column, and were eluted with 10 mM Tris buffer that contain 10 mM maltose (7, 13). Uricase-MBP (uricase fused to maltose binding protein) was digested with factor Xa as described by Maina *et al.* (13). Uricase-MBP was first denatured by dialysis in 8 M urea followed by dialysis in 10 mM Tris buffer pH 7.2. The concentration of factor Xa in digestions was 1%, by weight, of the fusion protein to be digested. After cleavage of uricase-MBP with factor Xa, the two domains were

separated by re-passage over a cross-linked amylose column.

6.3.5 Assay of uricase activity

Uricase activity was routinely measured aerobically as the decrease in absorbance at 293 nm due to the enzymatic oxidation of uric acid. During purification, the activity of the enzyme was measured in an assay mixture that contained 10 mM Tris buffer (pH 8.5). One unit was defined as the amount of enzyme required to transform 1 μmol of uric acid into allantoin in 1 min at 25 °C at pH 8.5. Protein concentration was estimated by the Bio-Rad Protein Assay, using bovine serum albumin as a standard. Reaction mixtures containing 5-100 μM substrate solution were used to determine the kinetic parameters.



6.4 Results

6.4.1 Design of the synthetic *Bacillus* spp. uricase gene

The *Bacillus* spp. uricase gene was designed using preferred codons common to all the three organisms. The next best codon was used when there was a conflict. Accordingly, the codon used were as follows: glycine, GGT/GGC; glutamic acid, GAA; aspartic acid, GAT/GAC; valine, GTT/GTA; alanine, GCT/GCA; serine, TCC/TCT/AGC; lysine, AAA; asparagine, AAC; methionine, ATG; isoleucine, ATC; threonine, ACC/ACT; tryptophan, TGG; cysteine, TGC; tyrosine, TAC; leucine, TTG; phenylalanine, TTC; histidine, CAC; and proline, CCG/CCA. The sequence was thoroughly analyzed with reference to GenBank databases and BLAST programs. The *Bacillus* spp. uricase gene was designed with *Eco*RI and *Nde*I sites at the 5' end and a *Hind*III site at the 3' end. Based on our previous experience, we used 5 to 15 base overlaps between each oligonucleotide.

6.4.2 Synthesizing the *Bacillus* spp. uricase gene using PCR

The assembly PCR protocol includes three steps: assembling the gene, amplifying the gene, and cloning. Because sixteen single-stranded oligonucleotides of complementary DNA fragments are filled in during the assembly the gene process, cycling with *rTth* polymerase results in the formation of increasingly larger DNA fragments until the full-length gene is obtained. DNA ligase is not used in the assembly process. Figures 6-2 to 6-4 show

experimental results concerning the protocol. The gene was also synthesized from sixteen single-stranded oligonucleotides fragments produced with overlapping sequence. For example SHH-N1~SHH-C2 was amplified from oligonucleotides SHH-N1 to SHH-C2; SHH-N3~SHH-C4 was amplified from oligonucleotides SHH-N3 to SHH-C4; SHH-N5~SHH-C6 was amplified from oligonucleotides SHH-N5 to SHH-C6; SHH-N7~SHH-C8 was amplified from oligonucleotides SHH-N7 to SHH-C8; SHH-N9~SHH-C10 was amplified from oligonucleotides SHH-N9 to SHH-C10; SHH-N11~SHH-C12 was amplified from oligonucleotides SHH-N11 to SHH-C12; SHH-N13~SHH-C14 was amplified from oligonucleotides SHH-N13 to SHH-C14; SHH-N15~SHH-C16 was amplified from oligonucleotides SHH-N15 to SHH-C16 (Figure 6-2, lanes 1- 8; first PCR products); SHH-N1~SHH-C4 was amplified from oligonucleotides SHH-N1 to SHH-C4; SHH-N5~SHH-C8 was amplified from oligonucleotides SHH-N5 to SHH-C8; SHH-N9~SHH-C12 was amplified from oligonucleotides SHH-N9 to SHH-C12; SHH-N13~SHH-C16 was amplified from oligonucleotides SHH-N13 to SHH-C16 (Fig. 6-3, lanes 1-4; second PCR products); SHH-N1~SHH-C12 was amplified from oligonucleotides SHH-N1 to SHH-C12; SHH-N5~SHH-C12 was amplified from oligonucleotides SHH-N5 to SHH-C12; SHH-N1~SHH-C16 was amplified from oligonucleotides SHH-N1 to SHH-C16 (Fig. 6-4, lanes 1- 3; third PCR products).

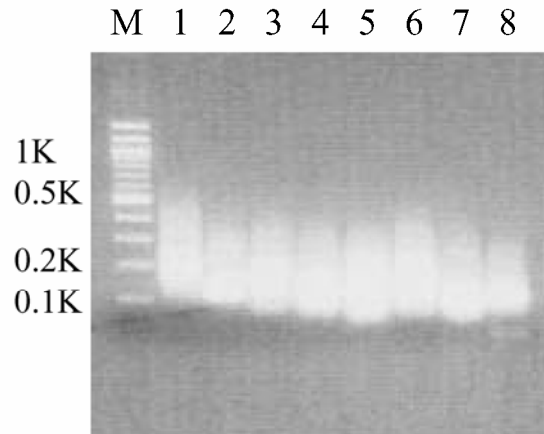


Figure 6-2. Agarose electrophoresis gel analysis of first PCR product (B). Lane M 1-Kb ladder; lane 1. SHH-N1~SHH-C2 ; lane 2. SHH-N3 ~ SHH-C4; lane 3. SHH-N5~SHH-C6; lane 4. SHH-N7~SHH-C8; lane 5. SHH-N9~SHH-C10; lane 6. SHH-N11~SHH-C12; lane 7. SHH-N13~SHH-C14; lane 8. SHH-N15~SHH-C16.

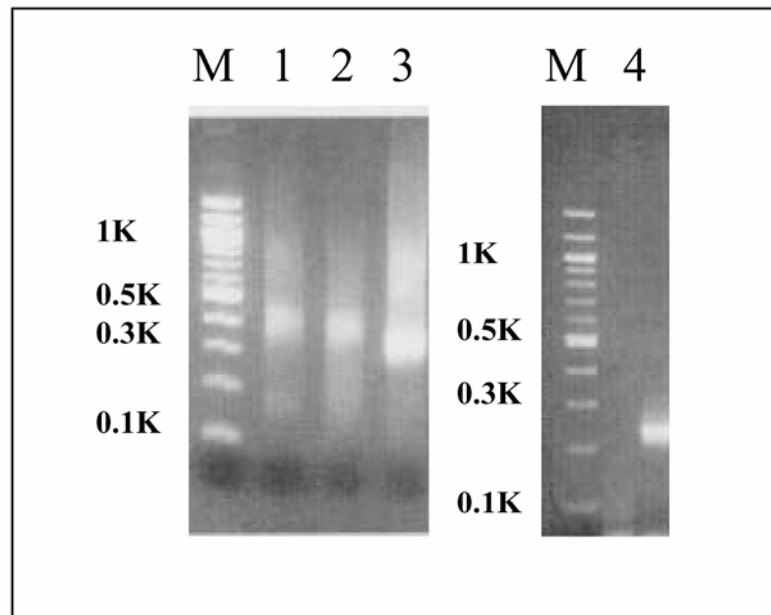


Figure 6-3. Agarose electrophoresis gel analysis of second PCR product (C). Lane M. 1-Kb ladder; lane 1. SHH-N1~SHH-C4 ; lane 2. SHH-N5 ~ SHH-C8; lane 3. SHH-N9~SHH-C12; lane 4. SHH-N13~SHH-C16.

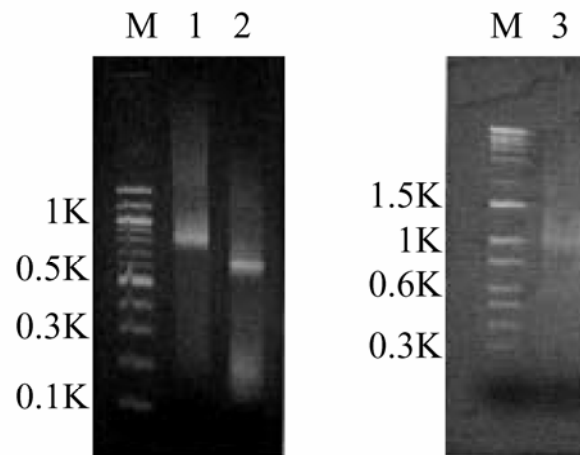
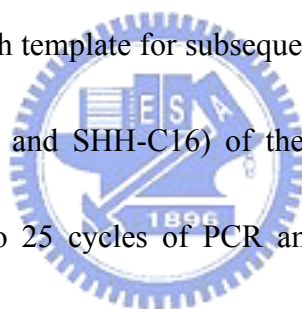


Figure 6-4. Agarose electrophoresis gel analysis of third PCR product (D). Lane M, 1 Kb ladder and 10 Kb ladder; lane 1. SHH-N1 ~ SHH-C12; lane 2. SHH-N5~SHH-C12 ; lane 3. SHH-N1~SHH-C16.

The amino acid sequence of the *Bacillus* spp. uricase protein was reverse translated into a nucleotide sequence based on an *E. coli* codon usage table. The resulting sequence was 999 nucleotides length and included a termination codon at its 5' and 3' terminus. Sixteen oligonucleotides, which spanned the length of the 999-base pair synthetic gene, were synthesized. These single-stranded oligonucleotides included 5-15 nucleotide overlaps, which upon annealing, serve as primers for the *rTth* polymerase in a PCR reaction. Additionally, the oligonucleotides SHH-N1 and SHH-16 contained flanking restriction enzyme sites to facilitate cloning into pMAL-c2. Gel purification of the oligonucleotides was unnecessary. A full-length template for subsequent PCR was generated using the 5'- and 3'- flanking primers (SHH-N1 and SHH-C16) of the synthetic *Bacillus* spp. uricase gene. This reaction was subjected to 25 cycles of PCR amplification as described above. The product of this reaction was a sharp band of the expected size. This fragment was successfully cloned (Fig. 6-5, lane 1), and functional *Bacillus* spp. uricase protein was expressed in both *E. coli* and uricase expression systems.



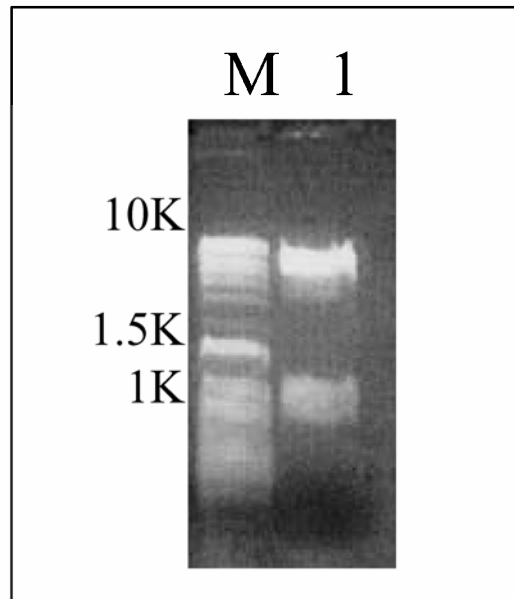


Figure 6-5. Agarose electrophoresis gel analysis of cloning (E). Lane M, 10 Kb ladder. Lane 1, 1 Kb synthetic *Bacillus* spp. uricase gene fragment were inserted into pMAL-c2, and were digested by *EcoRI/HindIII*.

6.4.3 Nucleotide and amino acid sequence of *Bacillus* spp. Uricase

Analysis of the nucleotide sequence of the synthetic *Bacillus* spp. uricase gene revealed the expected uricase ORF which began at the initiation codon ATG at nucleotide 1 and ended with the termination codon TGA at nucleotide 999 (Fig. 6-6). The ORF codes for a protein of 333 amino acid residues with a calculated molecular mass of 36.7 kDa. Thus, the approach was effective in generating a new uricase sequence.

6.4.4 Expression and purification of the *Bacillus* spp. Uricase

The uricase-MBP fusion protein was successfully purified from *E. coli* only after it was purified in an amylose column. The purified uricase-MBP fusion protein was eluted with maltose buffer and pooled. After cleavage of with factor Xa, the two domains was separated by re-passage over a cross-linked amylose column, concentrated and analyzed by SDS-PAGE (Fig. 6-7). The uricase protein, the major band on the gel, had an apparent molecular weight of 36.7 kDa. Specific activity of the uricase was determined to be 4.2 U/mg. Lineweaver-Burk plot estimates gave a K_M value of 25 M.

```

ma1E.....TCGAGCTCGAACAAACAACAACAATAACAATAACAACAACCTCGGGATCGAGGGAAGGATTTCAG
GAAATTCCATATGACCAAACACAAAAGAAAGGGTTATGTAATAACGGTAAAGGTGACGTTTTTCGCTTACCGT      60
      M T K H K E R V M Y Y G K G D V F A Y R      20
ACCTACTTGAAACCGCTCACCGGTGTTAGGACCATCCCGGAATCCCGGTTCTCCGGTCGTGACCACATC      129
T Y L K P L T G V R T I P E S P F S G R D H I      43
CTCTTCGGTGTTAACGTTAAAAATCTCCGTTGGTGGTACCAAATTCCTGACCTCCTTCACCAAAGGCGAC      198
L F G V N V K I S V G G T K F L T S F T K G D      66
AACAGCTTGGTTGTTGCTACCGACTCCATGAAAAAATTTCATCCAGAAACACTTGGCTAGCTACACCGGT      267
N S L V V A T D S M K N F I Q K H L A S Y T G      89
ACCACCATCGAAGGTTTCTTGGAAATACGTTGCTACCTCCTTCTTGAAAAAATACTCCACATCGAAAAAG      336
T T I E G F L E Y V A T S F L K K Y S H I E K      112
ATCTCCTTGATCGG TGAAGAAATCCCGTTGAAAACACCTTCGCTGTTAAAAACGGTAAACAGGGCTGCT      405
I S L I G E E I P F E T T F A V K N G N R A A      135
AGCGAGCTCGTTTTCAAAAAATCCCGTAAACGAATACGCTACCGCTTACTTGAACATGGTTTCGTAACGAA      474
S E L V F K K S R N E Y A T A Y L N M V R N E      158
GACAACACCCTGAACATCACCGAACAGCAGACGGTCTGGCTGGTCTCCAGTTGATCAAAGTCAGCGGT      543
D N T L N I T E Q Q S G L A G L Q L I K V S G      181
AACTCCTTCGTTGGTTTCATCCGTTGACGAATACACCACCCTGCCGGAAGACTCCAACCGTCCGCTGTTT      612
N S F V G F I R D E Y T T L P E D S N R P L F      204
GTTTACTTGAACATCAAATGGAAATACAAAAACACCGAGTGACATCGCTACCTCCGTTTTCCACGAAAC      681
V Y L N I K W K Y K N T E D S F G T N P E N Y      227
CGAAACCCCTGTCCATCCAGAGACTCATTCCGGTACCAACCCGGAAAACTACGTTGCTGCTGAACAGATCC      750
V A A E Q I R D I A T S V F H E T E T L S I Q      250
CACTTGATCTACTTGATCGGTAGTAGGATCTTGGAAAAGGTTCCCGCAGCTGCAGGAAGTTTACTTCGAA      819
H L I Y L I G S R I L E R F P Q L Q E V Y F E      273
TCCCAGAACCACACCTGGGACAAAATCGTTGAAGAAATCCCGAAATCCGAAAGTAAAGTTTACACCGAA      888
S Q N H T W D K I V E E I P E S E G K V Y T E      296
CCGCGTCCGCCGTACGGTTTCCAGTGCTTACCAGTTACCAGGAAAGACTTGCCGCAGGAAAAACATCCTG      957
P R P P Y G F Q C F T V T Q E D L P Q E N I L      319
ATGTTCTCCGACGAACCGGACCATAAAGGTGCTCTGAAATGAAAAATGTCGGAGCCTGAAAGCCTGATG      999
M F S D E P D H K G A L K      333
GGAAAACCTGACAACCCATATTTTGAATTTAACCTGCGGCAAAACAGCGGCAAGCTTCTGCAGCGGCAC      1068
TGCCCGTCGTTTTACAACGTCGTGACTGGGAAAAACCCTGGCGTTACCCAACCTTAATCGCCTTG      1131

```

Figure 6-6. DNA sequence of the synthetic *Bacillus* spp. uricase gene. The deduced amino acid sequence is shown under the nucleotide sequence.

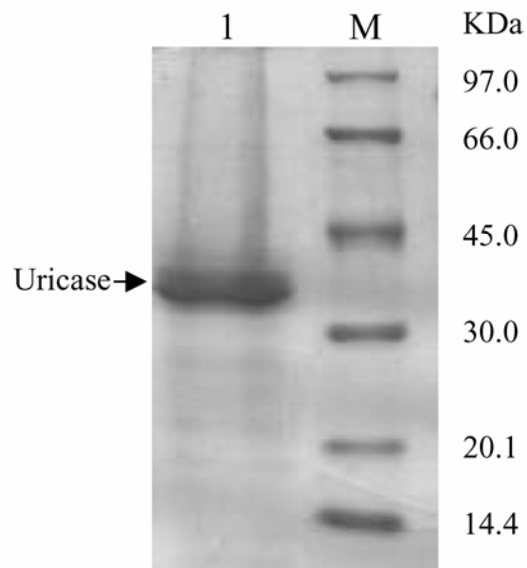


Figure 6-7. SDS-PAGE analysis of the uricase fragment from the flow-through of a second amylose column. Lane M: marker proteins: phosphorylase b (97 kDa), bovine serum albumin (66 kDa), ovalbumin (45 kDa), carbonic anhydrase (30 kDa), trypsin inhibitor (20 kDa); lane 1, uricase protein. The samples were loaded onto 12% polyacrylamide gel. The uricase protein, the major band on the gel, had an apparent molecular weight 36.7 kDa.

6.5 Discussion

We report the successful creation of a synthetic uricase gene codon optimized for *Bacillus* spp.. The synthetic gene was generated using a novel PCR approach using multiple synthetic long oligonucleotides spanning the coding region. The cloned synthetic uricase gene was expressed in *E. coli* and active enzyme was easily purified using a MBP-fusion system. The experiments described herein were designed to demonstrate that the gene assembly method can be used to construct any gene even if only the amino acid sequence is available or had been deduced. Other researchers have reported the construction of a synthetic gene using an approach like ours which does not use DNA ligase in any part of the assembly process. In one case, a two-step PCR protocol that involved thermostable *Taq* polymerase was used to create a synthetic gene for the HIV-2 Rev protein that contains codons preferentially utilized in *E. coli*. The resulting sequence was 303 nucleotides long and included a termination codon at its 3' terminus. Four oligonucleotides, which spanned the length of the 303-base pair synthetic gene were used in that work (4). In another example, Stemmer et al. (21) described the assembly by PCR of a 1.1 Kbp synthetic TEM-1 β -lactamase-encoding gene. The assembly was achieved in a single reaction that involved a total of 56 oligodeoxyribonucleotides, each 40 nucleotides long. The synthetic gene was amplified by PCR and cloned in a vector that contained the tetracycline-resistance gene as the sole selectable marker. Accordingly, the authors suggest that in assembly of other genes,

experiments screening a few colonies will suffice to identify the gene of interest.



6.6 References

1. Adamek, V., Suchova, M., Demnerova, K. and Kralova, B. (1990) Fermentation of *candida utilis* for uricase production. *J. Indu. Microbiol.* 6, 85-90.
2. Bhargava, A. K., Lal, H. and Pundir, C. S. (1999) Discrete analysis of serum uric acid with immobilized uricase and peroxidase. *J. Biochem. Biophys. Methods* 39, 125-136.
3. Burtic, C. A. and Ashwood, E. R. (1994) Teitz textbook of clinical chemistry, 2nd ed. Philadelphia:WB saunders company.
4. Dillon, P. J. and Rosen, C. A. (1990) A rapid method for the construction of synthetic genes using the polymerase chain reaction. *BioTechniques* 9, 298-300.
5. Eswara, U. S., Dutt, H. and Mottola, A. (1974) Determination of uric acid at the microgram level by a kinetic procedure based on a pseudo-induction period. *Anal. Chem.* 46, 1777.
6. Goeddel, D. V., Kleid, D. G., Bolivar, F., Heyneker, H. I., Yansura, D. G., Crea, R., Hirose, T., Kraszewski, K., Itakura, K. and Riggs, A. D. (1979) Expression in *Escherichia coli* of chemically synthesized genes for human insulin. *Proc. Natl. Acad. Sci. USA* 76, 106-110.
7. Guan, C., Li, P., Riggs, P. D. and Lnouye, H. (1988) Vectors that facilitate the expression and purification of foreign peptides in *E. coli* by fusion to maltose-binding protein. *Gene* 67, 21-30.
8. Hayashi, N., Welschof, M., Zewe, M., Braunagel, M., Dubel, S., Breitling, F. and Little, M. (1994) Simultaneous mutagenesis of antibody CDR regions by overlap extension and PCR. *BioTechniques* 17, 310-314.
8. Kawamura, S., Fukamizo, T., Araki, T. and Torikata, T. (2003) Expression of a synthetic gene coding for ostrich egg-white lysozyme in *Pichia Pastoris* and its enzymatic activity. *J. Biochem.* 133,123-131.
10. Keilin, J. (1959) The biological significance of uric acid and guanine excretion. *Biol. Rev.* 34, 265-296.

11. Kellerman, O. K. and Ferenci, Y. (1982) Maltose-binding protein from *Escherichia coli*. *Methods Enzymol.* 90, 459-467.
12. Koyama, Y., Ichikawa, T. and Nakano, E. (1996) Cloning, sequence analysis and expression in *Escherichia coli* of the gene encoding the *candida utilis* urate oxidase. *J. Biochem.* 120, 969-973.
13. Maina, C. V., Riggs, P. D., Grandea, A. G., Slatko, B. E., Moran, L.S. and Tagliamonte, J. A. (1988) An *E.coli* vector to express and purify foreign proteins by fusion to and separation from maltose-binding protein. *Gene* 74, 365-373.
14. Mandecki, W. and Bolling, T. J. (1988) *FokI* method of gene synthesis. *Gene* 68, 101-107.
15. Miland, E. A., Ordieres, J. M., Blanco, P. T. and Smyth, C. O. (1996) Poly (o-aminophenol)-modified bienzyme carbon paste electrode for the detection of uric acid. *Talanta* 43, 785-796.
16. Montalbini, P., Redondo, J., Caballero, J. L., Cardenas, J. and Pineda, M. (1997) Uricase from leaves: its purification and characterization from three different higher plants. *Planta* 202, 277-283.
17. Montalbini, P., Aguilar, M. and Pineda, M. (1999) Isolation and characterization of uricase from bean leaves and its comparison with uredospore enzyme. *Plant Science* 147, 139-147.
18. Nanjo, M. and Guilbault, G. G. (1974) Enzyme electrode sensing oxygen for uric acid in serum and urine. *Anal. Chem.* 46, 1769-1772.
19. Sambrook, J. and Russell, D. W. (2001) *Molecular cloning: A Laboratory Manual*. Cold Spring Harbor Laboratory Press. Cold Spring Harbor, NY.
20. Schiavon, O., Calicati, P., Ferruti, P. and Veronese, F. M. (2000) Therapeutic proteins: a comparison of chemical and biological properties of uricase conjugated to linear or

- branched poly(ethylene glycol) and poly(N-acryloylmorpholine). *Il Farmaco*. 55, 264-169.
21. Stemmer, W. P. C., Cramer, A., Ha, K. D., Brennan, T. M. and Heyneker, H. L. (1995) Single-step assembly of a gene and entire plasmid from large numbers of oligodeoxyribonucleotides. *Gene* 164, 49-53.
22. Uchiyama, S., Shimizu, H. and Hasebe, Y. (1991) Chemical amplification of uric acid sensor responses by dithiothreitol. *Anal. Chem.* 66, 1873-1876.
23. Wallrath, L. L. and Friedman, T. B. (1991) Species differences in the temporal pattern of drosophila urate oxidase gene expression are attributed to trans-acting regulatory changes. *Proc. Natl. Acad. Sci. USA* 88, 5489-5493.
24. Yamamoto, K., Kojima, Y., Kikuchi, T., Shigyo, T., Sugihara, K. and Takashio, M. (1996) Nucleotide sequence of the uricase gene from *Bacillus* sp. TB-90. *J. Biochem.* 119, 80-84.
25. Yuichi, H., Tetsuhiko, S. and Hajime, I. (2000) Cloning, sequence analysis and expression in *Escherichia coli* of the gene encoding a uricase from the yeast-like symbiont of the brown planthopper, *Nilaparvata lugens*. *Insect Biochemistry and Molecular Biology* 30, 173-182.
26. Yutaka, A., Hiroshi, I., Hiroomi, N., Tsugutoshi, A. and Mitsutatk, Y. (1992) Effects of serum bilirubin on determination of uric acid by the uricase-peroxidase coupled reaction. *Clin. Chem.* 38, 1350-1352.